ONCOGENE-INDUCED SIGNALING HETEROGENEITY IN LUNG CANCER

APPROVED BY SUPERVISORY COMMITTEE

_____

Steven J. Altschuler, Ph.D.

_____

Lani F. Wu, Ph.D.

_____

John D. Minna, M.D.

_____

Christine K. Garcia, M.D., Ph. D.

_____

Michael A. White, Ph.D.

_____

Melanie H. Cobb, Ph.D.

DEDICATION

I thank my mentors, Steve and Lani for their mathe-magical guidance, Dr. Minna for his onco-therapeutic guidance, and for giving me the opportunity and the independence to be a bridge between the scientific researches of two laboratories. I am indebted to my thesis committee members, Christine, Mike and Melanie, for their endless patience, advice and support. This work would not be complete without my friends, inside and outside the lab, for keeping me sane during difficult times. Finally, this is for my parents, for countless reasons. All acknowledgements would belong to those listed above. Any errors are mine.

ONCOGENE-INDUCED SIGNALING HETEROGENEITY IN LUNG CANCER

by

DHRUBA DEB

DISSERTATION

Presented to the Faculty of the Graduate School of Biomedical Sciences
The University of Texas Southwestern Medical Center at Dallas
In Partial Fulfillment of the Requirements
For the Degree of

DOCTOR OF PHILOSOPHY

The University of Texas Southwestern Medical Center

Dallas, TX

August, 2015

ONCOGENE-INDUCED SIGNALING HETEROGENEITY IN LUNG CANCER

Dhruba Deb, Ph.D.

The University of Texas Southwestern Medical Center at Dallas, 2015

Steven J. Altschuler, Ph.D.

John D. Minna, M.D.

Lani F. Wu, Ph.D.

Lung cancer causes the maximum number of cancer related deaths worldwide. In recent years, the cancer genome atlas (TCGA) initiative has identified 138 frequently occurring driver oncogenes and tumor suppressor genes in lung cancer. Currently, only 15 of these genes can be targeted therapeutically. Study of downstream signaling alterations of these oncogenes and tumor suppressor genes may identify novel therapeutic targets. Although studies on genetic heterogeneity in subclonal populations within one tumor using deep sequencing and multiple sectioning have gained popularity

recently, the signaling heterogeneity within tumor cells with identical genetic changes remain poorly understood. Hence, I focus on TP53, KRas and C-Myc as they are among the most frequently occurring oncogenic alterations in lung adenocarcinoma. The downstream signaling changes of these genes may be different from one cell to another. Here, I develop high throughput approaches to study alterations of 6 major signaling readouts – phospho-Erk1/2, phospho-Stat3, Smad2/3, β-catenin, P65, and Foxo1 and quantitatively analyze thousands of cells with defined set of genetic changes. I ask - Can I utilize oncogene-induced signaling alterations in single cells to identify novel targetable vulnerabilities? Using single-cell image analysis I show that the genetically transformed HBECs with all 3 oncogenic changes (TP53, KRas and C-Myc) show significant signaling heterogeneity. They exhibit downregulated Smad2/3 signaling in single cells. Next, using a dominant negative construct, I confirm that this phenotype is partially reversible by the removal of C-Myc oncogenic stress. I further observe that the transformed HBECs exhibit upregulated Stat3 signaling in single cells. In addition, the Stat3 inhibitor Stattic causes more cell death in transformed HBECs. Interestingly, our single-cell image analysis suggests that Stat3 upregulation and Smad2/3 downregulation are mutually exclusive. Hence, Stattic will not be able to target the Smad2/3 downregulated cells. To target Smad2/3 downregulated cells, I identify Bcl6, a downstream target of Smad2/3, and I show that Bcl6 is a novel targetable vulnerability in transformed HBECs. I observe that C-Myc and Bcl6 gene expressions are strongly correlated in cell populations as well as in single-cell level. I further show that Bcl6 can be a targetable vulnerability in a subset of c-Myc addicted non-small cell lung cancers. I

conclude that single-cell analysis of driver oncogenes and their downstream signaling can identify novel targetable vulnerabilities.

CONTENTS

Prior publications

1. Deb D., Vishveshwara S., Vishveshwara S. (2009) Understanding protein structure from a percolation perspective. Biophysical Journal 16:97(6): 1787.

2. Deb D. (2015) Understanding the unpredictability of cancer using techniques from chaos theory and modern art. Leonardo Journal, MIT press, USA, in press, DOI: 10.1162/LEON_a_01099

List of figures

List of tables

List of abbreviations

NSCLC – Non small cell lung cancer

HBEC – Human bronchial epithelial cells

P53 – Transcription factor p53

KRAS – Kirsten rat sarcoma viral oncogene homolog

C-MYC – Cellular Myc

MAX – Myc associated factor x

WNT – Wingless related integration

NFκβ - Nuclear factor kappa light chain enhancer of activated B cells

TGFβ - Transforming growth factor beta

IFNγ - Interferron gamma

JAK – Januse kinase

MAPK – Mitogen activated protein kinase

P65 – Transcription factor p65

STAT1 - Signal transducer and activator of transcription 1

STAT3 - Signal transducer and activator of transcription 3

ERK1/2 – Extracellular signal regulated kinase 1 and 2

FOXO1 – Fox head box protein O1

BSA – Bovine serum albumin

IF - Immunofluorescence

shRNA – short hairpin ribo nucleic acid

EMT – Epithelial to mesenchymal transition

FBS – Fetal bovine serum

PBS – Phosphate buffered saline

TBST – Tris buffered saline with Twin 20

PFA – Paraformaldehype in phosphate buffered saline

qRT-PCR – Quantitative reverse transcriptase polymerase chain reaction

BCL6 – B cell lymphoma 6

MMP7 – Matrix metallo proteinase 7

SOX2 - Sex determining region Y-box 2

FOXK1 – Fox head box protein K1

CDKN1A - Cyclin-dependent kinase inhibitor 1A

ATR - Ataxia telangiectasia and Rad3 related

CHEK1 - Checkpoint kinase 1

CDKN1B - Cyclin-dependent kinase inhibitor 1B

CDKN2A - Cyclin-dependent kinase inhibitor 2A

CDKN2B - Cyclin-dependent kinase inhibitor 2B

PTEN - Phosphatase and tensin homolog

NF-KB1 - Nuclear factor NF-kappa-B p105 subunit

PRDM1 - PR domain containing 1, with ZNF domain

IRF4 - Interferon regulatory factor 4

Oncogenes and Signaling Pathways in Lung Cancer

1.1 Introduction

Lung cancer is a lethal disease responsible for more than a million deaths worldwide each year (Siegel et al., 2013). Non-small cell lung cancer (NSCLC) comprises of 80%-85% of total number of lung cancer cases (Pao and Hutchinson, 2012). The conventional chemotherapeutics outcome has reached a plateau in terms of overall survival of the patients (Custodio et al., 2012). Hence, extensive advances were made in biomarker identification and targeted inhibition of specific signaling pathways (Stahel et al., 2013) dysregulated in NSCLC patients. But, further improvement of targeted therapy is necessary as we are still far from improving overall survival of all NSCLC cases.

The main reason for the failure of certain targeted therapies may be multiple salvage and resistant signaling pathways in solid tumors allowing them to bypass inhibition of a single pathway (Custodio et al., 2012). These signaling pathways, involved in growth and development of normal cells, are aberrated in tumor cells (discussed in section 1.2). Hence, understanding multiple dysregulated signaling pathways at the same time - is important.

To complicate the matter further, we have come across evidences that cells from different regions of solid tumors exhibit different genotypes and signaling phenotypes (Intra-tumor heterogeneity discussed in section 1.4.1). Therefore, most commonly used

population average measurements will miss the variability of the whole spectrum of possible signaling states and its connection to difference in their oncogenotypes. In other words, we need to understand concurrent alteration of these signaling pathways in single cancer cell level.

Some of the recent studies aimed to decipher the connection between oncogenotypes and signaling pathway alteration in the models of late stage cancers (Akiri et al., 2009; Bartis et al., 2013; Jeannot et al., 2014; Jung et al., 2013; Oliveras-Ferraros et al., 2011; Tan et al., 2013; Wang et al., 2013). But, oncogene induced signaling alteration in the early stages of lung cancer progression is not well understood. Signaling diversities in early stage lung cancer models are not as dramatic as that in late stage cancer models (Singh et al., 2010). But they are still indicative of the disease progression and hence their understanding may help diagnosis and therapy of early stage lung cancer.

Studying multiple signaling pathways simultaneously in single cancer cell level is difficult. This chapter describes the most commonly altered signaling pathways in lung cancer and the challenges involved in studying them. Next, it lists currently available tools and techniques to acquire single cell data on various attributes of cancer cells. At that point the specific need for single cell data acquisition and analysis becomes evident. Finally, this chapter presents the specific dissertation aims. We believe a molecular understanding of oncogene induced signaling pathway alteration in single cell level will provide an improved rationale for personalized targeted therapeutics in lung cancer.

1.2 Oncogenes and tumor suppressor genes of Lung

Search for known oncogenes and tumor suppressor genes using molecular genotyping in the lung cancer patients is routinely used now to guide the personalized therapy. This is mainly due to the superior efficacy of targeted inhibitors - Erlotinib and Crizotinib as opposed to standard platinum doublet chemotherapy (Ahn et al., 2013; Brunetto et al., 2010; Hohenforst-Schmidt et al., 2013; Paramanathan et al., 2013; Pennell, 2012; Tamiya et al., 2010) for patients with EGFR mutations and ALK alterations respectively (Cataldo et al., 2011; Kwak et al., 2010). In addition to them, earlier studies using array-based profiling of copy number changes (Weir et al., 2007), targeted sequencing of candidate protein-coding genes (Ding et al., 2008) and whole genome sequencing of a single tumor/normal pair (Ju et al., 2012) identified a list of significantly mutated genes in lung adenocarcinoma.

The recent report on comprehensive molecular profiling of lung adenocarcinoma by The Cancer Genome Atlas Research Network (TCGA (2014)) from the analysis of 412 tumor and matched normal tissue pairs reported several statistically significant mutated genes (Figure 1.1). As expected, P53 was most commonly mutated (46%) among all tumor suppressor genes. The other common tumor suppressors were STK11 (17%), KEAP1 (17%), NF1 (11%), RB1 (4%) and CDKN2A (4%). Among common oncogenes, KRAS (33%) and EGFR (14%) mutations were mutually exclusive. However, while KRAS mutations were significantly higher in transversion-high cohort, EGFR mutations were significantly enriched in transversion-low group. BRAF (10%), PIK3CA (7%), MET (7%),

RIT1 (2%) were other commonly mutated oncogenes. Previously identified ALK fusion occurred in transversion-low tumors. Among different Myc alterations, c-Myc amplification is the most common occurrence in lung cancer (20%)(Albihn et al., 2010).

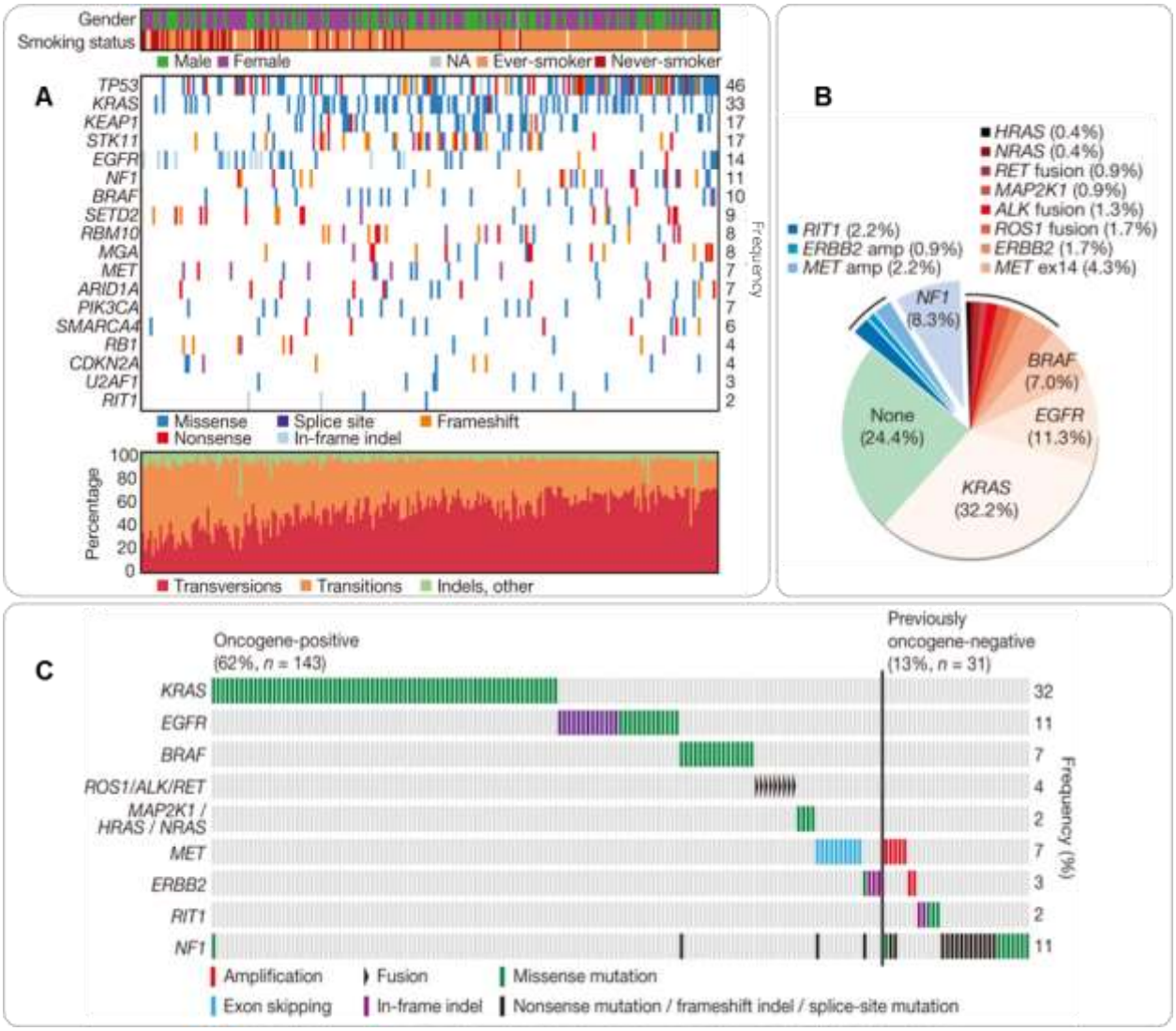

Figure 1.1 Molecular profiling of 230 lung adenocarcinoma (acquired and modified from TCGA (2014)). A) Co-mutation plot from whole exom sequencing. B) Known somatically activated driver oncogenic events (red, 63% of cases) and newly identified candidate driver oncogenes (blue, 13% of cases) associated with RTK/RAS/RAF pathways. C) Co-mutation plot of variants of known significance within RTK/RAS/RAF

pathways showing patterns of mutual exclusion. Many of these genetic alterations cannot be exploited therapeutically.

In addition, smokers and never-smokers exhibit substantial differences in mutational burden, spectrum and affected genes (Govindan et al., 2012). Smokers constitute 85% of the total lung cancer cases. In general, smokers show ten times the number of point mutations than never smokers. The occurrence of both P53 and KRAS mutations are significantly higher in smokers (Larsen and Minna, 2011). Although, various sequencing and mutational assay identifies the number of occurrence of the above mentioned common genetic alterations, unfortunately, many of these alterations are difficult to exploit therapeutically (Imielinski et al., 2012).

1.3 Signaling Pathways as Biomarker for Targeted Therapy

The term “targeted therapy” may be applied to all cancer treatments, including conventional cytotoxic chemotherapy which targets DNA replication or mitotic microtubules. But, in general clinical usage, “targeted therapy” refers to two types of treatments - monoclonal antibodies and small-molecule Tyrosine kinase inhibitors (Larsen et al., 2011). A molecular target should be uniquely altered (overexpressed or mutated) in cancer cells compared to the normal cells so that a therapy against that target kills the cancer cells and not the normal cells, achieving a broad therapeutic window i.e. a promising efficacy-to-toxicity profile.

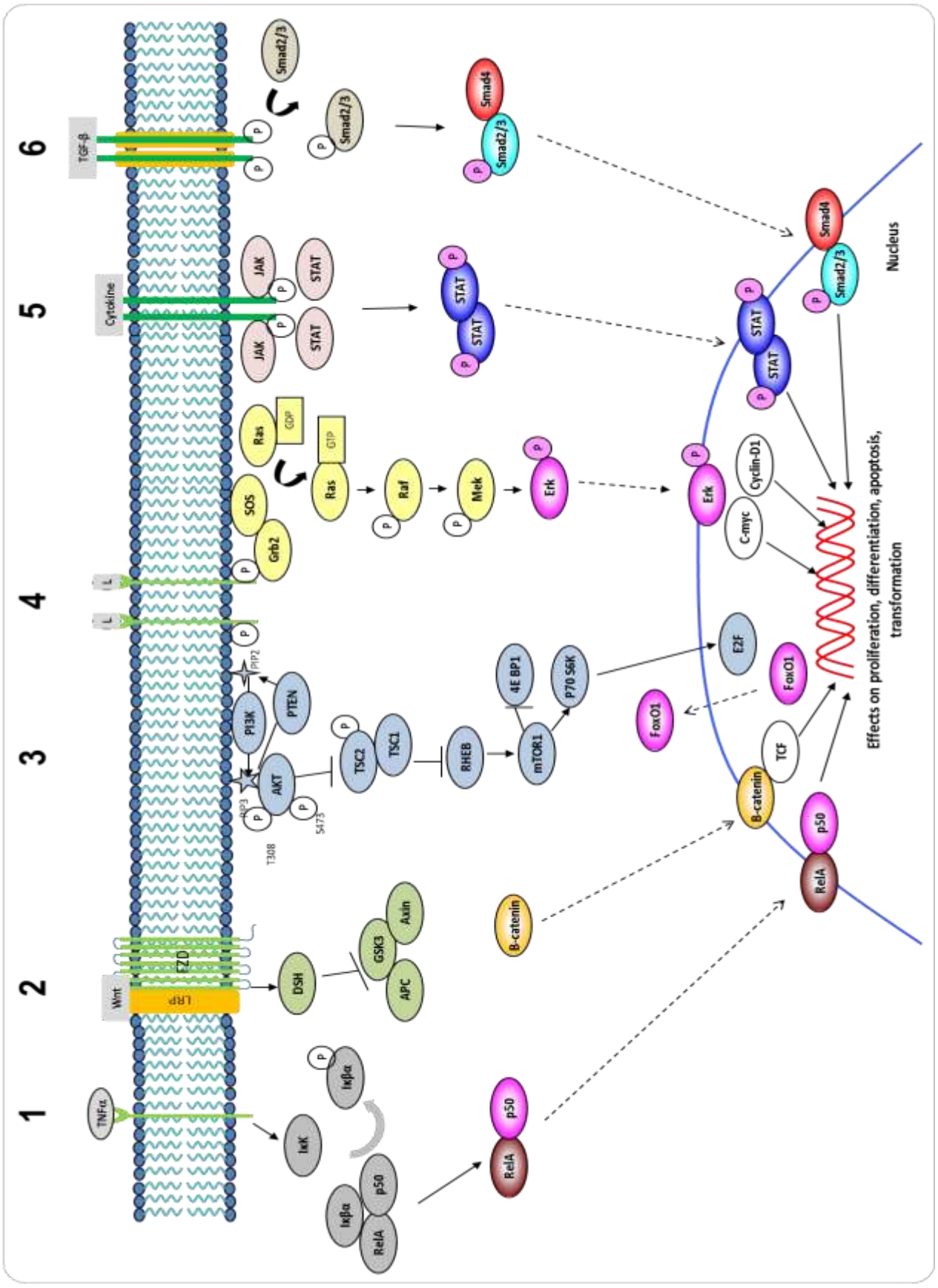
1
2
3
4
5
6
TNFα
IκK
IκBα
p50
RelA
Wnt
LRP
EZD
DSH
GSK3
Axin
APC
β-catenin
PI3K
PTEN
PIP2
PIP3
AKT
T308
S473
TSC2
TSC1
RHEB
mTOR1
4E BP1
P70 S6K
E2F
FoxO1
TCF
β-catenin
p50
RelA
TGF-β
Smad2/3
Smad4
Cytokine
JAK
STAT
Ras
GDP
GTP
SOS
Grb2
Raf
Mek
Erk
C-myc
Cyclin-D1
Nucleus
Effects on proliferation, differentiation, apoptosis, transformation

Figure 1.2 Signaling readouts in various pathways in lung cancer (simplified diagram of canonical signaling, cross talks are not shown) that change their cellular location upon pathway activation. 1) TNFα pathway: NFκβ/RelA/P65 is bound and inhibited by IκB. Proinflammatory cytokines such as TNFα activates the IKK complex which phosphorylates IkB. This leads to ubiquitination and proteosomal degradation of IκB freeing P65/P50 heterodimer which can translocate to nucleus. 2) WNT pathway: Binding of WNT ligand to Frizzled receptor causes displacement of GSK3β from the APC/Axin/GSK3b complex freeing β-catenin to translocate to nucleus. 3) PI3K/AKT/mTOR pathway: One of the major receptor tyrosine kinase (RTK) pathways is activated by various ligands, which is activated via PI3K. PI3K phosphorylates PIP2 to PIP3 which binds to AKT to position it in the membrane which can be phosphorylated. This inactivates TSC2 to prevent inhibition of mTORC1. The activity of AKT pathway causes FOXO1 to translocate from nucleus to cytoplasm. 4) RAS/RAF/MEK/ERK pathway: Another important RTK pathway known as MAPK pathway. This pathway involves stepwise phosphorylation of RAS, RAF, MEK and ERK. Phosphorylated ERK1/2 translocates to nucleus. 5) JAK/STAT pathway: Binding of cytokines such as IL-6 causes phosphorylation of STAT which homo-dimerizes and transloactes to nucleus. 6) TGFb pathway: Binding of TGFβ ligand to its receptor causes phosphorylation of Smad2/3 which dimerizes with Smad4 and translocate to nucleus. These signaling pathways are affected by the oncogenic events and can be exploited therapeutically.

Oncogenic activation and loss of tumor suppressor genes in cancer cells may be potential therapeutic targets. But, because of multiple complexities involved in the long drug development pipeline (Phougat et al., 2014), sometime we do not end up with specific drugs to target them (not “clinically actionable”). In that scenario, downstream signaling dysregulation may act as potential targets. It has been shown that somatic mutations in primary lung adenocarcinoma for several tumor suppressor genes affect key signaling pathways (Ding et al., 2008). Figure 1.2 describes common signaling pathways in lung cancer and Table 1.1 lists respective targeted therapies for them

approved by Food and Drug Administration (FDA) or in clinical trials. Hence, understanding the very nature of alteration in these downstream signaling pathways induced by oncogenes may guide us towards specific targeted therapy.

However, the choice of readouts to study dysregulated signaling is tricky. Signaling pathways comprise of multiple components. Which component in the pathway can capture maximum amount of useful information (or alteration in this case)? Given enough time and manpower (or brainpower), we can study multiple components of multiple signaling pathways in multiple stages of lung cancer progression. However, when we are interested in understanding signaling alteration in single cell level, the problem becomes too complicated with multiple hypotheses. Hence, in the current work, we have made couple of “supervised” choices while selecting the signaling readouts (described in section 3.2).

1.4 The Intra-tumor Heterogeneity Problem

Heterogeneity within the cell phenotypes of the same tumor has been noticed for a long time. In nineteenth century, Virchow, the father of modern pathology, observed the pleomorphism of cancer cells within tumors (Brown and Fee, 2006). Later, in mid-twentieth century, studies of genetic and functional heterogeneity were carried out in animal models by assaying cytogenetic profiles and tumorigenicity in single cell level (Makino, 1956). Next came the studies of Fildler, Kripke and their colleagues on existence of distinct subpopulations of cancer cells within tumors varying in

tumorigenicity, metastatic potential and treatment resistance (Fidler, 1978; Fidler and Kripke, 1977; Heppner and Miller, 1983). The term “intra-tumor heterogeneity” was coined during this time. Moreover, clinical investigators recognized that the inter-tumor variability in biomarkers could assist in making personalized treatment decisions. But, intra-tumor variability of the same biomarker challenges the treatment outcome in patients (Hawkins et al., 1980).

With the advent of new technologies, characterization of intra-tumor heterogeneity became clearer than ever. In recent years, three studies on three types of cancer, renal carcinoma (Gerlinger et al., 2012), glioblastoma (Sottoriva et al., 2013) and endometrial cancer (Supernat et al., 2014) have taken similar approach - multiple biopsies from a single patient tumor were collected and genomic and proteomic studies were carried out on them. When the first two studies clearly depicted presence of intra-tumor heterogeneity and pointed towards Darwinian evolution of tumor cells and associated therapeutic consequences, the third study took it further by showing the degree of intra-tumor heterogeneity itself could serve as a clinically valid molecular marker.

1.4.1 Layers of heterogeneity

The multistep tumor initiation and progression involves certain biological capabilities known as the hallmarks of cancer which distinguish tumors from normal tissue (Hanahan and Weinberg, 2011). They include – sustaining proliferative signaling, evading growth suppressors, avoiding immune destruction, enabling replicative

immortality, tumor-promoting inflammation, activating invasion and metastasis, inducing angiogenesis, genome instability and mutation, resisting cell death and, deregulating cellular energetics. Individual cells within a given tumor may display considerable amount of variability in these traits (Figure 1.3). Additionally, the degree of variability in each of these traits may be different (Almendro et al., 2013). The presence of one dominating subclone in primary vs metastatic tumor will give rise to regional heterogeneity. But, a more complicated scenario involves presence of multiple subclones in varying proportions, intermingled in a tumor giving rise to a mosaiform structure.

One approach to study this multi-faceted problem is – “divide and conquer”. If a simpler cancer model system can be created to incorporate only few of the hallmarks of cancer, the induced heterogeneity may have reduced range as opposed to that in a fully malignant cancer situation. This simple model system would be easy to perturb and useful to study the heterogeneity in few hallmarks in isolation. Later this model can be further developed to incorporate other hallmarks. The current study used the oncogenic progression model developed in John Minna laboratory (described in section 3.1). The input in the model system (immortalized human bronchial epithelial cells) was successive introduction of most common lung oncogenes. The output that we have measured in single cell level was signaling alteration.

Figure 1.3 Intra tumor heterogeneity in hallmarks of cancer (acquired and modified from Hanahan, Weinberg(Hanahan and Weinberg, 2011) and Almendro *et. al.(Almendro et al., 2013)*). Late stage tumors may exhibit varying degree of diversity from cell to cell in each of these ten distinct biological properties simultaneously. Interestingly, early stage tumors may possess reduced range of heterogeneity. Hence, simple isogenic cell line model systems can be utilized to study the effect of altering one hallmark on others, e.g. effect of defined genetic alterations on signaling pathways in a controlled system.

1.4.2 Available tools and techniques to study heterogeneity

As the importance and need for single cell data in cancer biology was realized, significant advances were made in developing new tools and techniques. Now a days, both gene and protein expression data can be acquired in single cell level. We will discuss some of these exciting techniques below.

Fluidigm Corporation, CA, has come up with a microfluidic system that isolates up to 96 single cells, enables imaging of these isolated cells for consideration of varying sizes, and finally profiles expression of up to 96 genes in each cell within few hours. Combining this technique with SMART-seq (Ramskold et al., 2012), a recent study reported dynamic paracrine control of cellular variation (Shalek et al., 2014).

Matrix-assisted laser desorption/ionization mass spectrometry imaging, also known as MALDI imaging, allows spatial distribution of antibodies across tumor tissue sections. The advantage of this method – it does not require specific antibodies. Some of the available methods for single cell analysis in combination with MALDI involve – microinjection of matrix onto the cell of interest *in situ*, micro and induction- based-fluidics, laser capture micro-dissection of individual cells, ordered stretching of tissue and laser oversampling (Boggio et al., 2011).

Flow cytometry offers the ability to quantify simultaneously the abundance and modification of large number of proteins. When combined with immunophenotyping and

multifactorial statistical modeling, a recent study on B-cell receptor mediated signaling revealed proximal activation defect in chronic lymphocytic leukemia (Palomba et al., 2014). The limited number of precise measurements due to spectral spillover in flow cytometry can be addressed by combining them with mass spectrometry (Cotari et al., 2013).

CyTOF system (Fluidigm Corporation, CA) uses a time-of-flight inductively coupled plasma mass spectrometry to detect dozens of markers simultaneously. This technique can be described as variation of flow cytometry where antibodies are labelled with heavy metal ion tags instead of fluorochromes. A recent study has combined CyTOF mass cytometry with immunocytochemistry and immunohistochemistry techniques, to image 32 proteins and their modifications simultaneously at a cellular resolution of 1 μm (Giesen et al., 2014) in breast cancer tissue samples.

There are advantages and shortcoming of each of the above described approaches. However, standardization of large panels of antibodies and combination of these techniques with each other can generate astonishing amount of single cell data with high confidence.

1.4.3 Need for new analytical measures

With the availability of large amount of single cell data, the next obvious step becomes – data analysis. Altschuler and Wu laboratory has pioneered in high-throughput

immunofluorescence data acquisition and analysis. By adapting facial recognition software, earlier study has found distinct phenotypes of cells from immunofluorescence images (Slack et al., 2008). The same approach was utilized to classify populations of cells after their perturbation by a panel of drugs and finally to predict the mechanism of action of new drugs. Later, single cell imaging of basal signaling states of H460 clones and further analysis of distinct subpopulations of cells provided prediction on their paclitaxel sensitivity supporting the idea that signaling heterogeneity may have functional significance (Singh et al., 2010). However, at that point there was no intrinsic definition of each subpopulation. Moreover, for a given signaling readout, signaling activity was not clearly understood. In this work, we have tried to address some of these questions by combining the diverse expertise of Altschuler and Wu laboratory and John Minna laboratory.

1.5 Dissertation aims

This chapter tries to give an idea of the complexity associated with the studies on oncogenes and signaling pathways in lung cancer. The focus, specifically, has been lack of – a) tools and techniques to measure signaling diversity at single cell level, and, b) understanding of downstream signaling pathways of oncogenes and tumor suppressors during lung cancer progression. Additionally, the increase in complexity with measurements at single cell level is stated. In this dissertation, we present studies of oncogene induced signaling alterations on cell line models of lung cancer progression where we demonstrate distinct rewiring of certain signaling pathways.

In chapter 2, we establish rigorous, quantitative methods for studying signaling diversity from fluorescence microscopy images. Although diversity at single cell level is reported in many literatures, there has been lack of reliable quantitative measures using the level of signaling marker expression. We address this problem in a context specific way and establish three quantitative measures of signaling diversity. We apply our measures on a panel of twelve lung cancer cell lines which are representatives of various types of lung cancer and classify them based on their diversity profile.

In chapter 3, we make use of an isogenic cell line model of early stage lung oncogenic progression to study the signaling diversity in seven signaling readouts. As the word “heterogeneity” is relative and could only be understood from a reference, we use immortalized cell line without any oncogenic manipulations as a measure for baseline signaling activity. In addition, to address the lack of intrinsic meaning of cellular subpopulations, we define three subpopulations, based on their signaling activity as comparted to the baseline signaling. Here we identify combined effect of oncogenic manipulation in altering downstream signaling maximally and yet transiently. In particular, we identify that oncogenes distinctly rewire Smad2/3 signaling so that it gets insulated from chronic exposures to environmental stimuli. Finally, we identify interesting targetable vulnerabilities for oncogene induced signaling heterogeneity.

In chapter 4, we recapitulate studies on these targetable vulnerabilities in other types of cancer. In addition, using a small number of lung cancer cell lines, we show that these targets when druggable can be utilized as therapeutic vulnerabilities in a subset of lung cancers.

Pathway	**Target component**	**Drugs**
WNT	Frizzled	OMP-18R5
		OMP-54F28
	Disheveled	3289-8625
		FJ9
		NSC 668036
	Wnt	LGK974
		IWP-2
	Tankyrase	IWR-1
		XAV939
	CK1a	Pyrvinium
	b-catenin	PFK 115-584
		CGP049090
		iCRT3
		iCRT5
		iCRT14
	CBP	ICG-001
		PRI-724
		Retinoids
		Vitamin D3
TGFb	TGFb	STX-100
		LSKL
		Lerdelimunab
		Metelimunab
		Fresolimunab
		1D11

		LY2382770
	TGFbR	SR2F
		P144
		P17
		IMC-TR1
		IMC-MT1
		LY580276
		LY2109761
		LY2157299
		SB-505124
		SD-208
		Ki26894
		GW788388
		SM16
	Smad2/3 binding	TRX-FOXH1B
		TRX-LEF
RAS/RAF/MEK/ERK	RAS	Lonafernib
		Tipifarnib
		ISIS 2503
	RAF	GSK2118436
		Regorafenib
		Sorafenib
		AZ628
		ISIS 5132
		XL281
	MEK	GSK1120212
		PD325901

		Selumetinib
		Sorafenib
		AS 703026
		AZD8330
		GDC0973
		RDEA119
PI3K/AKT/mTOR	PI3K	BKM120
		GDC0941
		PX866
		XL147
		XL765
		BEZ235
		BGT226
		LY294002
	AKT	Nelfinavir
		MK2206
		Perifosine
	mTOR	Everolimus
		PX866
		Ridaforolimus
		Rapamycin
		Temsirolimus
		AZD8055
		BEZ235
		OSI027
JAK/STAT	JAK	Tofacitinib
		Ruxolitinib

		LY2784544
		AZD1480
		Cyt387
	STAT3	NSC74859
	STAT1	Fludarabine
TNFa	IKK	BX795

Table 1.1 Consolidated list of targeted therapy for various components of signaling in WNT (Kahn, 2014), JAK/STAT , TGFβ (Akhurst and Hata, 2012), TNFα , AKT(Larsen et al., 2011) , IFNγ , MAPK(Larsen et al., 2011) pathways.

Measures of Signaling Diversity at Single Cell Level

2.1 Introduction

In general laboratory practice, plate-to-plate, day-to-day or batch-to-batch variability is characterized by the Z factor (Zhang et al., 1999). The Z factor reflects both the assay signal dynamic range and the data variation associated with the signal measurements. To achieve further probabilistic interpretation, strictly standardized mean difference (SSMD) and coefficient of variability in difference (CVD) were created (Zhang, 2007). However, similar effort towards quantifying the variability or diversity in phenotype states for single cell analysis has not been taken extensively.

Earlier work in Altschuler and Wu laboratory has developed techniques to profile the cellular subpopulations (Loo et al., 2009). In this approach, based on an enhanced collection of phenotypic features extracted from a subset of markers, a classifier was trained to identify subpopulations. Next, in a step-wise method, subpopulation profiles were constructed using replicate experiments where the cells were further stained with some overlapping and different marker sets. In this way, a virtual subpopulation profiling was created for many markers to overcome the obstacle of being able to image only three or four markers correctly at a time.

There are other noteworthy approaches as well. A hybrid approach between single-cell and mixture-based stochastic sampling model was developed that applied probability theory to transcriptome-wide measurements. This method, further combined with maximum-likelihood estimation, provided single cell quantification of each regulatory state (Bajikar et al., 2014). In a separate study, quantification of heterogeneous

populations was achieved by using parallel-coordinates plots to obtain a qualitative understanding of the system and support vector machines to assess the performance of marker combinations (Hasenauer et al., 2012).

Although these analytical techniques to quantify heterogeneity proved to be valuable in various applications such as, drug discovery, pathway analysis and diagnostics, not until very recently, a set of indices were developed to identify, quantify and characterize the heterogeneity for inclusion in many screening and cellular profiling techniques (Gough et al., 2014). This study used four statistical measures for heterogeneity analysis – coefficient of variation, interquartile range, quadratic entropy and Kolmogorov-Smirnov distance. Using a binary decision tree it classified Stat3 signaling distribution into one of the following classes – homogeneous, micro-heterogeneous, macro-heterogeneous and each of these three classes with outliers. In this study, “homogenous” was a relative term as all the cell populations always exhibited “some heterogeneity”.

In this chapter, we describe our approach of understanding heterogeneity of several signaling markers in a panel of lung cancer cells as compared to those in immortalized normal cells developed in John Minna laboratory, hence, providing a “baseline” above which we considered the heterogeneity made a difference (Altschuler and Wu, 2010) in lung cancer. Specifically, we have made use of the high throughput and high content immunofluorescence image and analysis platform developed in the Altschuler and Wu laboratory. We also used three statistical measures for quantifying the signaling heterogeneity.

2.2 Fluorescence microscopy images to measure signaling

The advantage of immunofluorescence imaging lies in the visualization of the cellular localization of stained signaling readout. In traditional population average techniques like Western blot, both total and phosphor proteins need to be analyzed. However, in this case by measuring the amount of nuclear to cytoplasmic ratio of a given signaling marker we could calculate the activity of the corresponding signaling pathway. Figure 2.1 shows the pipeline of immunofluorescence staining and imaging used in our current study.

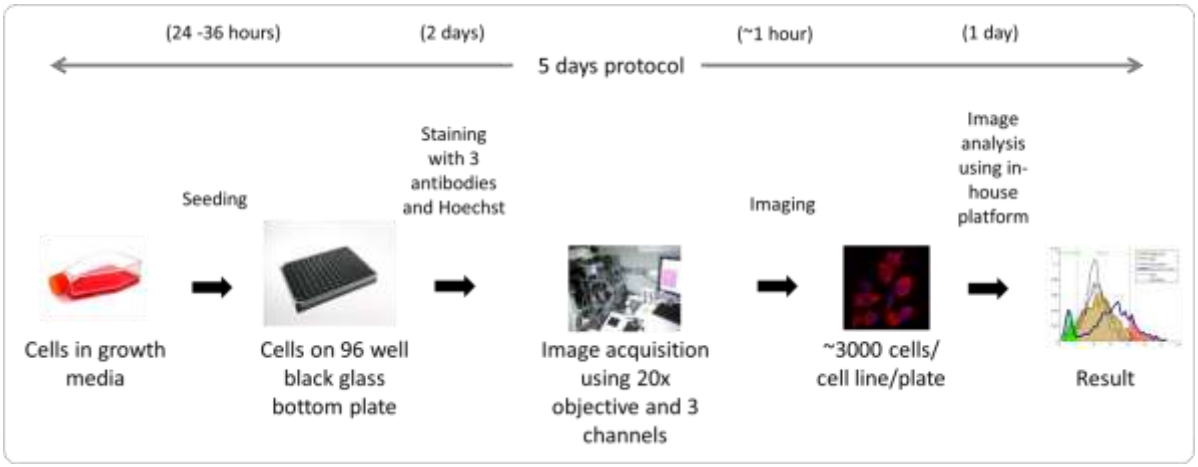

Figure 2.1 Pipeline for high throughput, high content image acquisition and analysis platform. The timeline, number of cells in each experiment etc are optimized for our specific experimental setup.

2.3 Image analysis to understand signaling diversity

There are multiple steps involved in the image analysis pipeline (Figure 2.2). After we acquire large number of immunofluorescence images, we process the images for background subtraction, segmentation (finding boundary of each cell and their nuclei) followed by manual quality control to discard signaling artifacts as described below. The

next step is – intensity feature extraction. Altschuler and Wu laboratory has developed a method to isolate multiple intensity features comprising of nuclear and cytoplasmic amount of each signaling marker, their pixel based localization, intensity and ratio of different markers at different cellular locations. Finally, we make use of some of the biologically meaningful features in a context specific way to identify the signaling alteration in single cells.

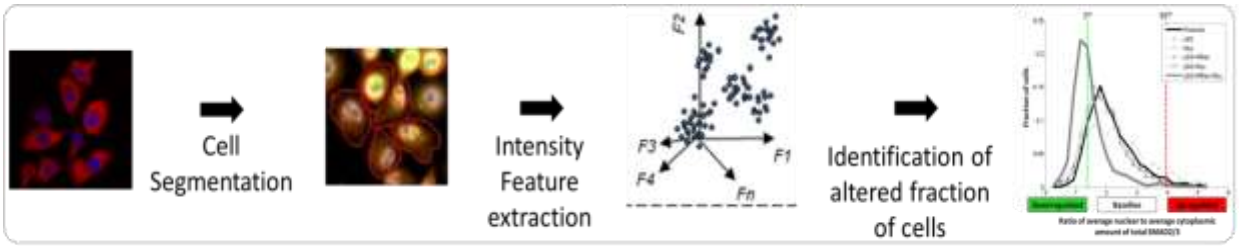

Figure 2.2 Pipeline for immunofluorescence image analysis. The main steps are background subtraction (not shown in figure), cell segmentation, intensity feature extraction and identification of altered fraction of cells.

2.3.1 Image processing

All fluorescence images were acquired using a TE-2000 epifluorescence microscope (Nikon) equipped with integrated Perfect-Focus System (PFS), Nikon Plan Apochromat 20x objective lens and Photometrics CoolSNAP HQ camera. Image acquisition was controlled by NIS-Elements software (Nikon). Image background correction was done using the National Institute of Health ImageJ rolling-ball background subtraction plug-in (Rasband et al., 1997-2009). Cellular regions were determined using a watershed-based segmentation algorithm (Loo et al., 2007) which first retrieves nuclear regions using DNA staining then combines multiple cytosolic region markers to identify cellular boundaries. Images were visually inspected, and images with severe focus, staining, or

cell-segmentation artifacts were discarded. We identified ~3,000 cellular regions per marker/well after applying automated cell segmentation to our image data.

2.3.2 Quality control

We manually inspected all fluorescence images and discarded those presenting obvious anomalies (e.g. focus issues and abnormal fluorescence staining). Next, images with poorly segmented cells were re-segmented with manually optimized segmentation parameters. Finally, frames containing poorly segmented cells were discarded.

2.4 Three measures of signaling diversity

2.4.1 Entropy

To measure the uncertainty of the signaling in lung cancer cell lines, we have taken an information theoretical measure.

$$Signaling\ diversity = -\sum_{i=1}^{n} Pi\ \log(Pi)$$

Where *i* is the number of signaling states (in our case, we define 3 states – baseline, upregulated and downregulated in parental HBEC) and *pi* is the probability of a cell to belong to a i^{th} signaling state.

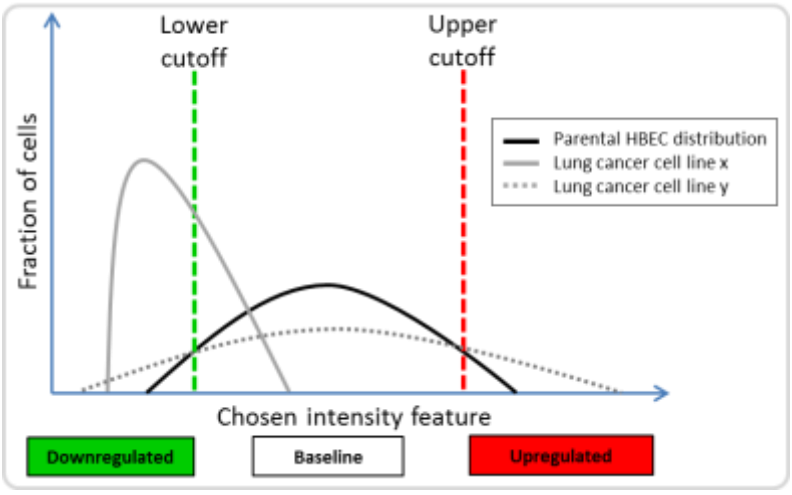

Figure 2.3 Measure of heterogeneity: Entropy. First the probability for each cell in a cell line is calculated for belonging to any of the three signaling states- baseline, downregulated and upregulated. This probability is correlated to the total number of cells in each signaling state. The entropy for the parental line always remains the same as we define three signaling states based on parental distribution.

2.4.2 Volume

To measure the deviation of the cells in the manipulated HBECs from those in the parental HBEC, we have measured the smallest volume that encloses 90% of cells in the intensity feature space. 10% cells are considered as outliers (Figure 2.3).

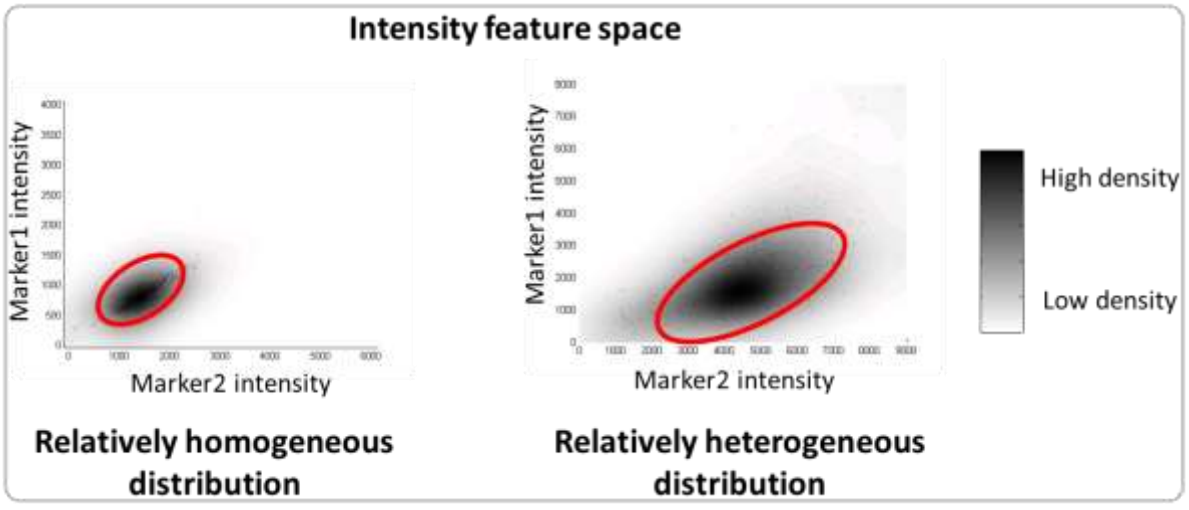

Figure 2.4 Measure of heterogeneity: Smallest volume in intensity feature space that encloses 90% cells. In the cartoon figure, the red ellipses represent the 90% volume.

2.4.3 Coefficient of variation

To measure the extent of signaling diversity in relation to mean signaling alteration in the population of manipulated cells we have quantified the coefficient of variation (*CV*) as –

$$CV = \frac{\sigma}{\mu}$$

Where σ is the standard deviation of log of chosen intensity feature and μ is the population average of all the cells in each well of the 96 well plate. The value of the intensity feature may range from 0 to 1, when average nuclear intensity is from smaller than to equal to average cytoplasmic intensity. On the other hand, this value may range from 1 to infinity, when average nuclear intensity is from larger than to equal to average cytoplasmic intensity. To take care of this asymmetry we used log transform of the raw intensity feature value.

2.5 Measuring reproducibility of signaling diversity

We have tested the reproducibility of our assay on signaling diversity using batch replicates (same cell line from different batch with varying number of splitting and freezing cycles in tissue culture), well replicates (during the same assay among various wells of the 96 well plate), plate replicates (among the results obtained from the same assay done at different time points in different 96 well plates). The standard deviation and P-value from two tailed student t test are summarized in the supplementary table x.

2.6 Signaling Diversity in a panel of Lung Cancer Lines

Lung cancer is considered a heterogeneous disease clinically, histologically, biologically and molecularly (Gazdar, 2010). There are approximately 200 lung cancer cell lines derived from patient tumors, established and maintained in John Minna laboratory. These cell lines harbor variety of mutations, copy number variations, methylation, acetylation etc. They also represent various histological subtypes of lung cancer, such as, adenocarcinoma, squamous cell carcinoma, large cell carcinoma, small cell lung cancer and carcinoids. In the current study we have selected a smaller subset of cell lines from those 200 lines representing various types of lung cancer.

2.6.1 Representative panel of lung cancer lines

The lung cancer cell lines in our study include A549, H2009, H1819, HCC4017, HCC366, H460, H1993, H2073, HCC827 and H2122.

Cell line	H1693	H1819	H1993	H2073	HCC827	HCC366	H2009	H2122	H460	A549
Tumor source	meta	meta	meta	primary	primary	primary	meta	meta	meta	primary
Anatomical site	Lymph node	Lymph node	Lymph node	lung	lung	lung	Lymph node	Pleural effusion	Pleural effusion	lung
Stage	3B	3	3A	3A	ND	ND	4	4	ND	ND
p53	MU	WT	MU	MU	MU	MU	MU	MU	WT	WT
KRas	WT	WT	WT	WT	WT	WT	MU	MU	MU	MU
Myc(DNA)	2	2.6	3	ND	8	ND	3	12	ND	ND

Table 2.1 A panel of lung cancer lines in our study with variety of tumor source, anatomical site, stage and most common genetic changes (p53, KRas and Myc).

2.6.2 Signaling readouts

An earlier study at Altschuler and Wu laboratory was conducted on general signaling markers most commonly related various biochemical signaling in cells(Singh et al.,

2010). To begin with, we have selected phosphorylated forms of Stat3 and Pten proteins from that list. Phospho-Stat3 (Y705) is expected to be localized in the nucleus to govern the expression of various genes involved in growth and development of healthy cells. However, it has been reported that many EMT transcription factors can be regulated by Stat3 (Wendt et al., 2014). On the other hand, phospho-Pten is known to be a master regulator of AKT pathway, in the vicinity of cellular membrane, converting PIP3 to PIP2. Despite the absence of a classical nuclear transport signal, Pten can be observed in the nucleus. Moreover, nuclear Pten may play role in cell cycle arrest, chromosome stability, and DNA repair (Planchon et al., 2008). Hence, variability in nuclear and cytoplasmic amount of these phospho proteins may point towards the underlying signaling alterations in lung cancer cell lines.

From the immunofluorescence images, we observed various signaling phenotypes of phospho-Stat3 and phospho-Pten within and among each lung cancer lines. As a point of reference we utilized immortalized human bronchial epithelial cells (parental HBEC and its triple manipulated counterpart, described in detail in section 3.1).

Figure 2.5 A panel of lung cancer cell lines and 2 HBEC lines stained with antibodies against phospho-STAT3 (red) and phospho-PTEN (green) and Hoechst for DNA (blue). Only representative images are shown here. The panel shows considerable diversity in various signaling phenotypes within and among each tumor cell lines.

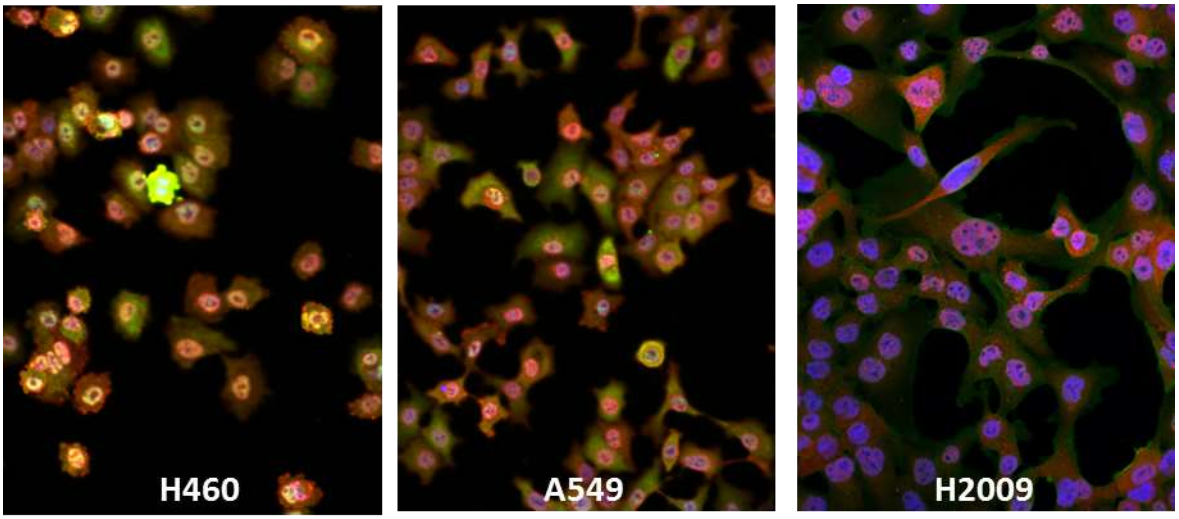

Interestingly, from the immunofluorescence images, we have observed more heterogeneity among the cancer cell lines than within each line (Figure 2.3). As we observed varying marker expression in single cell level we quantified the extent of heterogeneity using the techniques described in section 2.4

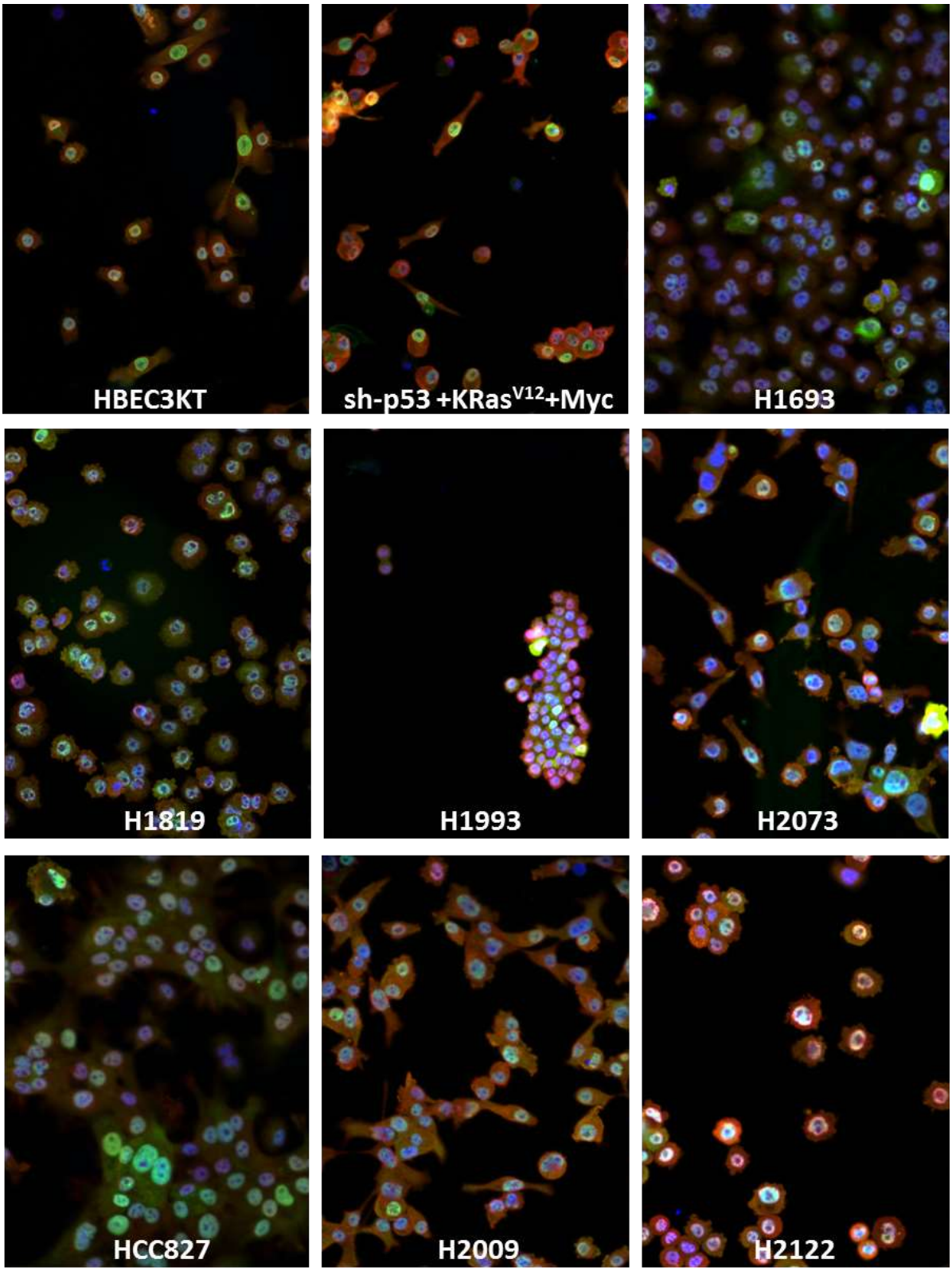
HBEC3KT
sh-p53 +KRas^{V12}+Myc
H1693
H1819
H1993
H2073
HCC827
H2009
H2122

Entropy

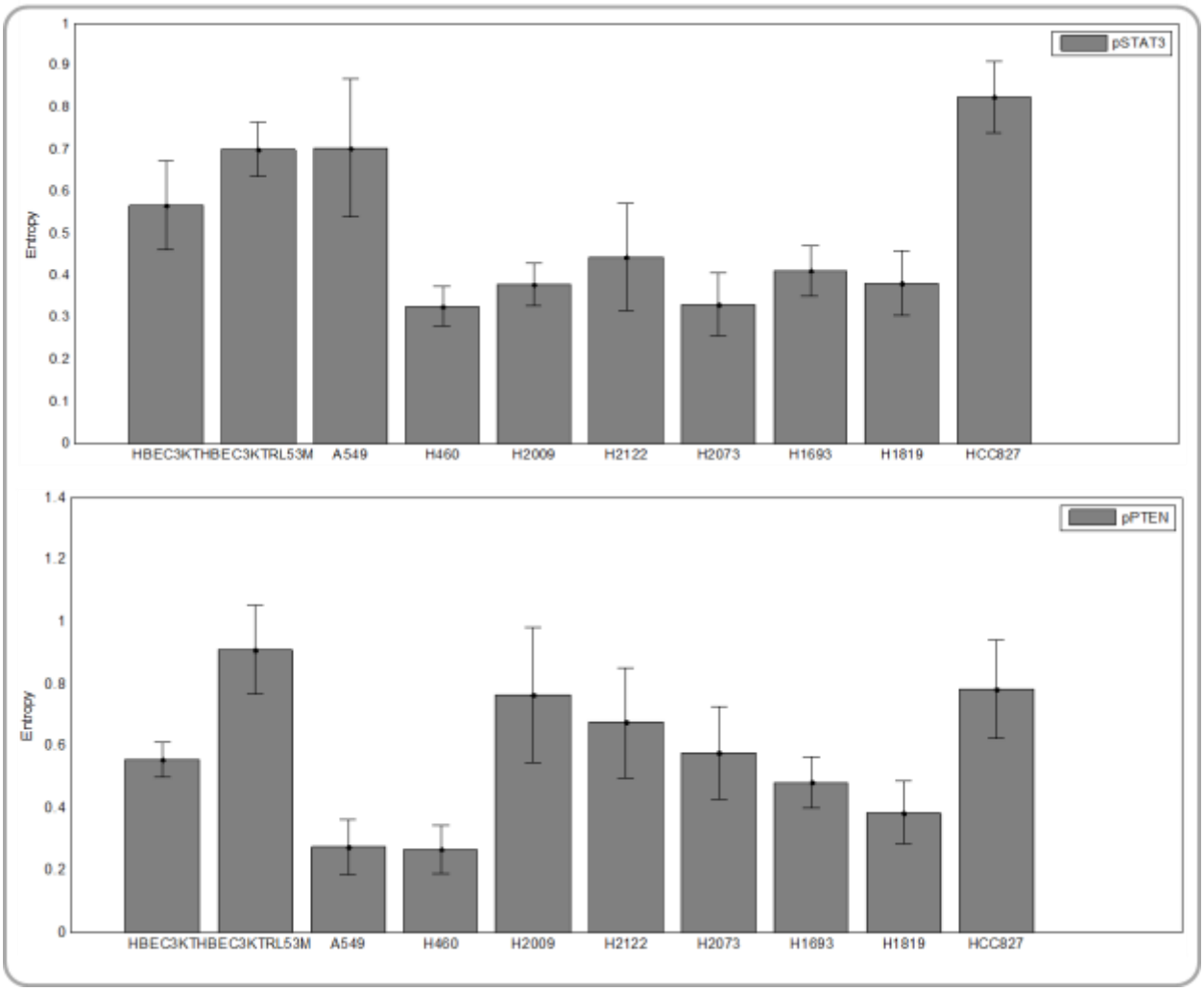

Figure 2.6 Normalized heterogeneity score using volume in intensity feature space. Lung cancer lines show varying level of heterogeneity.

Volume

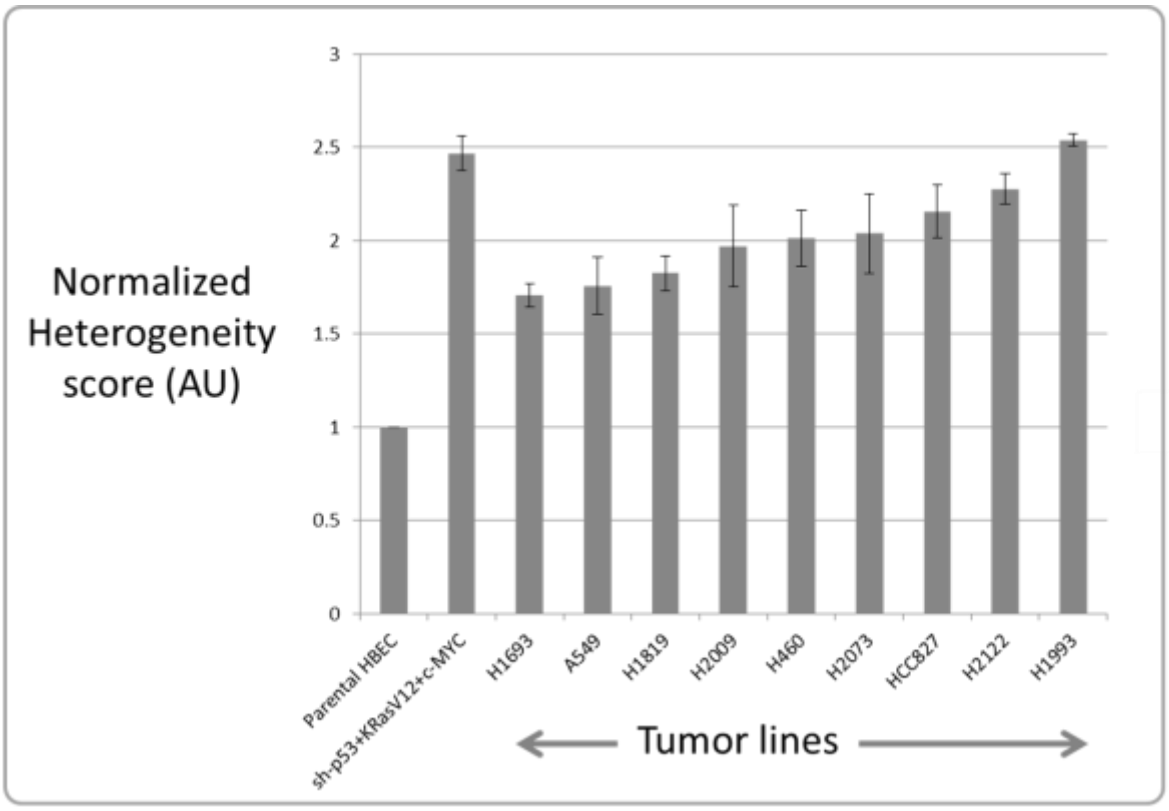

Figure 2.7 Normalized heterogeneity score using volume in intensity feature space. Lung cancer lines show more heterogeneity than normal immortalized HBEC. However, 3 oncogenic manipulations in HBEC increase its heterogeneity to the same level of that of NSCLCs.

Coefficient of variation

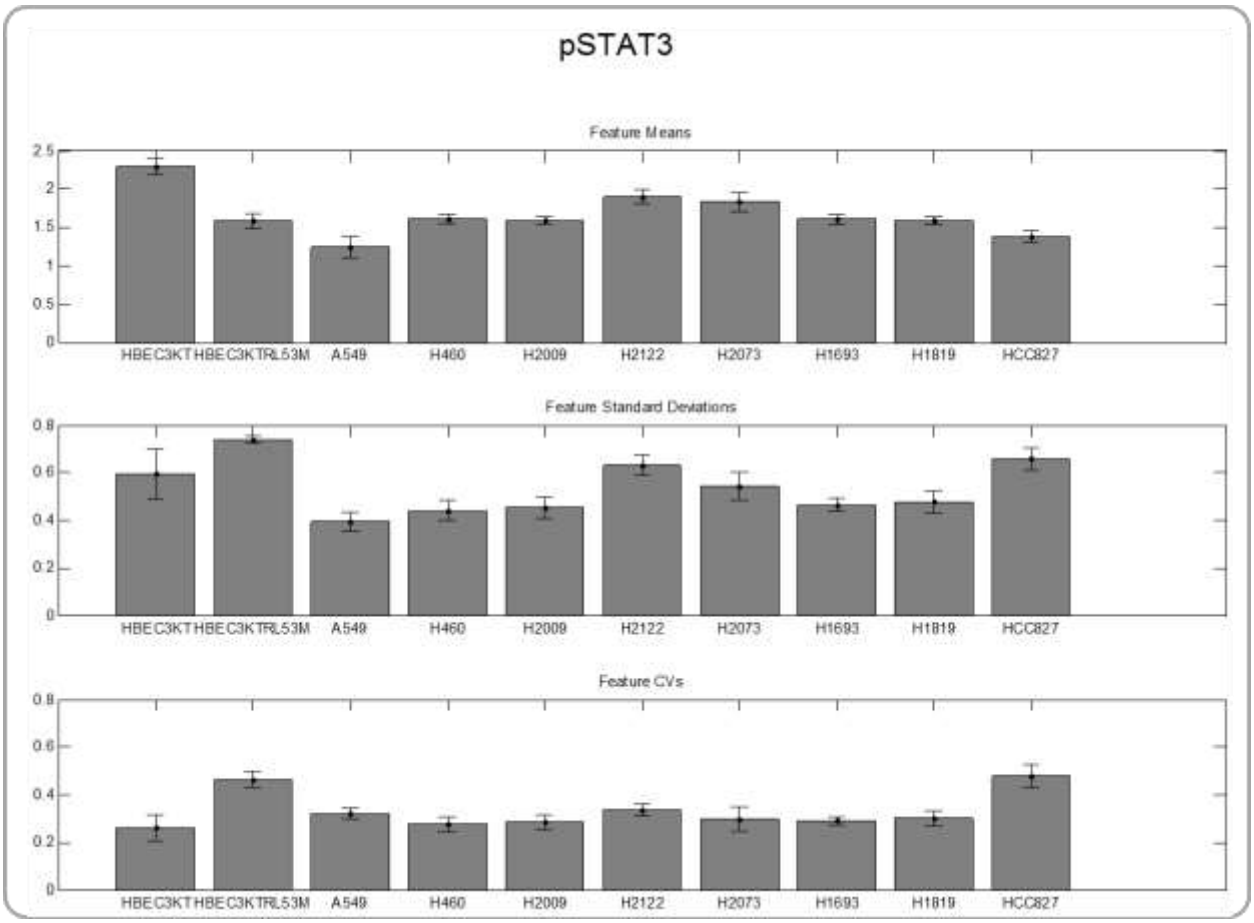

Figure 2.8 Normalized heterogeneity score using coefficient of variation in intensity feature space. Lung cancer lines show varying level of heterogeneity.

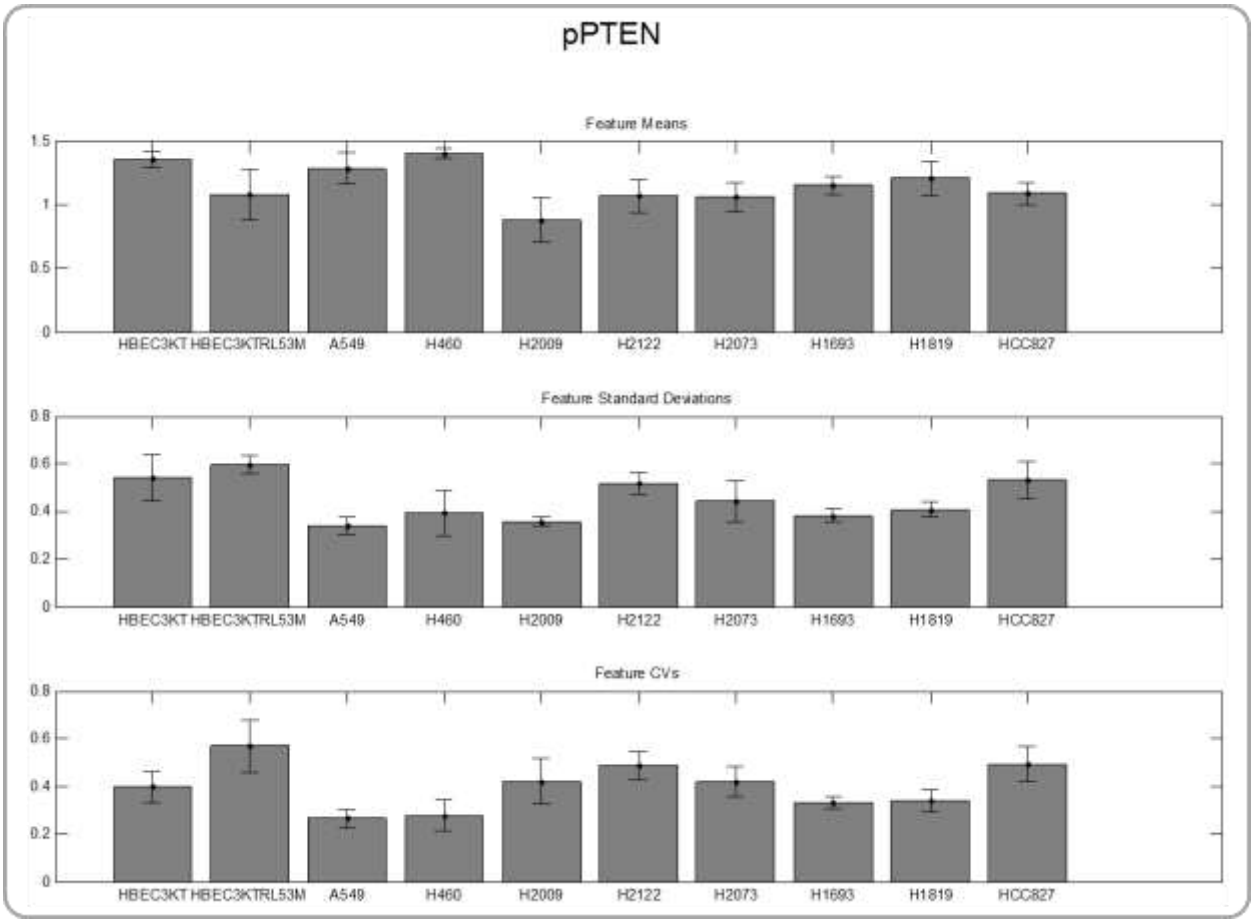

Figure 2.9 Normalized heterogeneity score using coefficient of variation in intensity feature space. Lung cancer lines show varying level of heterogeneity.

2.7 Discussion

In this chapter we have attempted to study the intra cellular signaling heterogeneity in a large panel of diverse types of lung cancer cell lines. We have looked into expression level of two signaling readouts previously studied in Altschuler and Wu laboratories. To objectively evaluate and quantify the cell-to-cell variation we used three analytical approaches. Interestingly, as each of these approaches captures specific properties of the signaling, all cell lines do not show the same level of heterogeneity compared

across all three measures. However, when studied carefully we can understand properties of specific subpopulations in these cell lines.

First, in general, for all the signaling markers, using all the three measures, triple manipulated HBECs show higher heterogeneity than the parental HBECs. In addition, the lung cancer line HCC827 show significantly higher heterogeneity in both phospho-Stat3 and phospho-Pten level than the parental HBECs.

Second, the panel of lung cancer lines shows varying range of heterogeneity. Using the 90% volume measure we show that the range of variations in all the lung cancer lines is higher than the parental HBEC when a two-dimensional feature space is considered with phospho-Stat3 and phospho-Pten. However, if the mean level of the marker is higher, they may have higher range of standard deviations. To make up for that we have used coefficient of variation measure. Using this measure we show that triple manipulated HBEC, H2122, A549 and HCC827 show higher heterogeneity in phospho-Stat3 level. But, for phospho-Pten level, A549 does not show higher heterogeneity than the parental HBEC. The entropy measure estimates the uncertainty of each cell belonging to an altered signaling state compared to the parental HBECs. Interestingly, using this measure only HCC827 showed higher heterogeneity than the parental HBECs. Our data suggests that the HCC827 cell line clearly contains the highest intra-cellular heterogeneity among our panel of lung cancer lines. Hence, future studies on correlation of functional studies and signaling heterogeneity on HCC827 will be interesting.

2.8 Methods

Cell lines and basal culture conditions

Normal and oncogenically manipulated immortalized Human Bronchial Epithelial Cells (HBECs) were cultured with Keratinocyte Serum Free Medium (KSFM; Life Technologies Inc., Carlsbad, CA) media containing 50 µg/mL of Bovine Pituitary Extract (BPE; Life Technologies Inc.) and 5 ng/mL of Epidermal Growth Factor (EGF; Life Technologies Inc.). Lung cancer cell lines, established in John Minna laboratory, were maintained in RPMI-1640 (Life Technologies Inc.) with 5% fetal bovine serum. All cell lines were DNA fingerprinted (PowerPlex 1.2 Kit, Promega, Madison, WI) and mycoplasma-free (e-Myco Kit, Boca Scientific, Boca Raton, FL).

Signaling readouts and immunofluorescence assay

Six signaling readouts were selected (Suppl. Table 3). Hoechst 33342 (Invitrogen Inc.) was used to identify nuclear regions. Cells were fixed with 4% paraformaldehyde for 5 minutes, permeabilized with ice cold 100% methanol at -20C for 10 minutes, washed with 0.1% TBST, blocked with 5% BSA solution in 0.1% TBST at room temperature for 30 minutes. 5% BSA in 0.1% TBST was used for primary and secondary antibody dilutions. Plates stained with primary antibodies were incubated at 4C overnight. They were washed with 0.1% TBST three times. Next, plates were incubated with secondary antibodies in the dark at room temperature for two hours and then washed again with TBST three times. After the final washing step, 100µl of TBST containing 0.1% sodium azide was added to each well.

Signaling Aberration in a Model of Lung Cancer Progression

3.1 Experimental model of lung oncogenic progression

To study the effect of most commonly occurring lung oncogenes on signaling alterations, we chose an *in vitro* model for our study. The isogenic series of immortalized human bronchial epithelial cells (HBECs) is one of the first reports of full malignant transformation of lung epithelial cells with defined genetic alterations (Sato et al., 2013). The series was created in John Minna laboratory by successive introduction of oncogenic manipulations to present various combinations of p53 null, oncogenic $KRAS^{V12}$, and C-MYC overexpression genotypes (Figure 3.1).

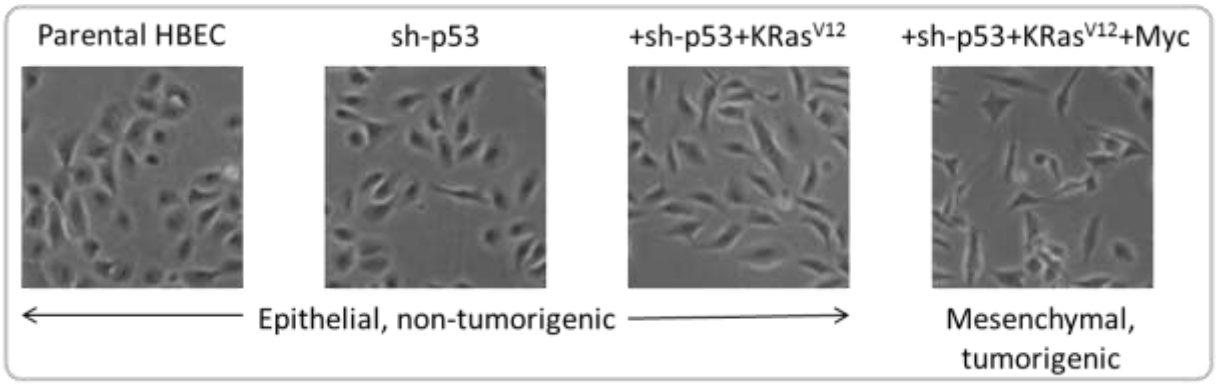

Figure 3.1 Successive oncogenic manipulations in HBECs. Brightfield images of four HBECs grown in culture. C-Myc overexpression in the background of p53 and KRas manipulations, introduces Epithelial to mesenchymal transition and tumorigenicity.

Loss of p53 function and oncogenic KRAS are two well-known genetic alterations in lung cancer occurring in approximately 50% and 30% of NSCLC, respectively (Larsen et al., 2011; Larsen and Minna, 2011). Aberrant expression of C-MYC, through amplification or over-expression, is found in approximately 20% of NSCLCs (Larsen et

al., 2011; Larsen and Minna, 2011). These genetic alterations are more common in smokers (~85% of total lung cancer) than non-smokers (~15%). While loss of p53 is believed to be an early event, oncogenic KRas mutation is considered relatively late events in lung cancer progression (Lubin et al., 1995). However, C-MYC amplification has been identified as a prognostic marker in early stage lung cancer (Iwakawa et al., 2011).

In reality, these genetic alterations can be heterogeneous at single-cell level (de Bruin et al., 2014; Gerlinger et al., 2012; Sottoriva et al., 2013; Zhang et al., 2014). To mimic this natural clinical situation we chose this "semi-controlled" system, where we control the type of oncogenic manipulations (p53, KRas and c-Myc) but we make use of the randomness of viral vector integration in the genome to create various levels of these genetic manipulations in single cells.

To evaluate the extent of genetic heterogeneity in the triple manipulated HBEC, we have studied the expression of P53, KRas and Myc genes in 20 single-cell clones of triple manipulated HBEC. The single-cell clones showed a range of expression for these oncogenes. For P53 all the single-cell clones of triple manipulated HBEC had lower expression than the parental HBEC3KT. For Myc, 18 out of 20 single-cell clones of triple manipulated HBEC had higher expression than the parental HBEC3KT. For KRas, 17 out of 20 single-cell clones of triple manipulated HBEC had higher expression than the parental HBEC3KT.

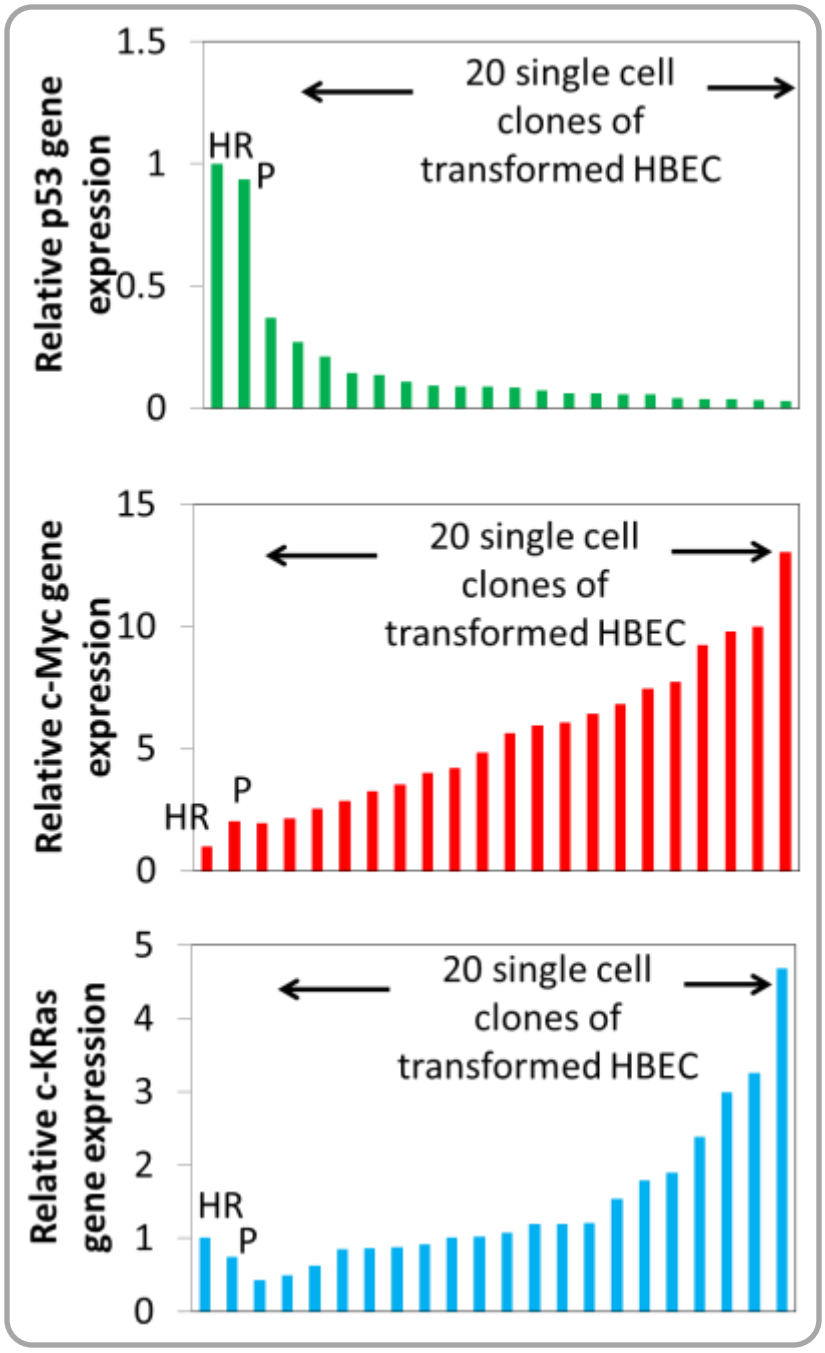

Figure 3.2 Single-cell clones of triple manipulated HBEC exhibit genetic heterogeneity. HR is human reference and P is parental HBEC3KT.

To quantify the heterogeneity of these manipulations in protein level we have made use of immunofluorescence image analysis of these single-cell clones. There was no

suitable KRas antibody for immunofluorescence image analysis. However, for P53 and C-Myc proteins we have observed considerable heterogeneity (Figure 3.3).

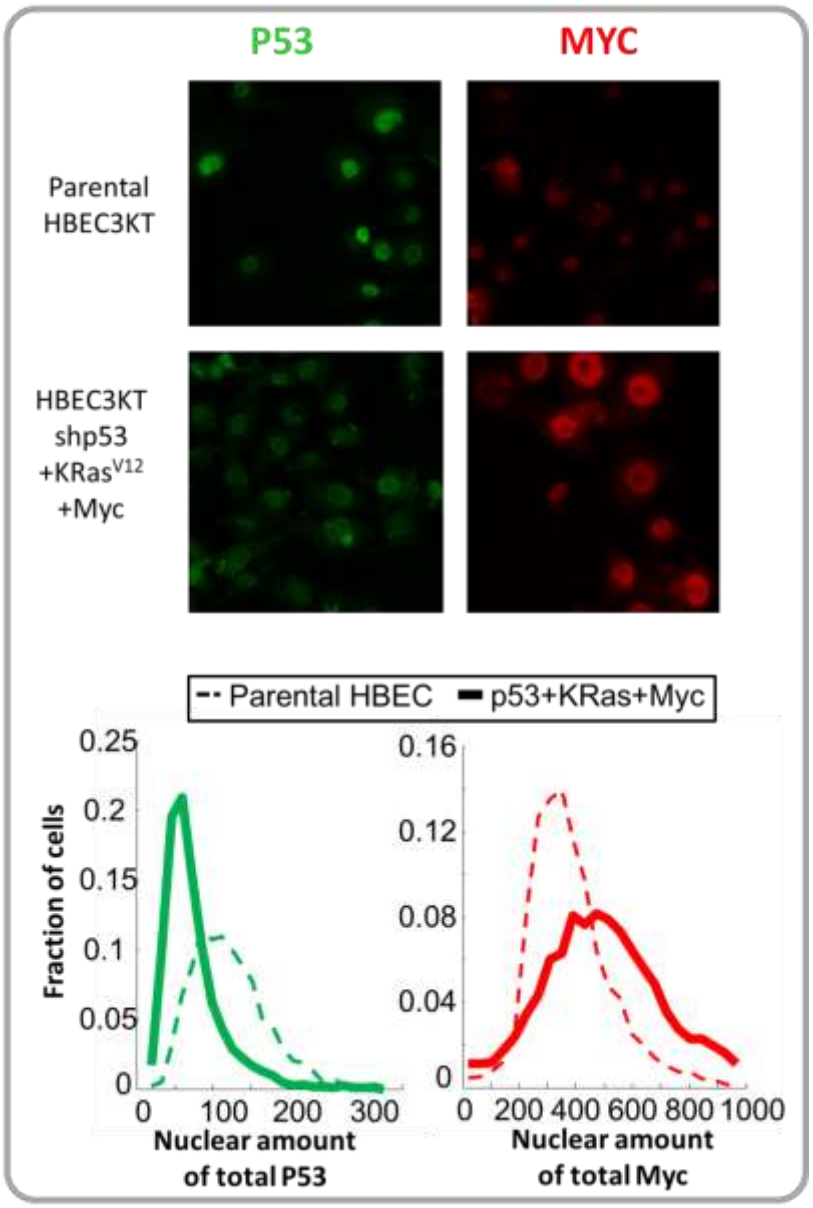

Figure 3.3 Heterogeneity in protein level for P53 and C-MYC in parental and triple manipulated HBEC.

Additionally, a recent study from John Minna laboratory reported the presence of divergent clonal heterogeneity in HBEC soft agar clones in terms of independent genetic events, distinct in vivo growth, tumor histology and differentiation (Sato et al.,

2013). Taken together, the isogenic series of HBECs provide us an ideal in vitro model system to study single cell variability in multiple signaling pathway alteration during oncogenic progression of early stage NSCLC.

3.2 Signaling readouts

The next challenge was the selection of signaling pathways and respective biomarkers for each of them. The focus of our study is a system level understanding of signaling pathways commonly dysregulated in lung cancer. Hence, we took a supervised approach and chose WNT, JAK/STAT, TGFβ, IFNγ, MAPK, AKT and TNFα pathways. For each of these pathways we selected downstream signaling markers that change cellular localization upon pathway activation (Figure 3.4, table 3.1 and discussed in section 1.2). These biomarkers, combined in our immunofluorescent assay, provided us an ensemble of snapshots of various signaling states and their alteration during oncogenic progression in HBECs.

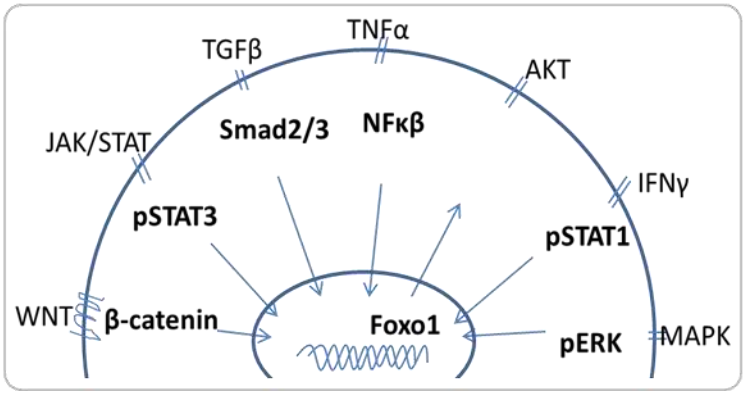

Figure 3.4 Specific signaling readouts downstream of various signaling pathways commonly altered in lung cancer. These markers were chosen for our immunofluorescence assay as they are known to change their cellular localizations upon pathway activation (Simple abstract images of canonical pathways are shown, no pathway crosstalks are shown here).

3.3 Determination of signaling state of each cell

To understand the activity in each signaling pathway, we have focused on a specific intensity feature – Ratio of average Nuclear to average Cytoplasmic amount of the

signaling marker (RNCav). For each cell we have extracted this intensity feature. Approximately, 3000 cells were analyzed per marker per cell line. Hence, each cell line gave us a distribution for a specific marker. In short, for any marker in parental HBEC, cells that fall within 5th and 95th percentile were defined to constitute the baseline signaling in parental HBEC. The top and bottom 5% (Total 10% of cells) were defined as outliers. The distribution of any manipulated HBEC when superimposed on this control parental distribution, gave us the altered fraction of cells from total population (Figure 3.5). The steps are explained in detail below.

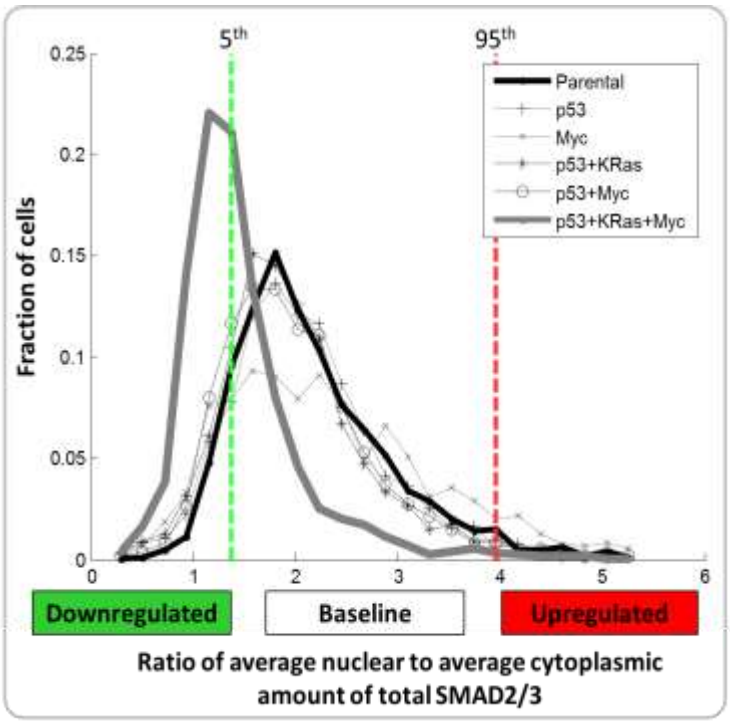

Figure 3.5 Definition of three signaling states (upregulated, baseline and downregulated) based on distribution of intensity features in parental HBECs. Any cells, which are within 5th and 95th percentile, are considered to show baseline signaling phenotype. Cells below 5th percentile are considered as downregulated and above 95th percentile are considered as upregulated. When the distribution of the same intensity feature from manipulated HBECs is superimposed, all the manipulated HBECs (except the triple manipulated line), looked similar to that of the parental HBEC. The distribution of cells of the triple manipulated HBEC line has shifted to the left consisting of ~40% of downregulated cells.

3.3.1 Compensation for difference in size of the cells

To determine if captured signaling alteration is due to the trivial effect of difference in the size of parental and manipulated cells, we compared manipulated cells to the parental cells of the same size. In short, we have found the dependence of our chosen

intensity feature (RNCav) on the nuclear and cytoplasmic size of the parental cells and manipulated cells. Using a polynomial surface fitting function we fitted the data to 5^{th} order polynomial. The two dimensions of the polynomial surface were made with nuclear and cytoplasmic intensity. We have used Matlab fit function with fitting surface poly55. We observed in our data that variation of our chosen intensity feature across cells of the same size is not constant with the change in cell size. However, the variation of feature across cells of same size roughly scales with mean value of the feature. For each manipulated cell, the size correction of the intensity feature value is carried out using this formula -

$$F_m' = (F_m – Poly_p(N_m, C_m) / Poly_p(N_m, C_m)$$

Where, F_m' is the size-corrected feature value for a manipulated cell, F_m is the initially measured feature value for a manipulated cell, $Poly_p(N_m, C_m)$ is the 5^{th} order polynomial used to fit nuclear and cytoplasmic intensity of manipulated cell (N_m and C_m respectively) to that of parental cell of the same size.

3.3.2 Reducing experimental noise by dropping outliers

We have set up our experiments in a way that we have replicate measures of alteration for each cell line from each 96 well plate. In general we have 6 well replicates for each cell line in each plate. Occasionally, due to experimental noise beyond our control certain rare well on the plate may show exceptionally high/low value of intensity feature (RNCav) for all the cells in that well. The whole data can get skewed because of this outlier well. Hence, we decided to identify outlier wells and drop them from our analysis. To identify the outlier wells for a cell line on a plate, we do pairwise comparison of

intensity feature between two wells. We measure the total standard deviation of the wells divided by difference in the mean of the wells. We used standard Z' score (Zhang et al., 1999).

Deviation score = $(\sigma_{wx} + \sigma_{wy}) / \Delta\mu_{wx,wy}$

Where, σ_{wx} and σ_{wy} are the standard deviation of intensity feature value of all the cells from well x and y respectively and $\Delta\mu_{wx,wy}$ is the difference in mean value of intensity feature from all the cells from well x and y respectively.

If this deviation score is greater than our choice of cutoff we consider these two wells similar, in other word, connected in a graph. Out of all the paired wells, using a graph theoretical approach, we find maximum connected component of wells. We keep the wells forming this largest connected component and we drop the wells forming the smaller components.

3.3.3 Classification of each cell into defined signaling state

The sorting of each cell according to their signaling state is a two-step process. First, we make use of the distribution of intensity feature value of all the parental cells (pooled from all the wells of a 96 well plate). We define baseline signaling between 5^{th} and 95^{th} percentile of this distribution. Any cell that falls below 5^{th} percentile is considered to be in downregulated signaling state. Similarly, any cell that falls above 95^{th} percentile is considered to be in upregulated signaling state. Second, we sort each cell (parental and manipulated) into above defined three signaling states – downregulated, baseline and upregulated. At this point we can calculate the standard deviation in fraction of altered cells (downregulated or upregulated) from each well of a 96 well plate. In the end we

could use this standard deviation to assess the difference in well replicates within the same plate.

3.4 Oncogene induced alteration in signaling markers

Based on immunofluorescent microscopy images, we have observed distinct behavior of each signaling readout (Figure 3.4). β-catenin showed the most dramatic change in the triple manipulated cell line. All other cell lines showed strong boundary and cytoplasmic β-catenin. The loss of β-catenin from the cell membrane and cytoplasm can be explained by the mesenchymal property of this line (Scharl et al., 2015; Yang et al., 2015). NFκβ showed strong cytoplasmic localization in all the cell lines suggesting possible inactivation of TNFα pathway in HBECs. While Smad2/3 showed relatively increased amount of cytoplasmic localization, Stat3 showed increased nuclear signal after three oncogenic manipulations indicating different activity in these two pathways. FOXO1 was distributed both in nucleus and cytoplasm throughout all the cell lines suggesting no obvious alteration during oncogenic progression. Although, majority of cells showed above mentioned signaling phenotypes, it is noteworthy that in all the cases, we have observed considerable amount of variation from cell to cell (Fig 3.7). The distinct behavior of each signaling marker and their substantial variation at single cell level – these two observations led us to quantification of signaling phenotypes.

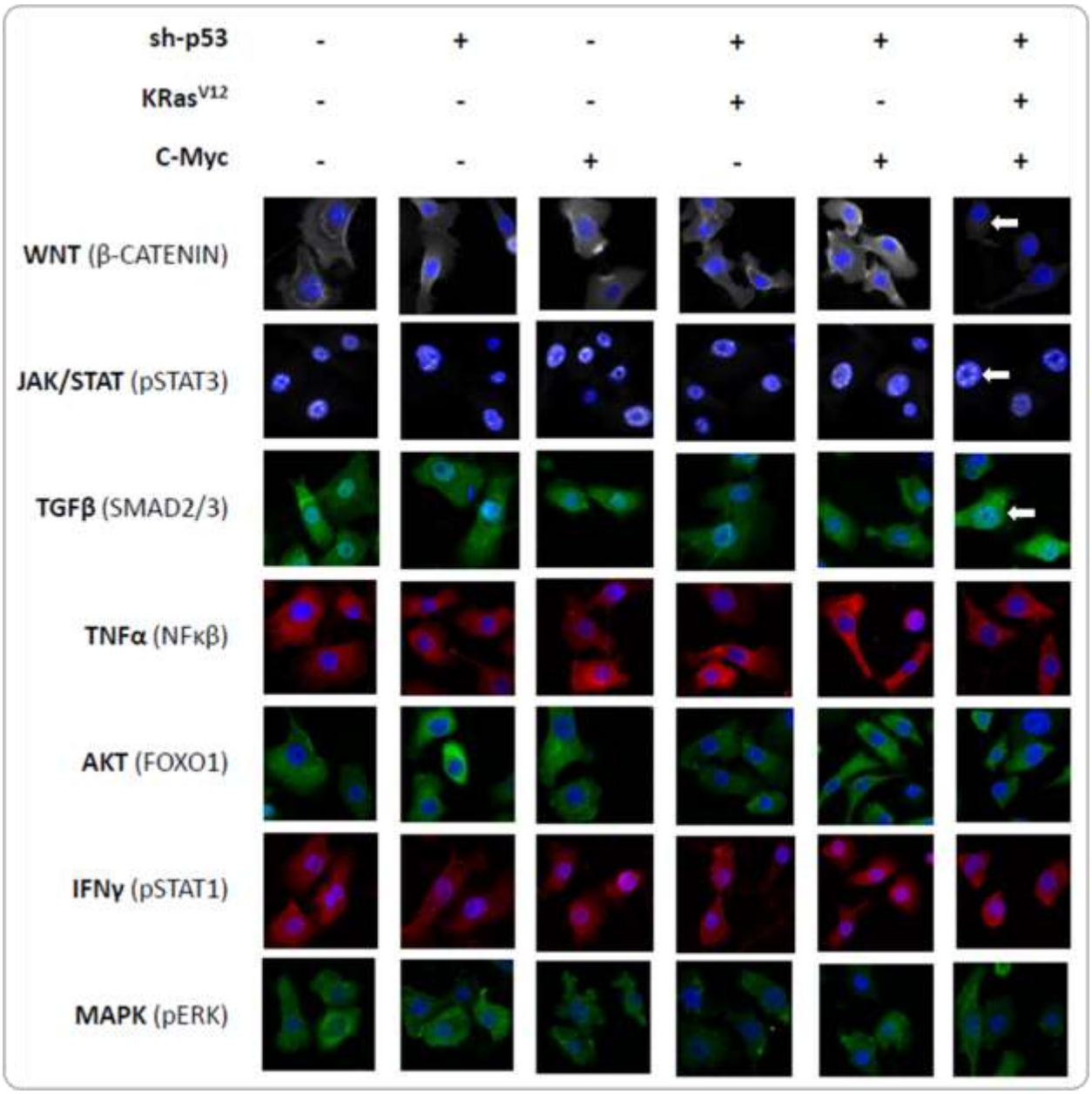

Figure 3.6 Signaling readouts and their phenotypes in oncogenically manipulated HBECs. β-catenin was used as a control marker to observe loss of boundary and cytoplasmic amount in the triple manipulated mesenchymal cell line. Apart from b-catenin, the other noticeable alterations were in Smad2/3 and phospho-Stat3 (shown with white arrow in the figure). Interestingly, the maximum alterations were found in the triple manipulated HBECs.

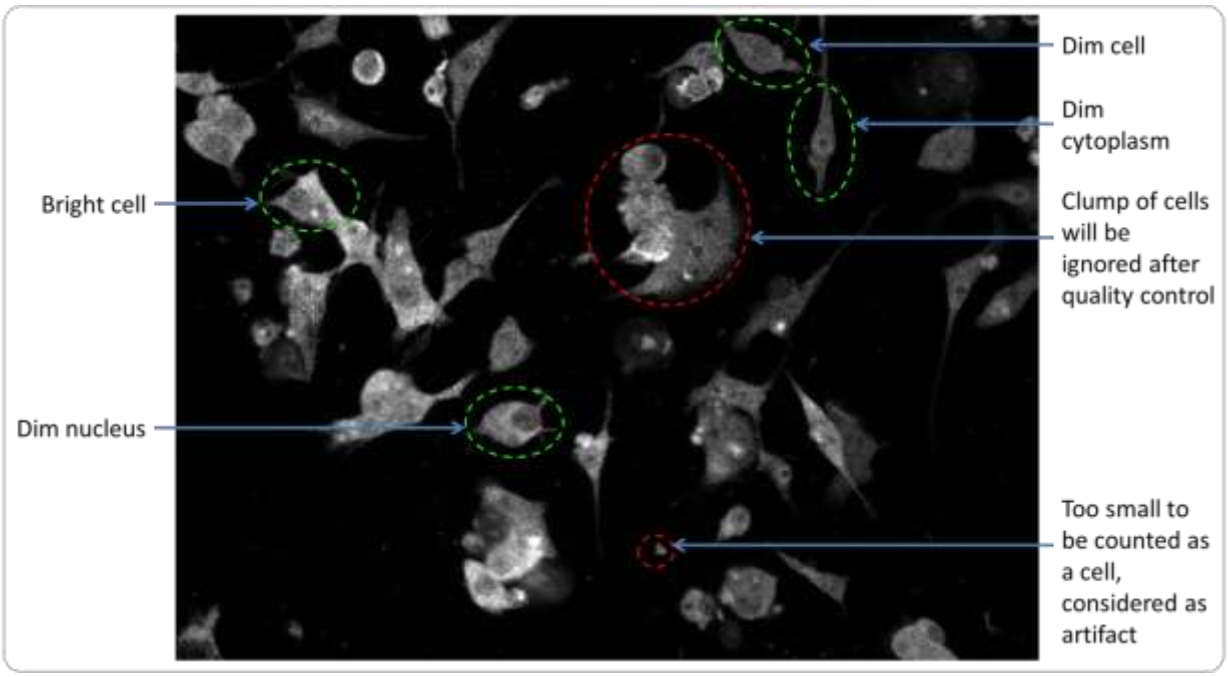

Figure 3.7 Considerable amount of variability from cell to cell in a raw image (before processing) using Smad2/3 as an example. Our focus is in the intensity of Smad2/3 in nucleus and cytoplasm of each cell. Cell clumps and small imaging artifacts are ignored after quality control.

Our single cell quantification of signaling alteration revealed that range of signaling alteration can be different from pathway to pathway. Among seven signaling pathways, the TGFβ and Jak-Stat pathways show the highest range of alteration. The alteration score, that varies from one pathway to another, shows one consistent trend for all the signaling pathways – the maximum alteration happens in the triple manipulated HBEC (PKM). However, the alteration in the signaling pathways does not increase gradually from one to two to three oncogenic combinations. The maximum alteration was observed in ~40% cells of the total population for both TGFβ and Jak-Stat pathways (Figure 3.6). Interestingly, when altered fraction of cells in Smad2/3 signaling is mostly downregulated, the fraction of Stat3 altered cells comprises of both downregulated and upregulated cells. Hence, it is evident that irrespective of being under the same genetic

alterations in PKM line, Smad2/3 and Stat3 show different signaling behavior. When the Myc-related upregulation of Stat3 was expected (Tran et al., 2008; Xiong et al., 2015; Zhang et al., 2012b), Smad2/3 downregulation in a mesenchymal cell line was less obvious. Hence, we decided to further explore the nature of oncogene induced Smad2/3 signaling alteration (figure 3.8).

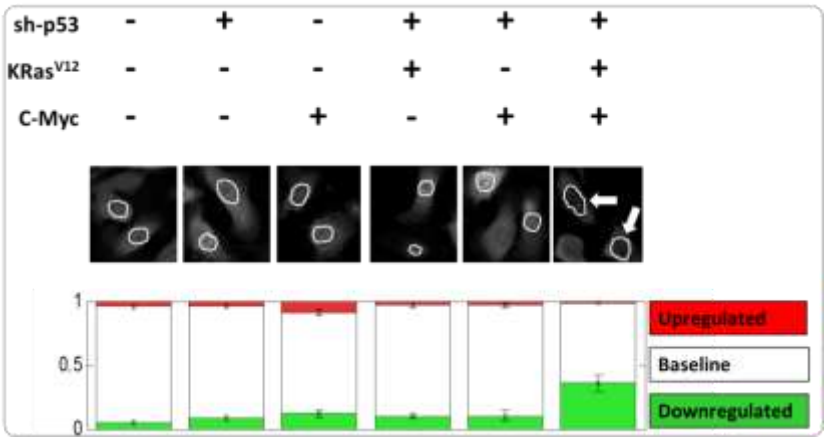

Figure 3.8 Oncogene induces Smad2/3 signaling alteration in HBECs. The quantification of signaling alteration among manipulated HBECs reveals that there is no gradual increase of altered cells with oncogenic progression. The maximum alteration occurs in the triple manipulated HBEC which comprises of 40% of downregulated cells.

3.5 Determination of cell cycle dependence

Do the cells with altered signaling belong to a different stage of cell cycle than the other cells in the population? Here, we have used an earlier developed *in silico* approach to separate the cells into G1 and G2M stages of cell cycle based on the distribution of their total DNA intensity (Nunez, 2001). We avoided drug induced cell cycle synchronization (e.g. nocodazole) as we have observed in our earlier studies that drug treatment could add additional layer of heterogeneous perturbation (Singh et al., 2010). Moreover, nocodazole treatment altered the morphology of parental HBEC suggesting additional perturbation on top of defined oncogenic manipulations (data not shown). Using this *in silico* technique, we have observed that the G2M cells were slightly more enriched with altered fraction of cells (Figure 3.9). Interestingly, we have observed that the altered

fraction of cells was distributed in all the stages of cell cycle suggesting that this signaling alteration is not cell cycle dependent.

3.6 Correlation and causality of oncogene induced signaling alteration

The way HBEC oncogenic progression system was created, the signaling alteration we observed here, can be induced by the oncogenes only. However, we like to grow our confidence with necessary and sufficient experiments. First, we chose to identify if the fraction of Smad2/3 downregulated cells have distinct level of oncogenic manipulations. The correlation of the level of expression of oncogenes and alteration of Smad2/3 should point us towards any possible connection. Second, we chose to test if we can reverse the altered fraction of cells by removing the oncogenic stress although it is quite possible that the sustained oncogenic stress might have pushed the cells to irreversible signaling state. This section describes the correlation and causality of oncogene induced Smad2/3 signaling alteration.

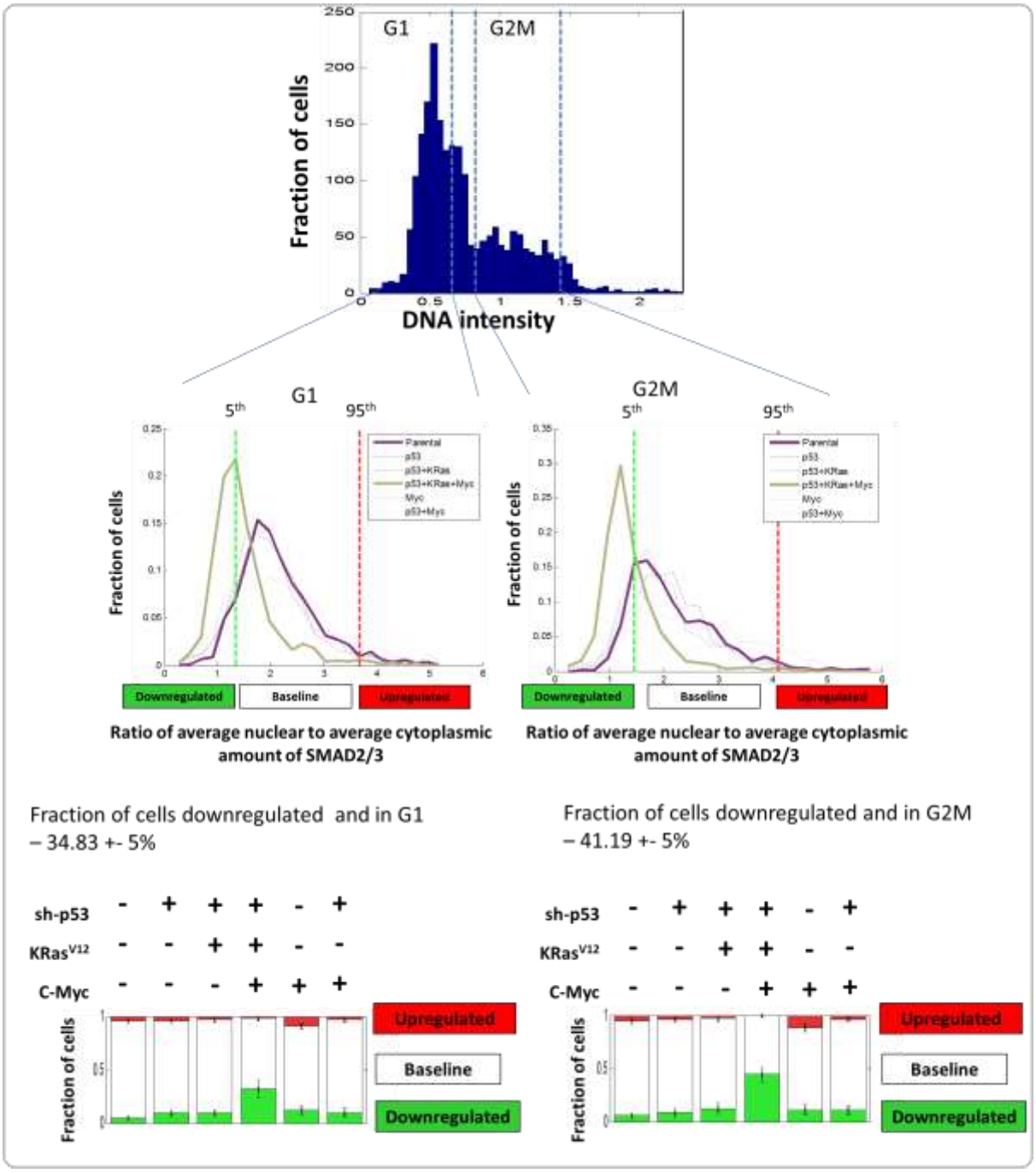

Figure 3.9 Cell cycle independence of Smad2/3 signaling alteration in the triple manipulated HBEC line. An *in silico* method is used to separate the G1 and G2M cells from the immunofluorescence images based the distribution of total DNA intensity. The G2M stage shows slight enrichment of the altered cells. Fraction of cells downregulated and in G1 and G2M stage comprises of 34.83 +- 5% and 41.19 +- 5% of total cells respectively.

3.6.1 Relationship of oncogenic manipulation and signaling alteration

To mimic the natural variation in the occurrence of oncogenic expression in different cells in the same tumor, the HBEC system was not created from single cell clones. Hence, the question remains - Is the level of oncogenic manipulations responsible for the Smad2/3 alteration in single cell level? A co-staining experiment with antibodies against all the three oncogenes (p53, $KRas^{V12}$ and C-Myc) with Smad2/3 could give us an idea of this correlation. In reality, antibodies were not available for the feasibility of a four channel microscopy experiment. Hence, we chose to co-stain Smad2/3 with these oncogenes one at a time. Moreover, there was no specific antibody available for oncogenic KRas. In Figure 3.10, we show that the parental and triple manipulated HBECs occupy different space in the scatter plots. As we stably knocked down p53, the overall dynamic range of this assay became smaller. On the other hand, C-Myc overexpression gave us a broader dynamic range for this assay. From the plots and Pearson's correlation coefficient, it became evident that level of c-Myc expression was correlated to Smad2/3 alteration in the triple manipulated HBECs.

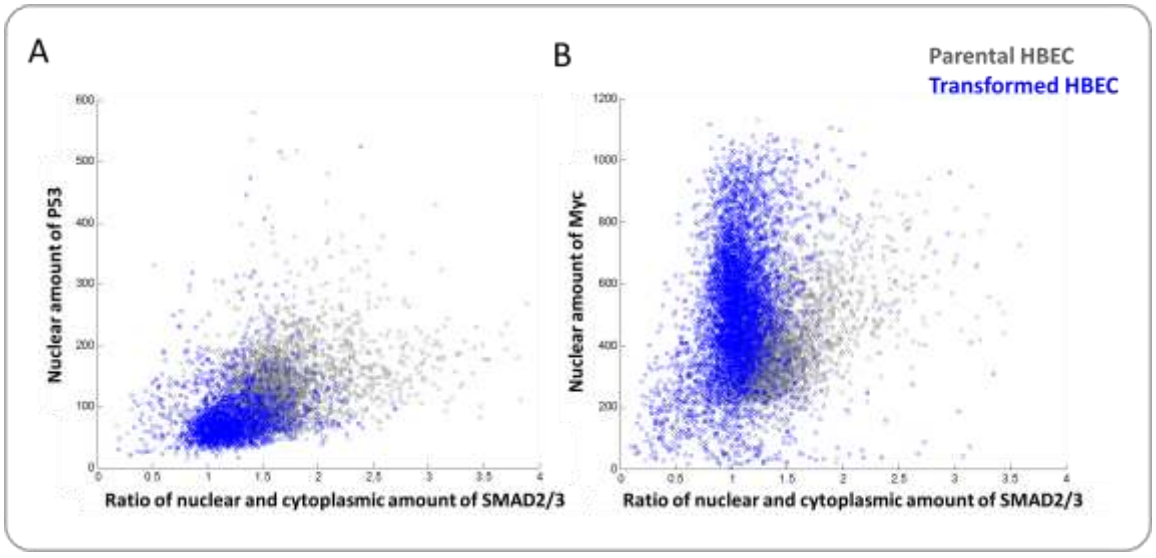

Figure 3.10 Correlation of level of oncogenic manipulations and Smad2/3 in single cell level. Each cell became a point in this scatter plot. The parental HBEC line is represented in grey and the triple manipulated HBEC line is represented in blue. The Pearson's correlation coefficient for p53 and Smad2/3 is very close in parental and triple manipulated HBEC (parental 0.38 and manipulated 0.33). However, the Pearson's correlation coefficient for c-Myc and Smad2/3 is considerably higher in the triple manipulated HBEC than that in the parental cell line (parental 0.42 and manipulated 0.63).

3.6.2 Reversibility of oncogene induced signaling alteration

Can we reverse the oncogene induced signaling alteration? Or, once transformed and pushed to a diseased state, do the cells continue to retain altered signaling even after the removal of the oncogenic stress? To answer this question, we decided to work with c-Myc manipulation. We have observed that with c-Myc overexpression in the background of p53 knockdown and oncogenic $KRas^{V12}$ expression, HBECs acquire signaling alteration. Hence, we hypothesized that inhibition of c-Myc's transcriptional activity might reverse the engineered signaling alteration. By stably introducing a Myc dominant negative construct, Omomyc, we would be able to inducibly inhibit Myc's transcriptional activity in the triple manipulated HBECs. Thus, we transduced the triple manipulated HBEC with Omomyc lentivirus (Figure 3.11).

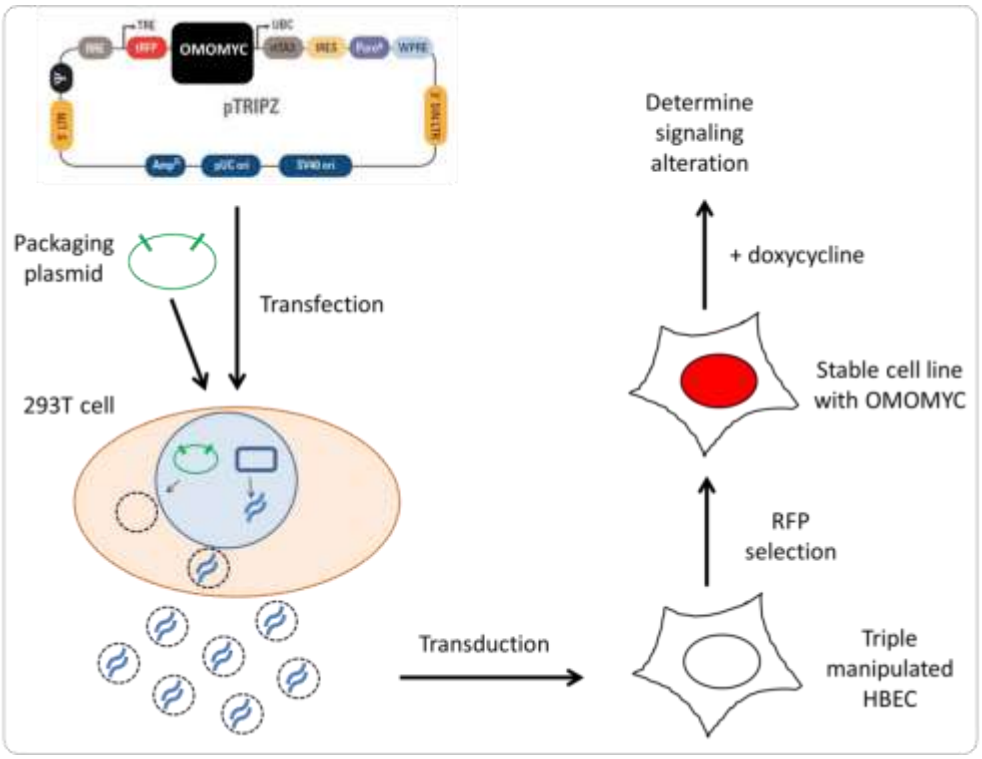

Figure 3.11 Stable knockdown of c-Myc target genes using Omomyc construct. pTRIPZ map was acquired from Open Biosystems website.

Upon induction of Omomyc, we showed a significant reduction in the expression of downstream target genes of c-Myc (RGS16 and ASS1), confirming functionality of the Omomyc construct. Next, when assayed for Smad2/3 signaling, we have observed significant alteration. The distribution of cells after downregulation of Myc transcriptional activity shifts closer to the distribution of parental HBECs (Figure 3.12). Hence, our data suggest that Smad2/3 signaling alteration is transient as it can be reversed by removing the c-Myc oncogenic stress. This observation also proves that the signaling alteration is clearly oncogene induced.

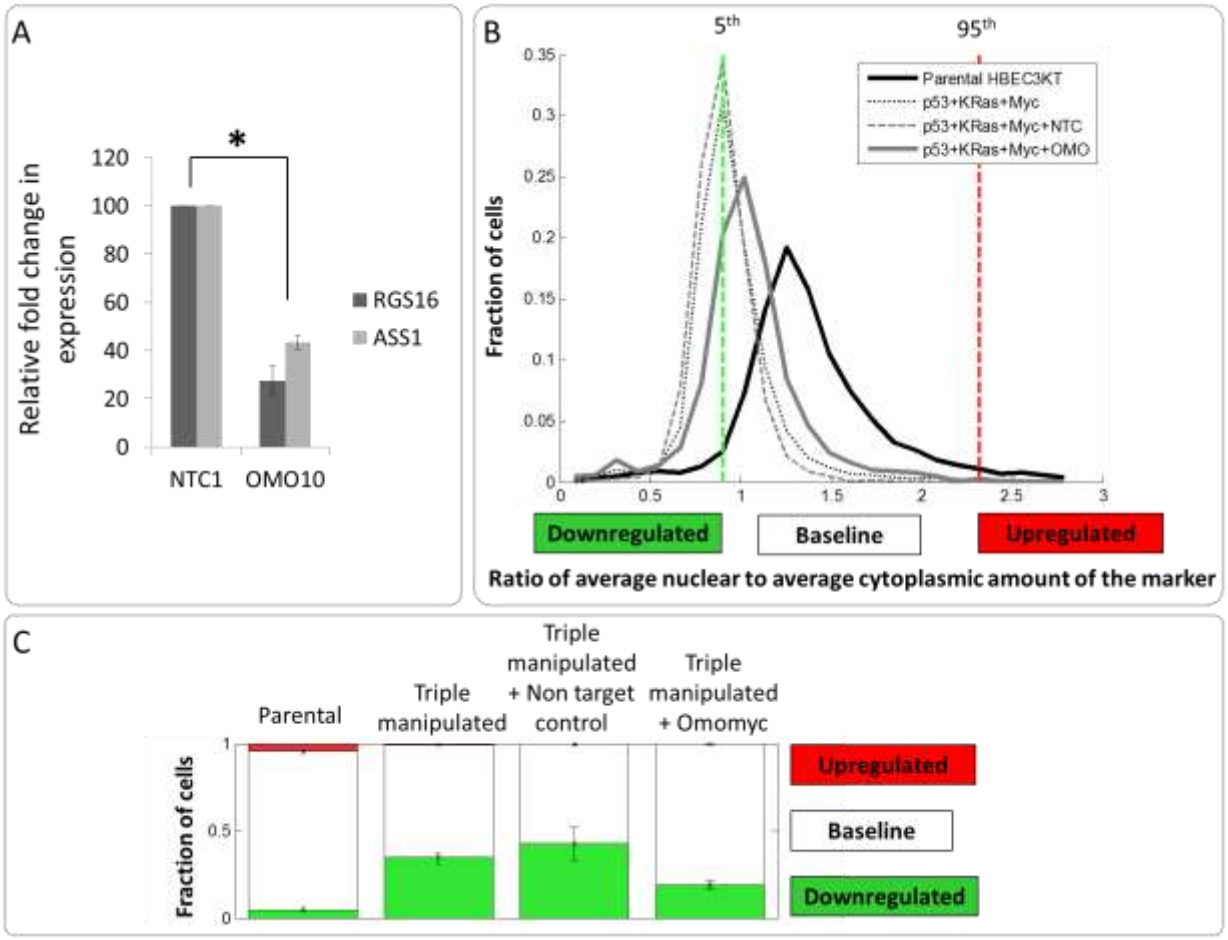

Figure 3.12 Reversibility of Smad2/3 alteration after Omomyc induction. A) Significant decrease in Myc downstream target genes such as Rgs16, Ass1 (p value<0.005) shown using qRT-PCR. B) The distribution of our specific intensity feature in parental HBEC, triple manipulated HBEC, and transduced with Omomyc and its non-target control. C) After Omomyc induction, the fraction of downregulated cells decreased significantly.

3.7 Comparison of Smad2/3 and Stat3 signaling alteration

So far, we have observed that C-Myc in the background of sh-p53 and $KRas^{V12}$, induced alteration in Smad2/3 signaling. But how distinct is this phenomenon? Do oncogenic manipulations altered multiple pathways in a single altered subpopulation of cells? Or, it created more than one subpopulations with distinct signaling phenotypes?

As phospho-Stat3 was another signaling marker that was altered after oncogenic manipulations, we chose to compare Smad2/3 signaling and Stat3 signaling in the triple manipulated HBECs. We co-stained the triple manipulated HBECs with antibodies against Smad2/3 and phospho-Stat3. In the scatter plot we have observed two distinct subpopulations – upregulated cells in Stat3 signaling and downregulated cells in Smad2/3 signaling (Fig. 3.13). In addition, a low Person's correlation coefficient suggested two distinct subpopulations. Hence, Smad2/3 signaling may be distinctly rewired in than any other signaling alteration by oncogenic manipulations.

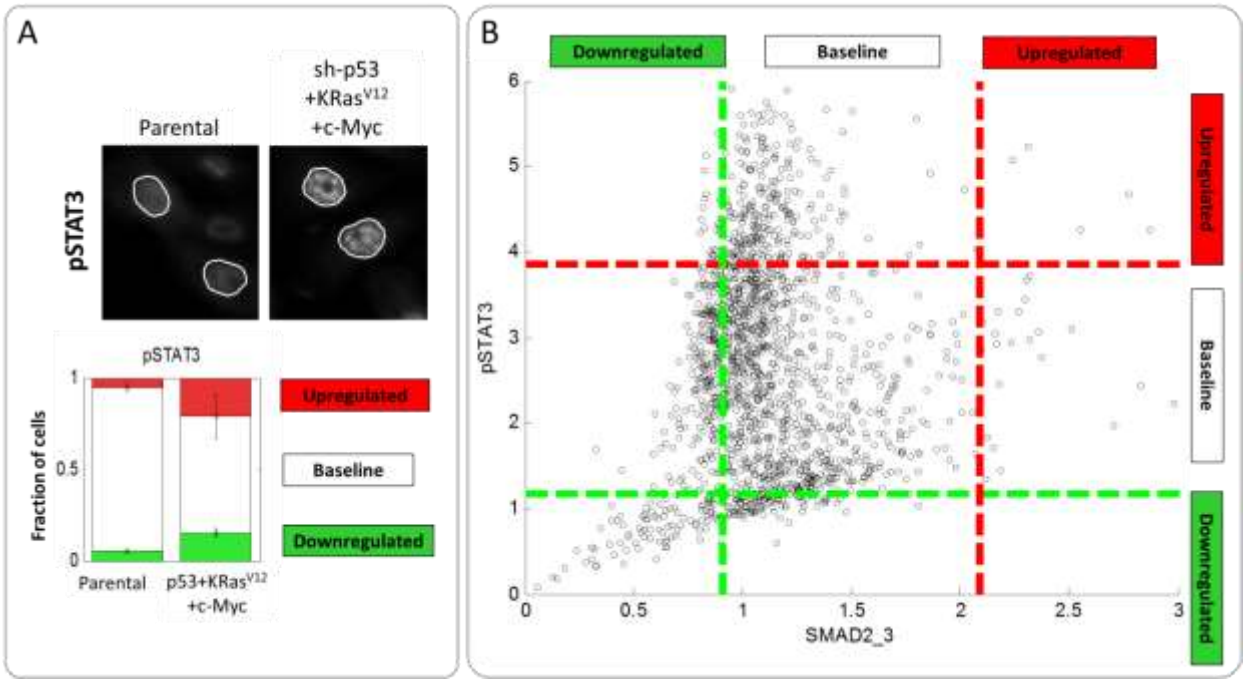

Figure 3.13 Smad2/3 alteration is distinct from Stat3 alteration. A) Phospho-Stat3 shows a fraction of cells with upregulated phenotype after oncogenic manipulations. B) Scatter plot of Smad2/3 and phospho-Stat3 showing majorly two subpopulations with a low Pearson's correlation coefficient (0.16) between Smad2/3 and phospho-Stat3 level in single cells.

3.8 Oncogenes vs environmental stimuli

Now that we have come across, a possible distinct rewiring in Smad2/3 signaling we became interested in further understanding the nature of this rewiring. For this purpose, we made use of response of the altered cells to environmental stimuli.

3.8.1 Signaling response to growth factors

As normal cells turn to malignancy their microenvironment starts to alter and the cells interact with altered microenvironmental stimuli. How stable is the engineered signaling alteration to microenvironmental stimuli? To evaluate this scenario, first, we have chosen to work on Smad2/3 signaling explicitly considering the availability of specific ligand (TGFβ) and inhibitor (SB431542 to TGFβ receptor) for this pathway. Using short term growth factor treatment (both TGFβ and 10% FBS) we showed the ability of Smad2/3 signaling pathway to respond to microenvironmental stimuli (Figure 3.12). Both parental and triple manipulated HBECs showed similar alteration in signaling upon short term treatment. However, in reality, cancer cells do not get pulses of microenvironmental signal. They experience long exposures to varying amount of stimuli. We hypothesized that over long period of treatment transformed cells and normal cells would exhibit different signaling response. We established the dynamic range of signaling response (varying concentration and time of treatment) in normal and transformed cells in the context of ligand and inhibitor addition. Interestingly, with physiological relevant dose of stimuli, all the cells in the population did not respond homogeneously. In both normal and transformed cells, we found subpopulations responding to given dose of growth factors. However, when a subpopulation of normal cells shifted to upregulated signaling state after long term treatment, the transformed cells behaved differently. A subpopulation of transformed cells exhibited downregulation

and hence the behavior of total population looked similar to its behavior under untreated condition (Figure 3.14). In essence, our data suggests that the transformed cells possess the ability to rewire the Smad2/3 signaling pathway differently where they could override the signals from the microenvironment.

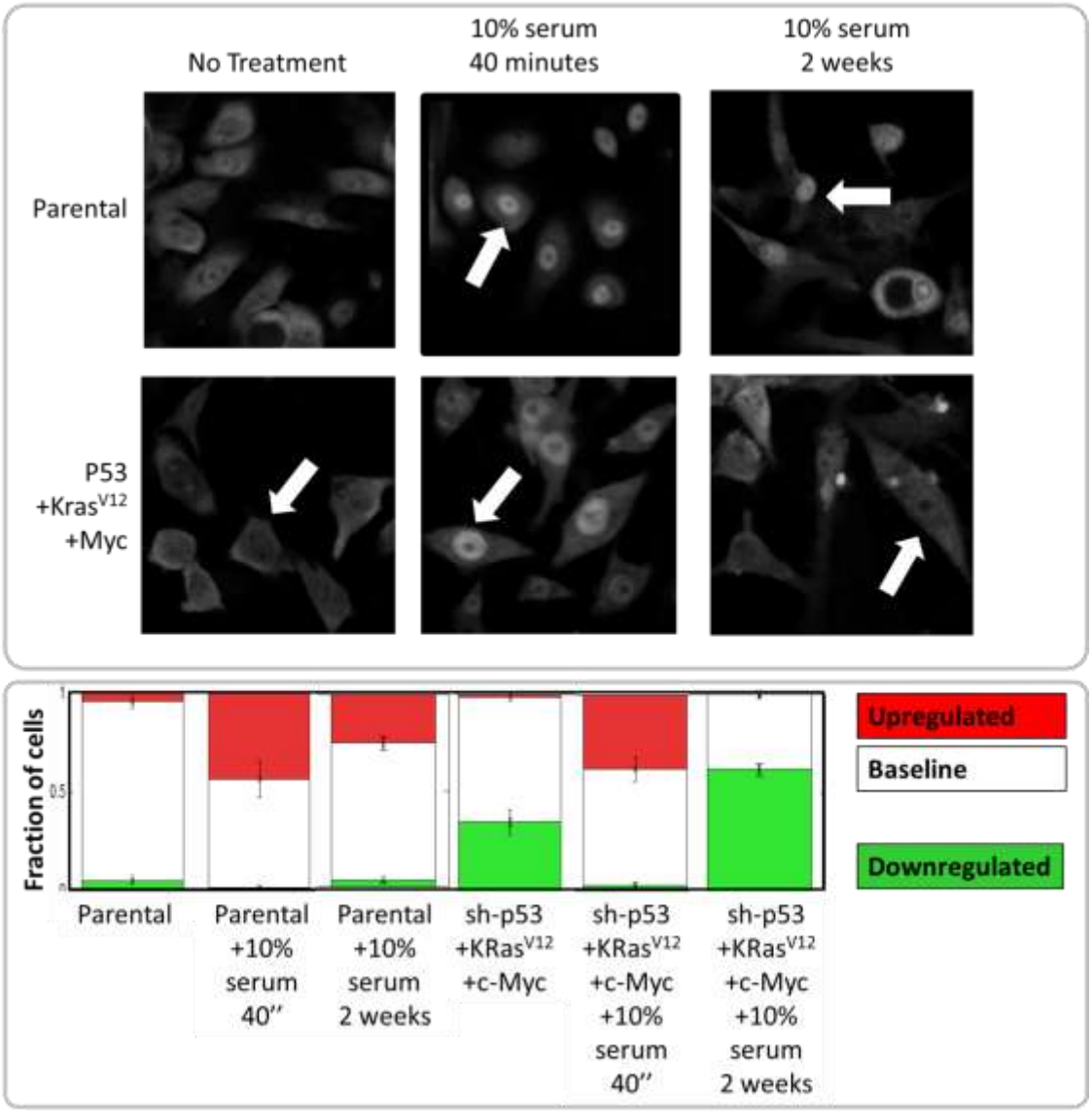

Figure 3.14 Response of Smad2/3 signaling to altered environment. In response to short term treatment of 10% serum (for 40 minutes) both parental and triple manipulated HBECs respond similarly showing increase in nuclear amount of Smad2/3. In response to long term treatment (for 2 weeks), the parental

HBEC continues to show higher nuclear Smad2/3, but the triple manipulated line showed low nuclear Smad2/3. Lower panel shows the quantification.

3.8.2 Signaling response to combination chemotherapy

After the malignancy of tumor cells are diagnosed, they undergo treatment. The most prevalent treatment options for lung cancer include combination chemotherapy. When the population of malignant cells comes across drug treatment their signaling may alter one more time. The drug treatment can create an “evolutionary bottleneck” by selecting pre-existing cells with altered signaling and/or the drugs can alter the signaling pathways during the treatment. In both the cases, the question remains: does combination chemotherapy treatment alter the Smad2/3 signaling in our transformed epithelial cells? We have optimized the clinically relevant combination dose of Cisplatin and Etoposide (Table xx) and applied them in pulses followed by a ‘no-drug’ time in the transformed cell.

Drug	C_pMax	MTD	Schedule (1 cycle)	TC equivalent dose	TC Schedule (1 cycle)
Cisplatin	5.6 ug/mL	80 mg/m^2	1 d followed by 3 weeks of remission	70 uM	6 hrs followed by 3 weeks of remission
Etoposide	15 ug/mL	100 mg/m^2	3 d followed by 3 weeks of remission	150 uM	6 hrs followed by 3 weeks of remission

Table 3.1 Optimization of Cisplatin and Etoposide combination treatment in parental and triple manipulated HBECs. The Tissue culture (TC) equivalent dose was found from the ratio of maximum plasma concentration (CpMax) to maximum tolerated dose (MTD).

We show that the drug treatment selects for altered fraction of cells. We further test how general is this phenomenon in lung cancer patient derived paired cell lines before and after Cisplatin and Etoposide combination therapy. H1693 and H1819 cell lines show significant reduction of altered cells in Smad2/3 signaling supporting the results in transformed epithelial cells.

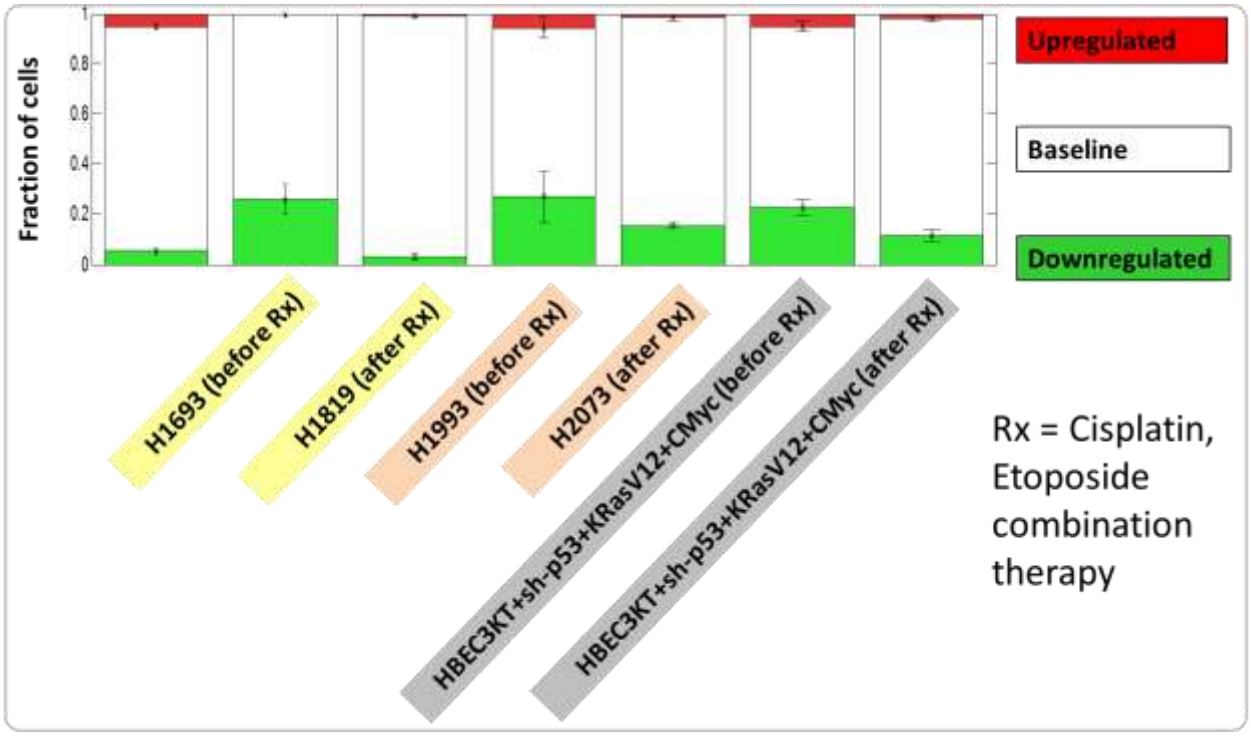

Figure 3.15 Smad2/3 signaling response to Cisplatin and Etoposide combination therapy.

3.9 Behavior of downstream target genes of SMAD2/3 signaling

Earlier using Smad2/3 phenotype as a readout we have shown that C-Myc overexpression in the background of stable knockdown of p53 and oncogenic KRas,

causes alteration in Smad2/3 signaling. This alteration was distinct from other signaling alterations like Stat3. In addition, we have observed that over chronic exposure to environmental stimuli parental and triple manipulated HBEC, give different response of Smad2/3. Hence, we hypothesize that oncogenes may rewire the Smad2/3 signaling by changing the response of Smad2/3 to environmental stimuli. To test this we have made use of the downstream target gene expression of Smad2/3 signaling under short and long term treatment of stimuli.

First, using microarray gene expression analysis we have shown that out of 30 known downstream targets of Smad2/3 downstream target genes, 10 are differentially expressed in the triple manipulated HBECs compared to all other HBECs. They include MMP7, SOX2, BCL6, FOXK1 family members (Figure 3.16). Second, using qRTPCR we confirm that MMP7, BCL6 and SOX2 expression increases and FOXK1 expression decreases significantly in triple manipulated HBEC in no treatment condition (as was observed earlier in microarray data. Second, in terms all the gene expression and under both short and long treatment conditions, triple manipulated HBEC shows significant difference from the parental HBEC. The evidences from multiple experiments confirm oncogene induced Smad2/3 signaling alteration persists in the presence of environmental stimuli.

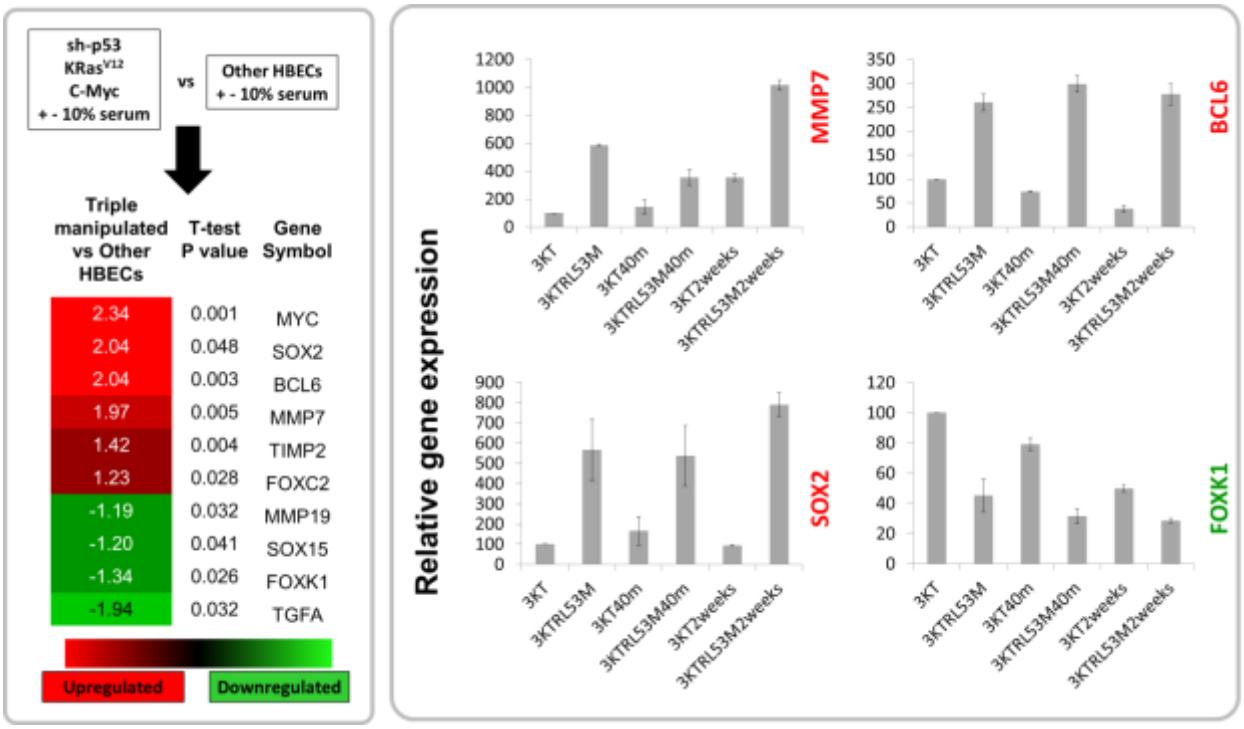

Figure 3.16 Downstream target gene expression of Smad2/3 signaling. The differential expression of downstream target genes of Smad2/3 signaling persists under the change in environmental stimuli.

Interestingly, the data suggests that the behavior of individual downstream targets is unique (Figure 3.16). For MMP7, both short and long term serum treatment increased expression significantly. This data suggests that the environmental stimuli adds up to oncogenic manipulations in regulating matrix metalloprotease 7 (MMP7). However, for BCL6, with serum treatment its expression decreases in parental line. But it remains similar (within standard error range) in triple manipulated HBEC with short and long treatment suggesting BCL6 expression is mostly controlled by oncogenic manipulation and not environmental stimuli. FOXK1 expression increases in the parental HBEC after long treatment but remains similar to no treatment condition in the triple manipulated HBEC. Collectively, this data suggests that oncogene induced Smad2/3 alteration may translate uniquely in each downstream target gene expression in the presence of

environmental stimuli pointing towards complexity (many crosstalks) associated with long treatment condition.

3.10 Targetable vulnerabilities

Is there any targetable vulnerability associated with the oncogene-induced signaling alterations? We have employed the Stat3 inhibitor Stattic to target the subpopulation with upregulated Stat3 signaling. The triple manipulated HBECs showed 4-fold increased sensitivity to Stattic compared to the non-manipulated HBECs (Figure 3.17). Hence, Stat3 is a potential targetable vulnerability in the triple manipulated HBEC.

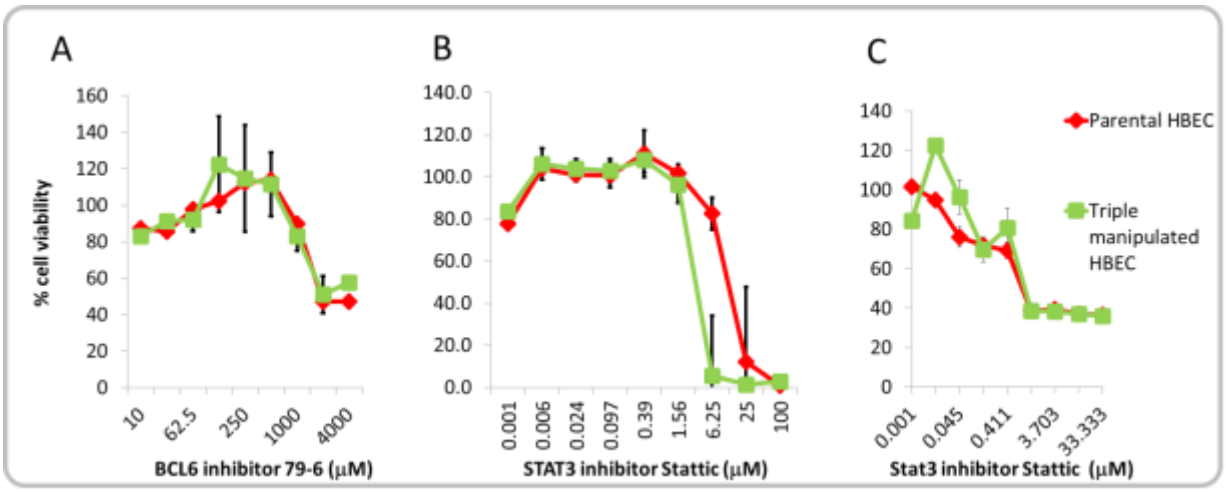

Figure 3.17 Response of parental and triple manipulated HBEC to Stat3 inhibitor Stattic, Bcl6 inhibitor 79-6 alone and in combination. Triple manipulated HBEC shows considerable difference (4 fold change) in viability from parental HBEC after Stattic treatment (B). 79-6 did not show any differential effect alone (A) or in combination (C) between the parental and triple manipulated HBECs.

However, as we have observed Stat3 upregulated cells and Smad2/3 downregulated cells were mutually exclusive (Fig. 3.13), we wanted to confirm if we depleted the subpopulation of Stat3 upregulated cells after Stattic treatment. From the co-staining

immunofluorescence experiment with antibodies directed towards Smad2/3 and phospho-Stat3, we observe that the subpopulation with upregulated Stat3 is killed after Stattic treatment (Fig. 3.18). But, the subpopulation with downregulated Smad2/3 still exists.

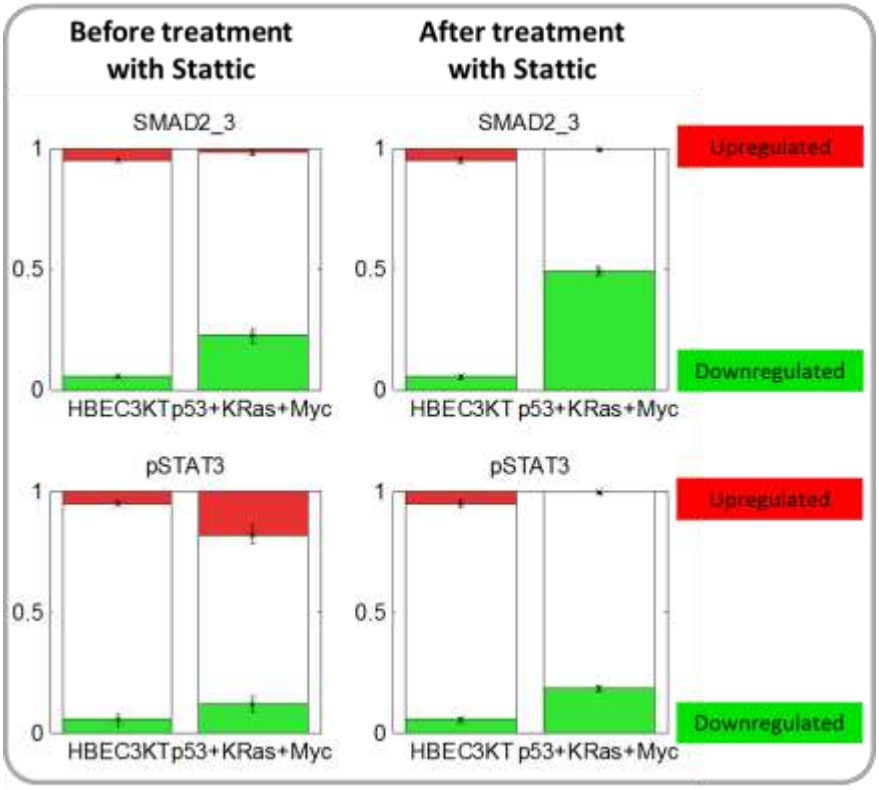

Figure 3.18 Altered fractions of cells, upregulated in red and downregulated in green, for Smad2/3 and phospho-Stat3 signaling before and after treatment with Stat3 inhibitor Stattic. Before Stattic treatment we observe both subpopulations with Smad2/3 downregulation and Stat3 upregulation in transformed HBEC. But, after Stattic treatment Stat3 upregulated cells die and Smad2/3 downregulated cells remain alive.

To target the subpopulation with downregulated Smad2/3, using gene expression analysis, we have identified Bcl6, a differentially expressed downstream target of Smad2/3 signaling (Figure 3.16). Triple manipulated HBEC shows 3-fold increased expression of Bcl6 compared to parental HBEC. Interestingly, this increased Bcl6 level is not changed by the alteration in environmental stimuli (10% FBS short and long treatment). Moreover, knockdown of Myc target genes reduces Bcl6 level by 2-fold. This low Bcl6 level after c-Myc target downregulation is comparable to the level of Bcl6 in the

parental HBEC (Figure 3.19). Hence, our data suggests that Bcl6 may be a potential target of c-Myc-induced signaling alterations.

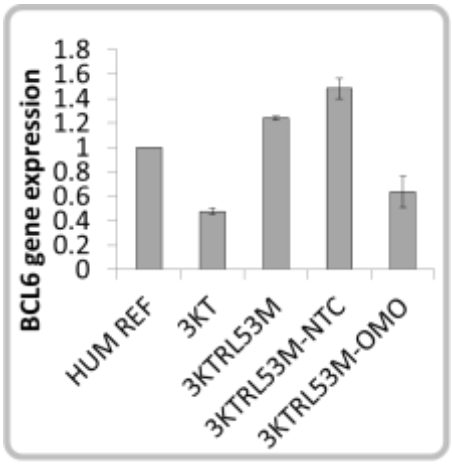

Figure 3.19 Bcl6 gene expression. Triple manipulated HBEC has higher Bcl6 than Parental HBEC under same growth condition. The introduction of a non-target-control vector does not change the Bcl6 expression significantly in the triple manipulated HBEC. However, introduction of Myc dominant negative lentiviral construct Omomyc targets the downstream genes of Myc. In this case, we observe significant reduction of Bcl6 gene expression.

To target cells with upregulated Bcl6, we have used the Bcl6 inhibitor 79-6. The IC50 of this drug calculated from MTS assay did not show any significant difference between the parental (2.9 mM) and triple manipulated HBEC (2.3 mM). Our data suggests that although Bcl6 is a potential therapeutic target, Bcl6 inhibitor alone may be insufficient (Figure 3.17). Next, we wanted to test if combination of Bcl6 and Stat3 inhibitor can provide a better outcome. To test this we have chosen a constant dose of 79-6 (0.3 mM) and varying dose of Stattic. Although we observed a decrease in IC50 values, the parental and triple manipulated HBECs showed no difference in their responses to the drug combination (Figure 3.17). Our data suggested that the Bcl6 inhibitor 79-6 may not be exploited in targeting cells with higher level of Bcl6 in our cell line model. Hence, we focused on genetic knockdown of Bcl6 and any resulting change in viability.

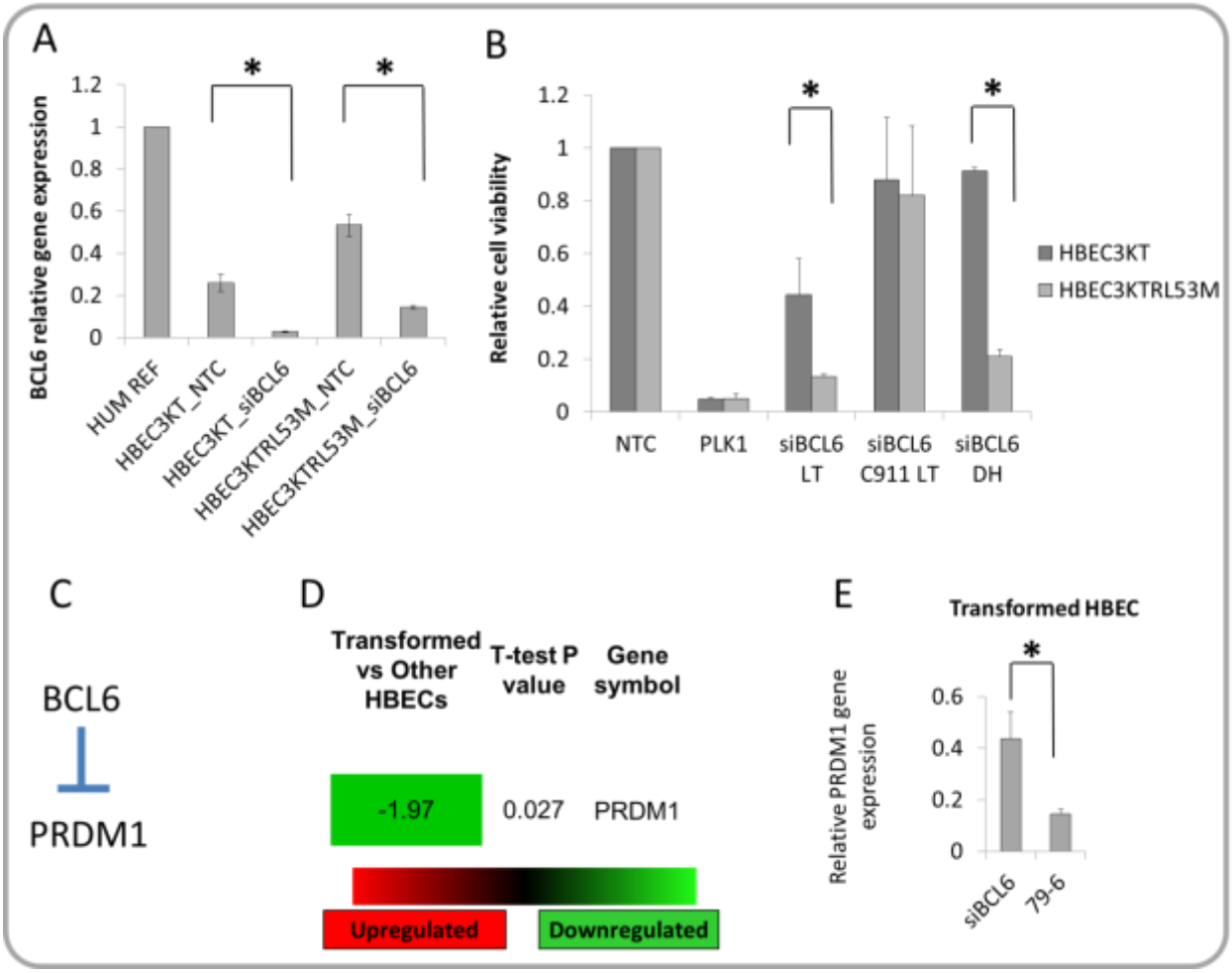

Figure 3.20 Knockdown of Bcl6 using siRNA. Panel A shows decrease in Bcl6 expression after siRNA transfection after 2nd day of transfection. The transfection efficiency is higher in parental HBEC (90%) compared to that in triple manipulated HBEC (75%). Panel B shows difference in viability of parental and triple manipulated HBEC on 5th day after siRNA transfection. Panel C, D and E show the well described BCL6 target gene PRDM1 expression in triple manipulated vs other HBECs and after siBCL6 and 79-6 treatment.

After siRNA mediated knockdown of BCL6 we have observed that the parental HBECs showed higher viability than the triple manipulated cells (Figure 3.20). Our data suggests that Bcl6 can be a potential therapeutic vulnerability in the triple manipulated HBECs.

We wondered if there is a difference between the knockdown of BCL6 gene expression by the pharmacological and the genetic knockdown approaches. We have utilized a well-described BCL6 target gene called PRDM1 to answer this question (Walker et al., 2015). BCL6 is known to inhibit PRDM1 expression. First using microarray data analysis we have found that PRDM1 was approximately 2 fold downregulated in the triple manipulated HBECs (Figure 3.20). This supports our previous result of BCL6 upregulation in the triple manipulated HBEC and hence explains downregulation of PRDM1. Next, we compared the PRDM1 expression after siRNA mediated BCL6 knockdown and 79-6 treatment. We observed significantly higher PRDM1 expression in siRNA mediated knockdown scenario suggesting higher level of BCL6 knockdown. The higher level of genetic knockdown may explain the difference in viability from the 79-6 drug treatment.

In summary, we used specific pharmacological inhibition and genetic knockdown of distinct subpopulations as a proof-of-principle. We conclude that the combination of p53null, KRasV12, and c-Myc lead to signaling heterogeneity and potentially targetable vulnerabilities (Stat3 and Bcl6) which may provide new treatments for early-stage lung cancer.

3.11 Discussion

In this chapter we attempted to understand oncogene induced signaling alteration in single cell level. We have observed that the c-Myc overexpression in the background of stable knockdown of p53 and expression of oncogenic $KRas^{V12}$ led to significant signaling alteration in HBECs. However, the level of c-Myc overexpression was

heterogeneous in single cells possibly due to the randomness of lentiviral vector integration in the genome of HBECs. Hence, we carried out costaining experiments with c-Myc and Smad2/3 and found a strong positive correlation (Pearson's correlation coefficient 0.63). Next, the knockdown of Myc target genes using Omomyc construct reversed the Smad2/3 alteration. These results confirm that c-Myc overexpression in the already existing oncogenic background, was causing alteration in Smad2/3 signaling. We have also identified the type of this Smad2/3 alteration as majorly downregulation. This downregulation was interesting to us because upregulation of TGFβ pathway is known to be correlated with mesenchymal properties of the cells in a context dependent fashion (Massague, 2012). In an earlier study, it has been shown that the triple manipulated HBECs secrete significantly higher amount of TGFβ pointing to autocrine-paracrine signaling in TGFβ pathway (Larsen, Minna in press). However, using long term serum treatment we show that Smad2/3 signaling can be insulated from the environmental stimuli upon chronic exposure. Upon short term treatment, there is no insulation. These evidences point towards a time dependent switch of Smad2/3 signaling activation and inactivation. In addition, we show that the observed Smad2/3 alteration is translated in the expression of downstream target genes such as BCL6. Interestingly, positive correlation of both Myc and BCL6 expressions are considered as prognostic markers in double hit lymphoma (Lin and Medeiros, 2013). However, BCL6 is known to repress Smad signaling in TGFb growth resistance (Wang et al., 2008). Hence, we may deduce that c-Myc overexpression initially increased signaling in Smad2/3 pathway which led to BCL6 overexpression. But, this BCL6 repressed Smad2/3 via a negative feedback loop leading to Smad2/3 downregulated phenotype.

We should note that the above described Smad2/3 alteration only occurred in a subpopulation of triple manipulated HBECs. C-Myc overexpression also altered Stat3 signaling as observed in our data. From our costaining experiment we observed that Stat3 overexpression occurs in a different subpopulation of cells. However, downregulated Smad2/3 and downregulated Stat3 appeared to be in the same subpopulation. Hence, oncogenic manipulations created more than one type of altered subpopulations. In addition, Jak-Stat signaling is known to transcriptionally repress BCL6 expression in primary mediastinal B-cell lymphoma (Ritz et al., 2013). Hence, in the Stat3 upregulated subpopulation, BCL6 may be repressed and hence is unable to downregulate Smad2/3 signaling. Taken together, all these evidences point to the identification of two interesting altered subpopulation of cells due to oncogenic manipulations in HBEC. One of them is downregulated in Smad2/3 and yet expresses high level of BCL6. The other has upregulation of Stat3 and possible downregulation of BCL6 (Figure 3.21).

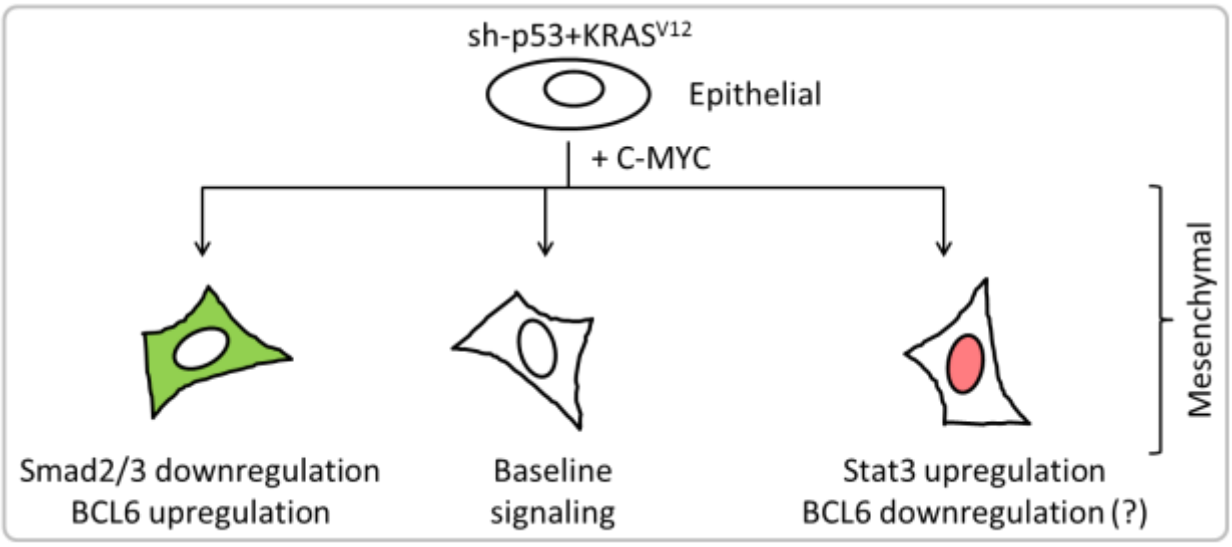

Figure 3.21 Proposed model of oncogene induced signaling diversity in HBECs.

In future studies, it will be important to carefully decipher the mechanism of such signaling diversity. Our choice of indirect immunofluorescence assay had couple of shortcomings: a) As immunofluorescence assay was a fixed cell assay we were not able to functionally characterize these subpopulations, b) The temporal fluctuation of signaling was not studied. Both of these problems can be addressed using live cell markers for Smad2/3 and Stat3 in future.

Antibody	Vendor	Catalog #	Lot #	Dilution
β-catenin	Cell Signaling	4627S	5	1:300
p-Stat3	BD	612543	28597	1:400
Smad2/3	Cell Signaling	8685S	1	1:800
NFκβ	Cell Signaling	4764S	3	1:400
Foxo1	Cell Signaling	2880B	5	1:300
pStat1	Cell Signaling	8183S	2	1:200
pErk1/2	Cell Signaling	9101S	27	1:200
pSmad2/3	Cell Signaling	8828S	4	1:400

Table 3.2 Details of antibodies used in the current study.

3.11 Methods

Cell lines and basal culture conditions

Normal and oncogenically manipulated immortalized Human Bronchial Epithelial Cells (HBECs) were cultured with Keratinocyte Serum Free Medium (KSFM; Life Technologies Inc., Carlsbad, CA) media containing 50 µg/mL of Bovine Pituitary Extract (BPE; Life Technologies Inc.) and 5 ng/mL of Epidermal Growth Factor (EGF; Life Technologies Inc.). Lung cancer cell lines, established in John Minna laboratory, were maintained in RPMI-1640 (Life Technologies Inc.) with 5% fetal bovine serum. All cell lines were DNA fingerprinted (PowerPlex 1.2 Kit, Promega, Madison, WI) and mycoplasma-free (e-Myco Kit, Boca Scientific, Boca Raton, FL).

Treatment with growth factors and inhibitors

To perturb the microenvironment of the cells grown in 2D culture condition, we have used varying concentration of Epidermal Growth Factor (EGF; Life Technologies Inc.), Transforming Growth Factor Beta 1 (TGFβ1; Life Technologies Inc.), SB431542 (Sigma-Aldrich Co. LLC.), Interferon Gamma 1 (IGF1; R&D Systems) and Fludarabine (Selleck Chemicals).

Liquid colony formation assay

For anchorage dependent liquid colony formation assay, 500 cells were seeded in each well of 6-well-plates (in triplicates for each cell line) for varying concentration of EGF as 0, 0.5, 5, 50, 500, 5000 pg/mL in KSFM. The cells were cultured for 2 weeks and then the colonies were stained with methylene blue.

Viral transfection and transduction of Omomyc construct

c-Myc target gene knockdown was achieved by the use of the Omomyc construct with pTripZ vector backbone. This virus was originally made by Laura Su-chek (from xxx lab). Cell lines were transduced as described previously and single cell clones with the highest range of RFP (inducible by doxycycline) intensity were selected.

qRT-PCR

The mRNA was isolated using QiaCube (Qiagen, xxx), the cDNA was made by iScript (Life Sciences Research). Quantitative Reverse Transcription PCR (qRT-PCR) was performed using validated Taqman primers and probes (Applied Biosystems, Foster City, CA) using Applied Biosystems 7500 qRT-PCR machine and relative expression was calculated using the $2^{-\Delta\Delta CT}$ method.

Treatment with c-Myc inhibitor

10058-F4 (Selleck Chemicals) was used for varying concentration (0, 23.5, 46.1, 70.6, 94.1, 117.6 µM) in liquid colony formation assay. Treatment of manipulated HBECs with 30 µM of drug was used for 3 days of treatment before qRT-PCR and immunofluorescence assay.

Treatment with chemotherapy drugs

Two chemotherapy drugs were used (Suppl. Table 2). Their Maximum tolerated dose (MTD), maximum plasma concentration ($C_P$max) were selected following xxx *et. al*. The tissue culture equivalent dose was calculated from MTD and $C_P$max as described by xxx *et. al*. The schedule was optimized for manipulated HBECs.

Treatment with Stat3 and Bcl6 inhibitors

BCL6 inhibitor 79-6 (Calbiochem, EMD Millipore) and Stat3 inhibitor Stattic (Calbiochem, EMD Millipore) was used for varying concentration in MTS drug sensitivity assay.

siRNA mediated knockdown

siRNA transfections were performed as described below. Cells were harvested48 h post-transfection to seed in *in vitro* tumorigenicity assays. 6-well siRNA invasion assays were performed with siRNAs at 20nM, RNAiMAX lipid (Life Technologies, Carlsbad, CA), and 50000 cells per well. At 48 hours cells were washed with PBS, trypsinized and mRNA was isolated using RNeasy Mini Kit (Qiagen).After 96 hours, cells were counted for viability. siRNA oligos were commercially validated and included positive siPLK1 (positive cell death phenotype), negative (non-silencing) controls (Qiagen, Hilden, Germany) and C911 controls (Buehler et al., 2012) (Sigma, USA).

Signaling readouts and immunofluorescence assay

Six signaling readouts were selected (Suppl. Table 3). Hoechst 33342 (Invitrogen Inc.) was used to identify nuclear regions. Cells were fixed with 4% paraformaldehyde for 5 minutes, permeabilized with ice cold 100% methanol at -20C for 10 minutes, washed with 0.1% TBST, blocked with 5% BSA solution in 0.1% TBST at room temperature for 30 minutes. 5% BSA in 0.1% TBST was used for primary and secondary antibody dilutions. Plates stained with primary antibodies were incubated at 4C overnight. They were washed with 0.1% TBST three times. Next, plates were incubated with secondary antibodies in the dark at room temperature for two hours and then washed again with

TBST three times. After the final washing step, 100µl of TBST containing 0.1% sodium azide was added to each well.

BCL6 as a novel targetable vulnerability

4.1 Bcl6 as a targetable vulnerability in a subset of lung cancers

4.1.1 BCL6 as a transcriptional repressor

B Cell Lymphoma 6 (BCL6) is a transcription repressor with various critical roles in cell types contributing to the innate and adaptive immune response. During the humoral response, BCL6 functions as a master regulator of the germinal center (GC) B cell phenotype (Hatzi and Melnick, 2014). GC B cells uniquely manifest under physiological conditions some of the characteristic hallmarks of tumor cells: they proliferate rapidly, evade growth checkpoint controls, and tolerate ongoing genomic instability occurring as a byproduct of somatic hypermutation. BCL6 enables and maintains the GC phenotype by repressing genes that control the cell cycle, cell death, terminal plasma cell differentiation, and DNA damage response(Phan and Dalla-Favera, 2004; Phan et al., 2005; Ranuncolo et al., 2007; Ranuncolo et al., 2008; Shaffer et al., 2000). For example, BCL6 represses TP53, CDKN1A, ATR, and CHEK1, allowing cells to sustain proliferation while rendering them resistant to DNA-damage induced apoptosis. BCL6 binds and represses numerous other tumor suppressors including CDKN1B, CDKN2A, CDKN2B, PTEN, and other genes (Ci et al., 2009). BCL6 also regulates genes involved in B cell signaling, thereby preventing premature termination of affinity maturation by T cells such as CD69, CD44, CD23b, and NF-KB1(Harris et al., 1999; Li et al., 2005; Shaffer et al., 2000), and silences genes that mediate terminal differentiation downstream of these signaling pathways such as PRDM1 and IRF4 (Shaffer et al., 2000) and (Tunyaplin et al., 2004).

4.1.2 BCL6 as a therapeutic target for B cell lymphoma

As BCL6 is expressed in majority of Diffused Large B Cell Lymphomas, and is required to maintain the survival of established lymphoma cells, created interest in utilizing BCL6 as a therapeutic target. Features that make the BCL6 BTB domain an attractive target include: a) residues through which BCL6 interacts with the SMRT, NCOR, and BCOR are unique to BCL6 and not conserved in other BTB domains, raising the possibility of developing specific inhibitors less likely to disrupt other related transcription factors; b) the BCL6 BTB domain corepressor interface is not involved in the lethal inflammatory phenotype that is caused by total loss of the BCL6 protein, thus reducing the likelihood of on-target toxicity; and c) the BTB corepressor interface contains structural epitopes involved in key intermolecular interactions that can be targeted by the design of competitive inhibitors. Drug design efforts led to the development of truncated, retro-inverso BCL6 peptidomimetic inhibitors (RI-BPIs), which display favorable pharmacokinetic properties and can fully eradicate established lymphomas in mouse models (Cerchietti et al., 2010; Cerchietti et al., 2009). RI-BPIs and other BCL6 small molecule inhibitors are currently being translated for use in humans. Computer-aided drug design enabled identification of a small molecule lead compound called 79-6 with similar anti-lymphoma activity. RI-BPIs and 79-6 do not induce any toxicity in animals, even when administered for up to 1 year in a continuous manner, which is consistent with the $Bcl6^{BTBmut}$ mouse model.

4.1.3 BCL6 as a therapeutic target in breast cancer

BCL6 was found to be highly expressed in breast cancer cell lines (Walker et al., 2015). In addition, the BCL6 locus was found to be amplified in many primary breast cancers.

Interestingly, BCL6 regulates a unique cohort of genes in breast cancer cell lines compared to B-cell lymphomas. Hence, BCL6 transcriptional mechanism may vary in a cell type-specific manner. It is important to note that the expression of the well described target gene PRDM1 was altered in lymphoma as well as breast cancer. It was shown that BCL6 expression promotes breast cancer cell survival and targeting BCL6 with a peptidomimetic inhibitor leads to apoptosis. Finally, a combination treatment using both BCL6 inhibitor and Stat3 signaling inhibitor provided enhanced cell death in triple-negative breast cancer. These results suggest that in addition to lymphoma and breast cancer, BCL6 can be a targetable vulnerability in other types of cancer as well.

4.2 BCL6 as a novel target in a subset of lung cancers

In the previous chapter, we have observed that the triple manipulated HBEC shows Smad2/3 downregulation and Bcl6 upregulation. We have utilized pharmacological inhibition and genetic knockdown techniques to observe BCL6 as a targetable vulnerability. Although BCL6 was a novel target in our simplified model of lung cancer – HBECs, we wondered if we can identify any patient derived primary lung cancer cell lines with high BCL6 expression.

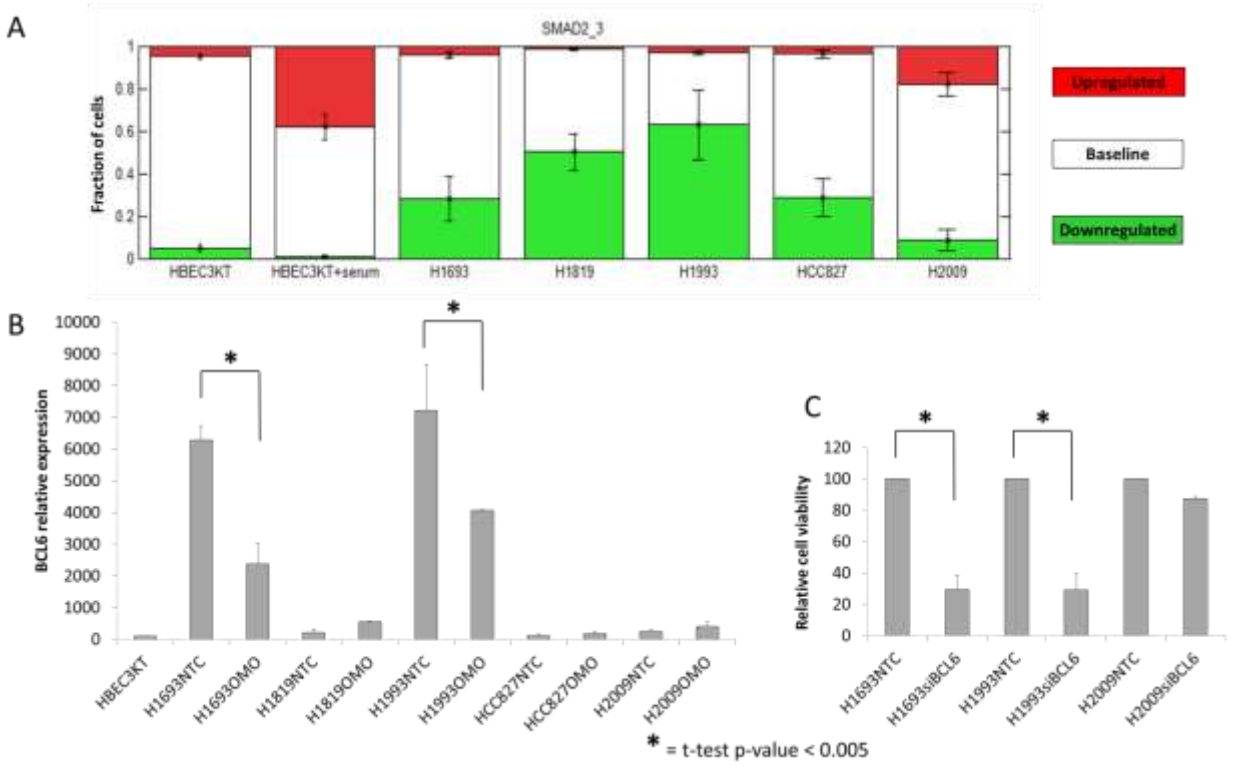

Figure 4.1 BCL6 can be a targetable vulnerability in a subset of c-Myc addicted lung cancers

Can we identify Myc-addicted lung cancer cell lines that have Smad2/3 downregulation and Bcl6 upregulation? In our HBEC system we have observed that the transformed HBECs decrease their Bcl6 expression after Myc target genes are knocked down. However, recent studies from John Minna's laboratory suggest that in lung cancer, Myc-addiction is functionally more important than Myc-overexpression. Hence, we tested five lung cancer cell lines among which H1693, H1819, H1993, HCC827 are addicted and H2009 is not addicted to Myc. We observed that H1693, H1819, H1993 and HCC827 show increased number of Smad2/3 downregulated cells compared parental HBEC (Fig. 6A). But, H2009 showed increased number of cells with Smad2/3 upregulation. Parental HBEC treated with 10% serum for 40 minutes was used as a positive control. Next, we tested if any of these cell lines had high level of Bcl6. H1693 and H1993

showed surprisingly high level of Bcl6 gene expression compared to parental HBEC in our qRTPCR assay (Fig. 6B). Interestingly, the high level of Bcl6 decreases significantly after Myc target gene knockdown using the Omomyc construct, a trend that we observed in the transformed HBECs (Fig. 5C). Finally, after siRNA mediated knockdown of BCL6 we have observed that H1693 and H1993 showed significantly higher cell death than H2009 (Figure 6C). Hence, our data suggests that Bcl6 can be a targetable vulnerability in a subset of Myc-addicted lung cancers.

4.3 Methods

Cell lines and basal culture conditions

Normal and oncogenically manipulated immortalized Human Bronchial Epithelial Cells (HBECs) were cultured with Keratinocyte Serum Free Medium (KSFM; Life Technologies Inc., Carlsbad, CA) media containing 50 µg/mL of Bovine Pituitary Extract (BPE; Life Technologies Inc.) and 5 ng/mL of Epidermal Growth Factor (EGF; Life Technologies Inc.). Lung cancer cell lines, established in John Minna laboratory, were maintained in RPMI-1640 (Life Technologies Inc.) with 5% fetal bovine serum. All cell lines were DNA fingerprinted (PowerPlex 1.2 Kit, Promega, Madison, WI) and mycoplasma-free (e-Myco Kit, Boca Scientific, Boca Raton, FL).

siRNA mediated knockdown

siRNA transfections were performed as described below. Cells were harvested48 h post-transfection to seed in *in vitro* tumorigenicity assays. 6-well siRNA invasion assays were performed with siRNAs at 20nM, RNAiMAX lipid(Life Technologies, Carlsbad, CA), and 50000 cells per well. At 48 hours cells were washed with PBS, trypsinized and

mRNA was isolated using RNeasy Mini Kit (Qiagen).After 96 hours, cells were counted for viability. siRNA oligos were commercially validated and included positive siPLK1 (positive cell death phenotype), negative (non-silencing) controls (Qiagen, Hilden, Germany) and C911 controls (Buehler et al., 2012) (Sigma, USA).

Signaling readouts and immunofluorescence assay

Six signaling readouts were selected (Suppl. Table 3). Hoechst 33342 (Invitrogen Inc.) was used to identify nuclear regions. Cells were fixed with 4% paraformaldehyde for 5 minutes, permeabilized with ice cold 100% methanol at -20C for 10 minutes, washed with 0.1% TBST, blocked with 5% BSA solution in 0.1% TBST at room temperature for 30 minutes. 5% BSA in 0.1% TBST was used for primary and secondary antibody dilutions. Plates stained with primary antibodies were incubated at 4C overnight. They were washed with 0.1% TBST three times. Next, plates were incubated with secondary antibodies in the dark at room temperature for two hours and then washed again with TBST three times. After the final washing step, 100µl of TBST containing 0.1% sodium azide was added to each well.

qRT-PCR

The mRNA was isolated using QiaCube (Qiagen, USA), the cDNA was made by iScript (Life Sciences Research). Quantitative Reverse Transcription PCR (qRT-PCR) was performed using validated Taqman primers and probes (Applied Biosystems, Foster City, CA) using Applied Biosystems 7500 qRT-PCR machine and relative expression was calculated using the $2^{-\Delta\Delta CT}$ method.

Conclusion and Future Direction

5.1 Questions unanswered and looking forward

The unavailability of "clinically actionable" targets for the majority of driver oncogenes in lung cancer begs for the search of novel targetable vulnerabilities (McCutcheon and Giaccone, 2015). In this thesis, we have studied Smad2/3 signaling alteration after three major oncogenic changes (p53null, $KRas^{V12}$, c-Myc overexpression) (Sato et al., 2013) at single-cell level. From downstream targets of Smad2/3 signaling (Massague, 2008; Massague and Gomis, 2006; Massague et al., 2005; Padua and Massague, 2009) we have identified Bcl6 as a targetable vulnerability in lung cancer. We have further shown that Bcl6 can be a novel targetable vulnerability in a subset of c-Myc addicted lung cancers.

In our single-cell image analysis, we have identified changes in cellular localization of β-catenin and Stat3 in addition to Smad2/3 in the transformed HBECs. Although β-catenin has been studied widely in epithelial and mesenchymal lung cancer cells (Scharl et al., 2015; Yang et al., 2015), the connection between c-Myc and β-catenin signaling is not well understood (Higgs et al., 2013; Juan et al., 2014; Lee et al., 2014; Li et al., 2012; Xie et al., 2014; Xu et al., 2015; Zhang et al., 2012a). c-Myc overexpression and Jak-Stat pathway signaling has been studied in breast cancer (Ref). In lung cancer upregulation of Stat3 signaling has been connected with ALDH1A3 positive lung cancer stem cells. However, these signaling pathways have not been studies widely in single-cells. Further single-cell studies will be interesting to understand if c-Myc dependent b-catenin and Stat3 signaling alterations occur in the same cells of the population.

To identify targetable vulnerabilities in Smad2/3 signaling we have observed high differential overexpression of 3 genes in the transformed HBECs - Sox2, Bcl6 and Mmp7. We focused on Bcl6 as in double-hit lymphoma cases Bcl6 is known to strongly correlate with c-Myc expression (Cinar et al., 2015; Lindsley and LaCasce, 2012; Oki et al., 2014; Yan et al., 2014), which was also observed in our transformed HBECs. However, Sox2 amplification has been well studied in lung cancer as a progenitor cell marker (Chou et al., 2013; Ischenko et al., 2014). Similarly, Mmp proteins have been characterized in understanding of matrix proteins and their connection with lung cancer pathogenesis (Leinonen et al., 2006; Safranek et al., 2007; Sasaki et al., 2001; Yamamoto et al., 2012). It would be interesting to study the connection of Sox2 and Mmp7 signaling with c-Myc addicted lung cancers to identify novel targetable vulnerabilities.

In the current study we have identified a strong correlation between c-Myc and Bcl6 expression in both population as well as single-cell level. Our panel of cell lines includes HBECs and lung cancer lines - H1693, H1993 and H2009. It will be interesting to screen a large panel of lung cancer cell lines for the correlation between c-Myc and Bcl6 to identify "double-hit" lung cancers. Additionally, further understanding of downstream targets of Bcl6 via RNA-seq studies are required to identify Bcl6-dependent cells (Walker et al., 2015). Finally, c-Myc and BCL6 protein expression in lung cancer patient tumor tissues need to be analyzed.

In the end, we show that single-cell analysis of driver oncogenes and their downstream signaling pathways can be utilized to identify novel targetable vulnerabilities. Further single-cell studies on other important oncogenes in lung cancer such as KRAS, LKB1,

and their downstream signaling will be useful (Kim et al., 2013). With the advent of high throughput studies, combining deep sequencing assays and high throughput immunofluorescence imaging assays to study the connection of intra tumor genetic heterogeneity and their downstream signaling heterogeneity in patient tissue samples can provide novel targetable vulnerabilities in lung cancer.

Appendix

1. Considerable variability at single cell level

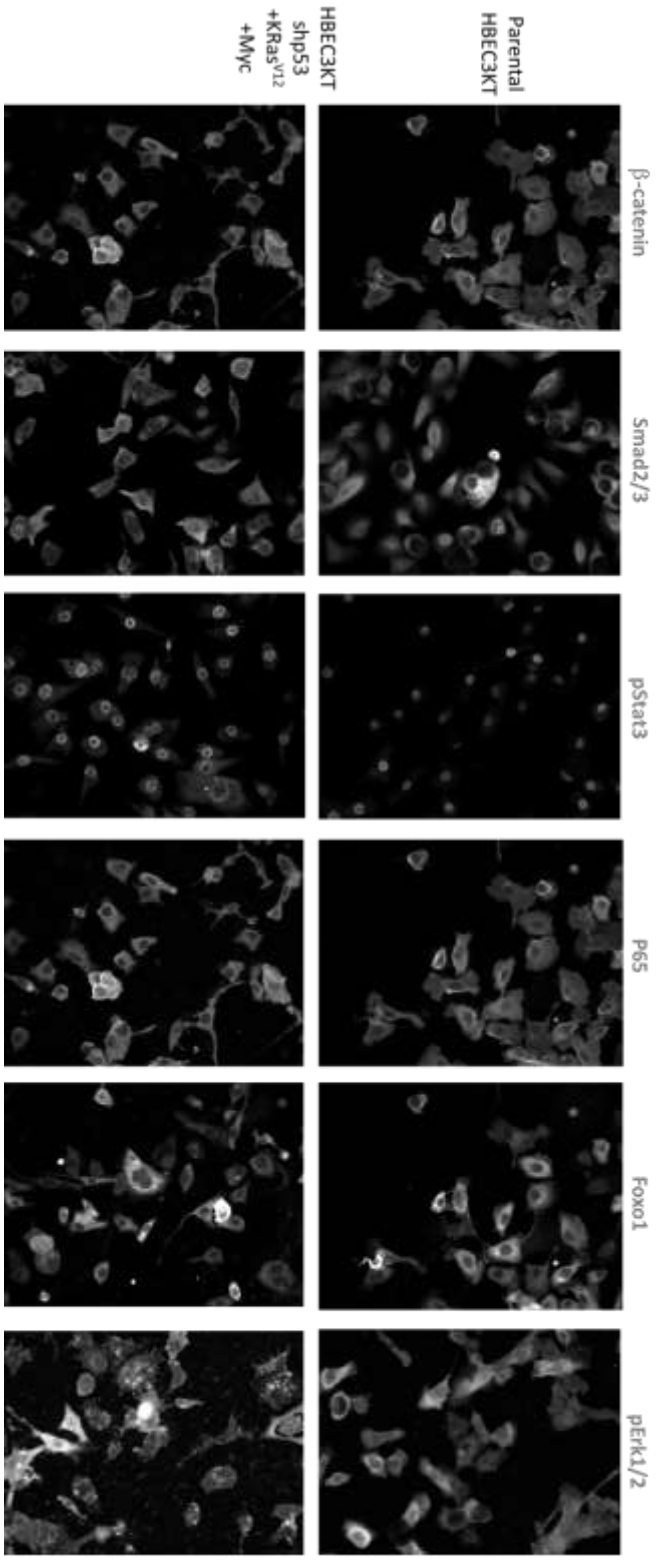

2. Reproducible signaling phenotype with total and phospho antibodies

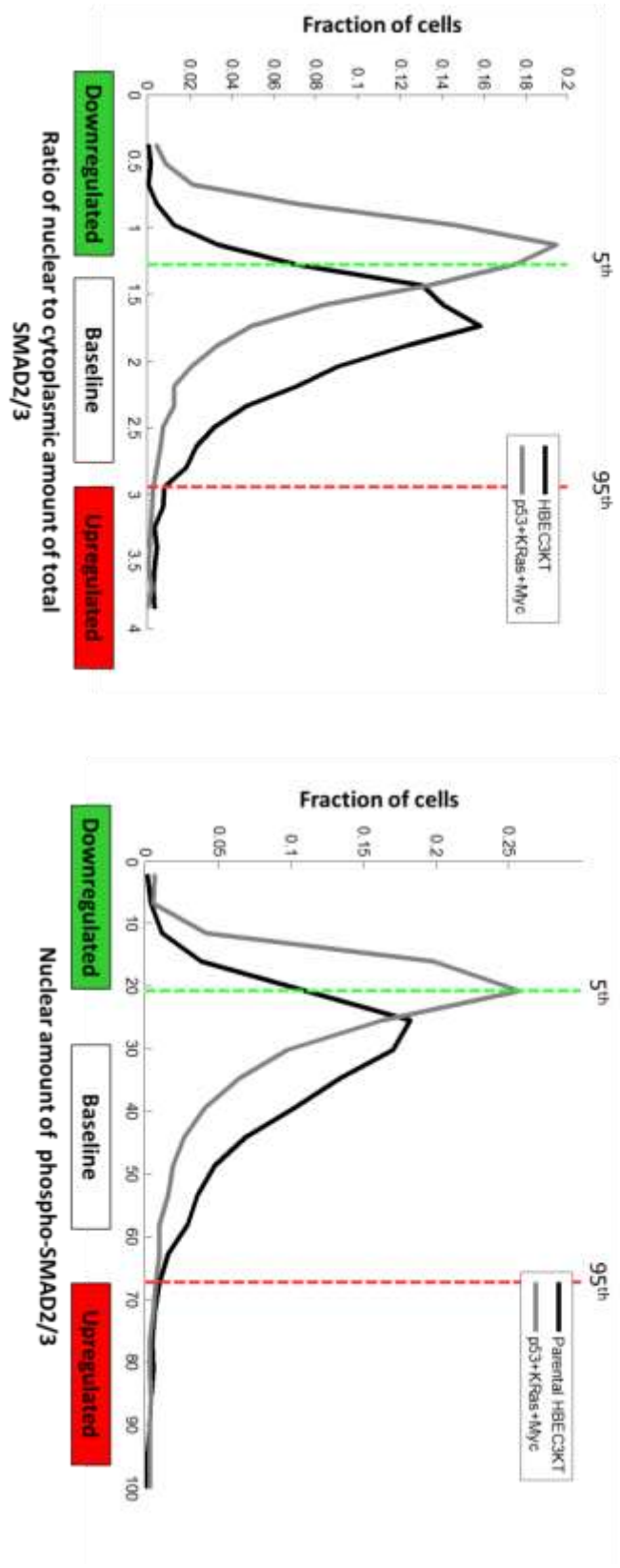

3. No difference in ERK1/2 protein level and in sensitivity to drugs targeting ERK pathway

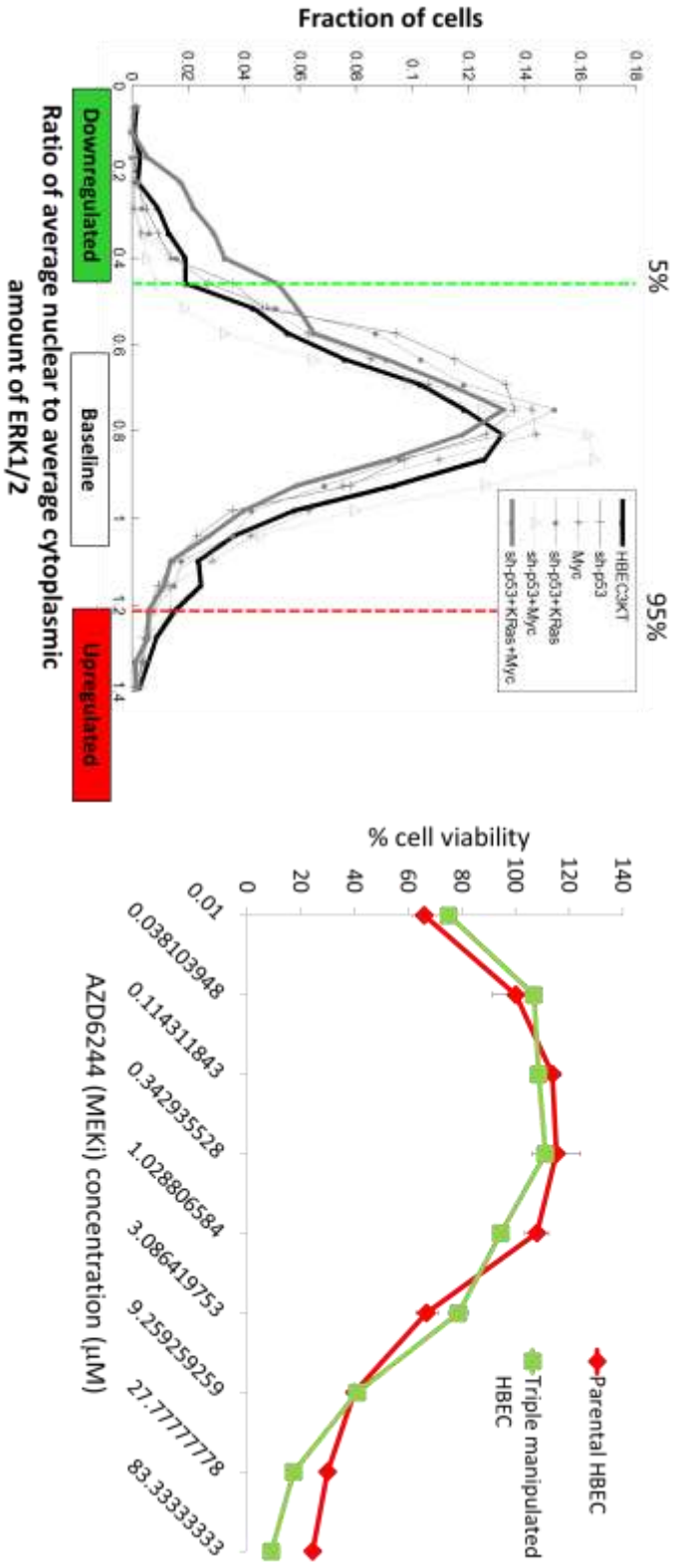

4. Dynamic range of SMAD2/3 response to TGFβ stimulus

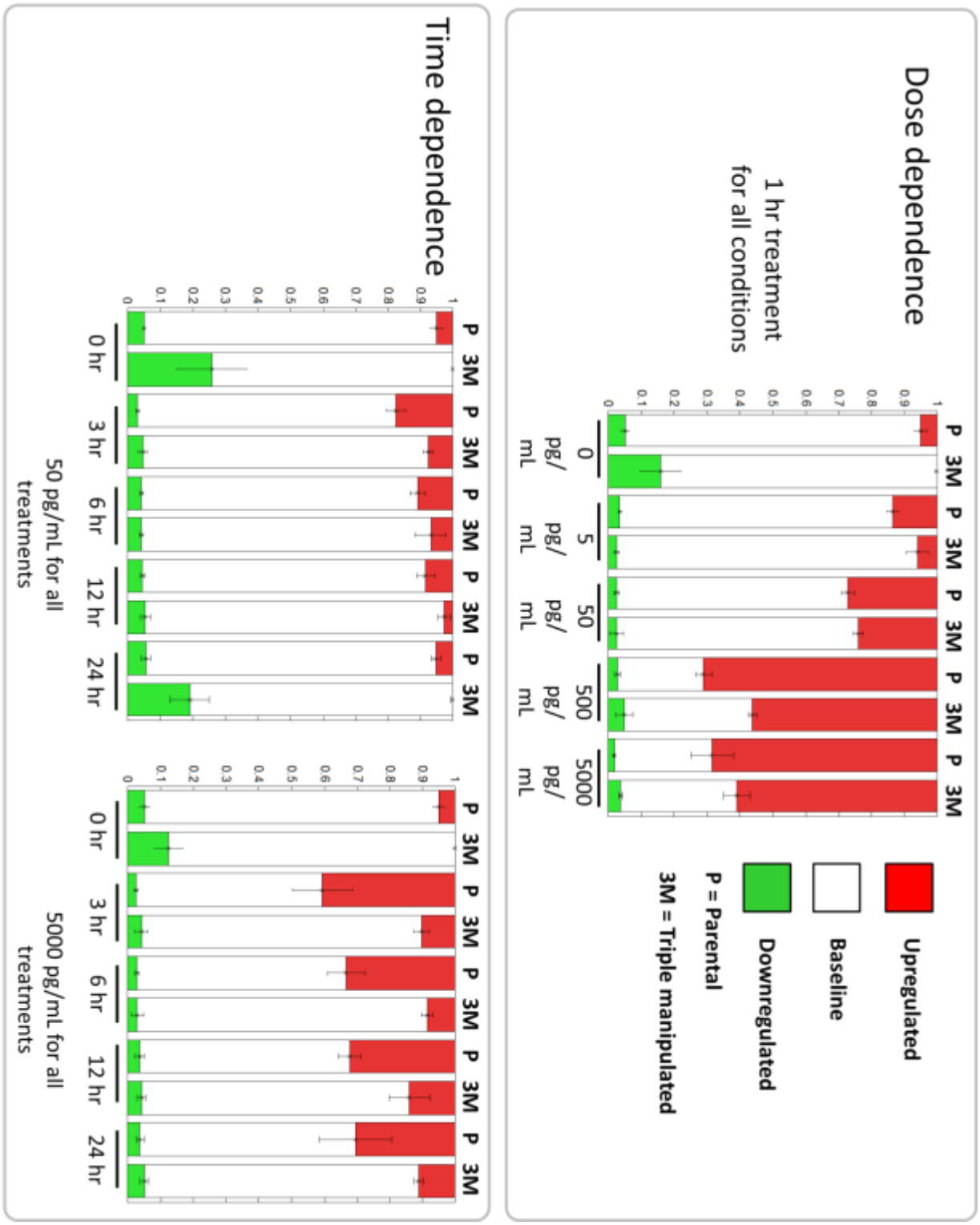

5. Altered fraction of cells are distributed in all stages of cell cycle

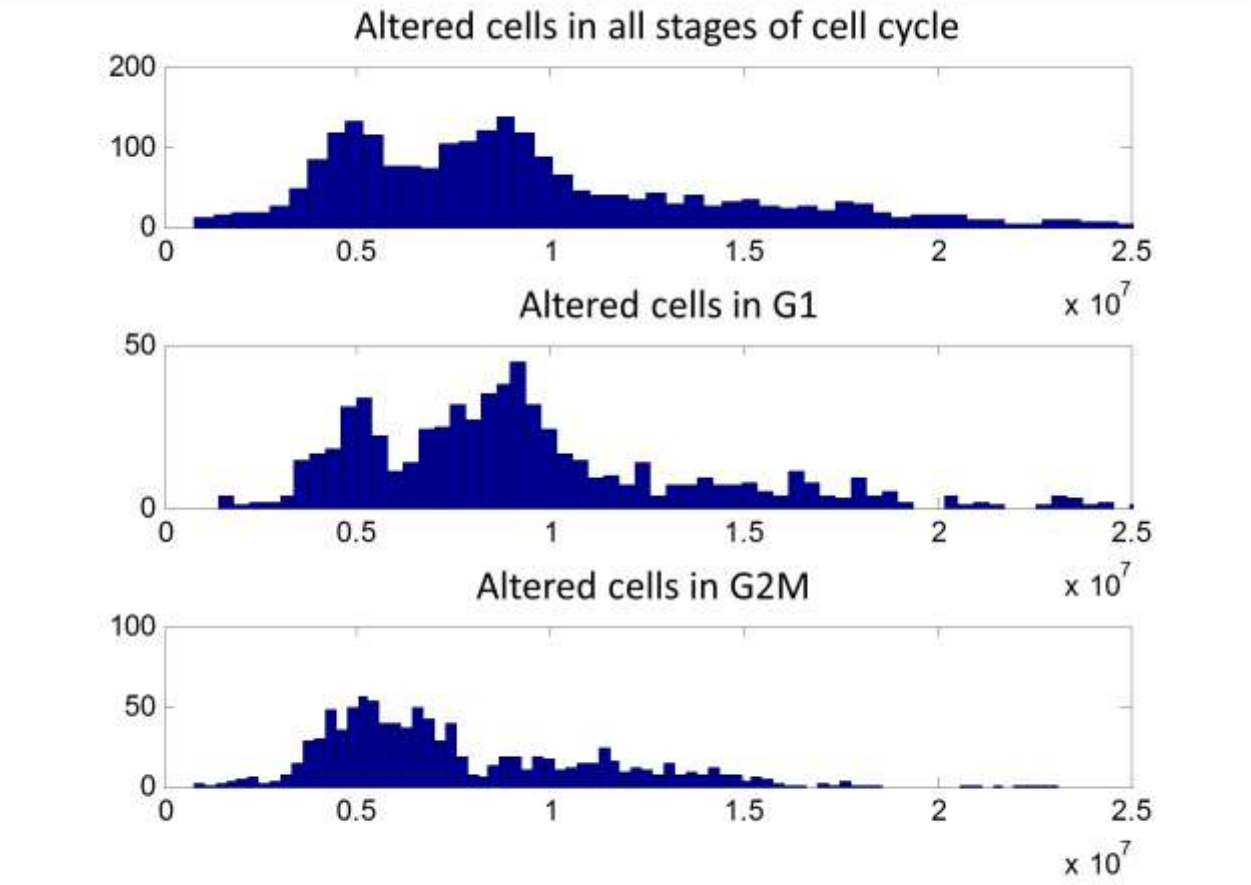

6. Smad2/3 and pStat3 correlation in parental HBEC3KT

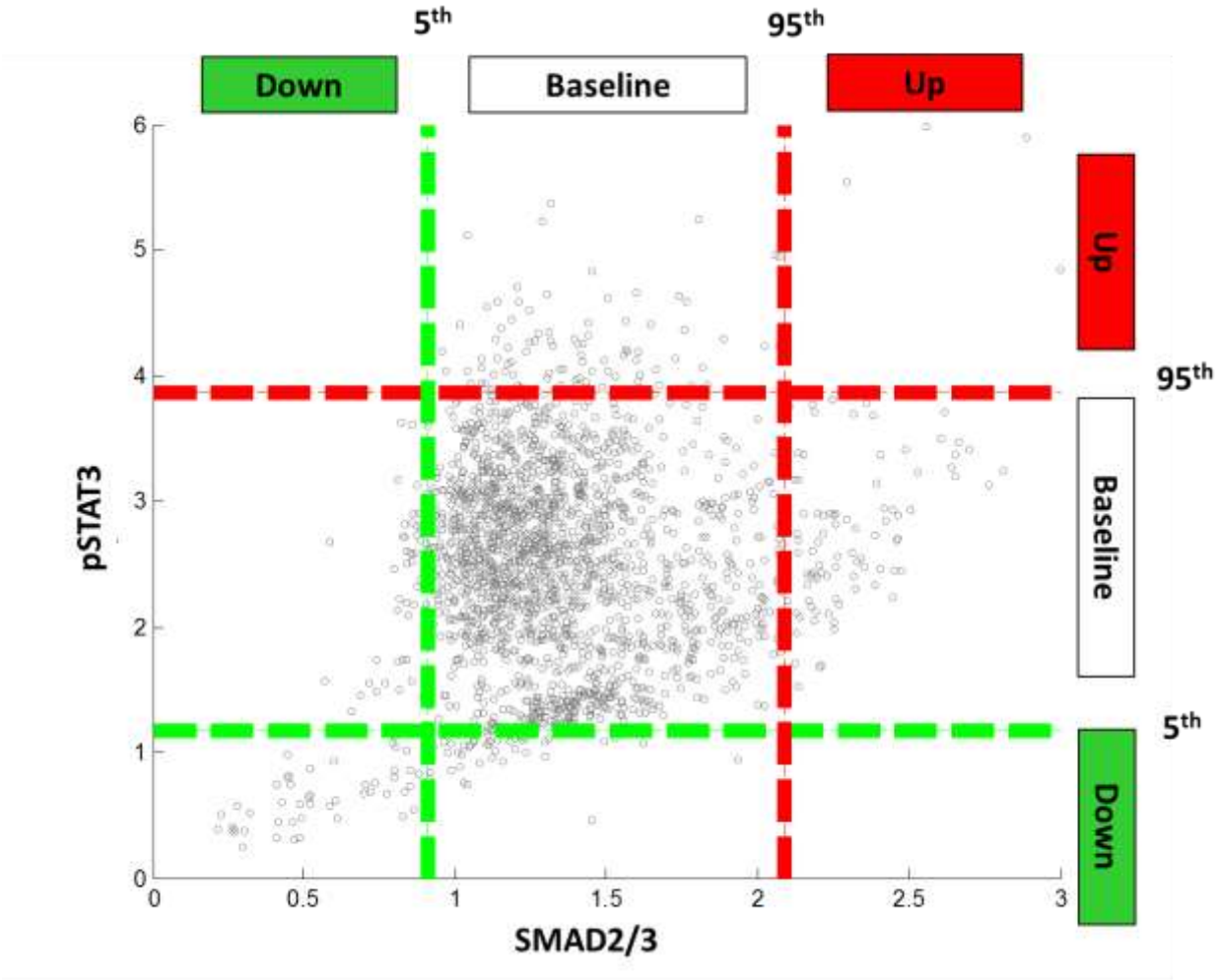

7. Atlas of heterogeneity (using volume in feature space measurement) in lung cancer oncogenic progression

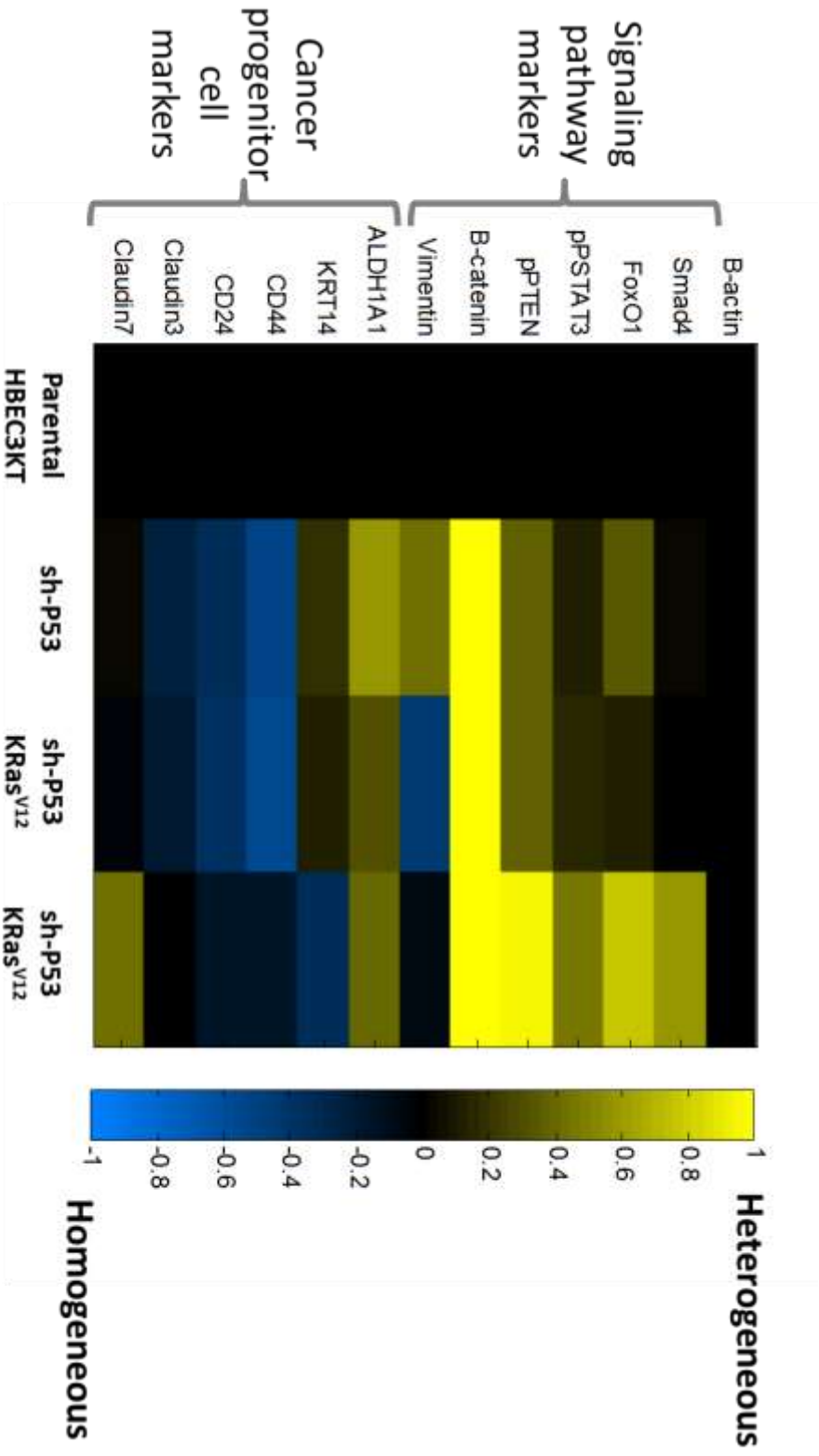

Bibliography

(2014). Comprehensive molecular profiling of lung adenocarcinoma. Nature *511*, 543-550.
Ahn, J.S., Lee, K.H., Sun, J.M., Park, K., Kang, E.S., Cho, E.K., Lee, D.H., Kim, S.W., Lee, G.W., Kang, J.H.*, et al.* (2013). A randomized, phase II study of vandetanib maintenance for advanced or metastatic non-small-cell lung cancer following first-line platinum-doublet chemotherapy. Lung cancer (Amsterdam, Netherlands) *82*, 455-460.
Akhurst, R.J., and Hata, A. (2012). Targeting the TGFbeta signalling pathway in disease. Nature reviews Drug discovery *11*, 790-811.
Akiri, G., Cherian, M.M., Vijayakumar, S., Liu, G., Bafico, A., and Aaronson, S.A. (2009). Wnt pathway aberrations including autocrine Wnt activation occur at high frequency in human non-small-cell lung carcinoma. Oncogene *28*, 2163-2172.
Albihn, A., Johnsen, J.I., and Henriksson, M.A. (2010). MYC in oncogenesis and as a target for cancer therapies. Advances in cancer research *107*, 163-224.
Almendro, V., Marusyk, A., and Polyak, K. (2013). Cellular heterogeneity and molecular evolution in cancer. Annual review of pathology *8*, 277-302.
Altschuler, S.J., and Wu, L.F. (2010). Cellular heterogeneity: do differences make a difference? Cell *141*, 559-563.
Bajikar, S.S., Fuchs, C., Roller, A., Theis, F.J., and Janes, K.A. (2014). Parameterizing cell-to-cell regulatory heterogeneities via stochastic transcriptional profiles. Proceedings of the National Academy of Sciences of the United States of America *111*, E626-635.
Bartis, D., Csongei, V., Weich, A., Kiss, E., Barko, S., Kovacs, T., Avdicevic, M., D'Souza, V.K., Rapp, J., Kvell, K.*, et al.* (2013). Down-regulation of canonical and up-regulation of non-canonical Wnt signalling in the carcinogenic process of squamous cell lung carcinoma. PloS one *8*, e57393.
Boggio, K.J., Obasuyi, E., Sugino, K., Nelson, S.B., Agar, N.Y., and Agar, J.N. (2011). Recent advances in single-cell MALDI mass spectrometry imaging and potential clinical impact. Expert review of proteomics *8*, 591-604.
Brown, T.M., and Fee, E. (2006). Rudolf Carl Virchow: medical scientist, social reformer, role model. American journal of public health *96*, 2104-2105.
Brunetto, A.T., Carden, C.P., Myerson, J., Faria, A.L., Ashley, S., Popat, S., and O'Brien, M.E. (2010). Modest reductions in dose intensity and drug-induced neutropenia have no major impact on survival of patients with non-small cell lung cancer treated with platinum-doublet chemotherapy. Journal of thoracic oncology : official publication of the International Association for the Study of Lung Cancer *5*, 1397-1403.
Buehler, E., Chen, Y.C., and Martin, S. (2012). C911: A bench-level control for sequence specific siRNA off-target effects. PloS one *7*, e51942.
Cataldo, V.D., Gibbons, D.L., Perez-Soler, R., and Quintas-Cardama, A. (2011). Treatment of non-small-cell lung cancer with erlotinib or gefitinib. The New England journal of medicine *364*, 947-955.
Cerchietti, L.C., Ghetu, A.F., Zhu, X., Da Silva, G.F., Zhong, S., Matthews, M., Bunting, K.L., Polo, J.M., Fares, C., Arrowsmith, C.H.*, et al.* (2010). A small-molecule inhibitor of BCL6 kills DLBCL cells in vitro and in vivo. Cancer cell *17*, 400-411.
Cerchietti, L.C., Yang, S.N., Shaknovich, R., Hatzi, K., Polo, J.M., Chadburn, A., Dowdy, S.F., and Melnick, A. (2009). A peptomimetic inhibitor of BCL6 with potent antilymphoma effects in vitro and in vivo. Blood *113*, 3397-3405.
Chou, Y.T., Lee, C.C., Hsiao, S.H., Lin, S.E., Lin, S.C., Chung, C.H., Chung, C.H., Kao, Y.R., Wang, Y.H., Chen, C.T.*, et al.* (2013). The emerging role of SOX2 in cell proliferation and survival and its crosstalk with oncogenic signaling in lung cancer. Stem cells (Dayton, Ohio) *31*, 2607-2619.

Ci, W., Polo, J.M., Cerchietti, L., Shaknovich, R., Wang, L., Yang, S.N., Ye, K., Farinha, P., Horsman, D.E., Gascoyne, R.D*., et al.* (2009). The BCL6 transcriptional program features repression of multiple oncogenes in primary B cells and is deregulated in DLBCL. Blood *113*, 5536-5548.
Cinar, M., Rosenfelt, F., Rokhsar, S., Lopategui, J., Pillai, R., Cervania, M., Pao, A., Cinar, B., and Alkan, S. (2015). Concurrent inhibition of MYC and BCL2 is a potentially effective treatment strategy for double hit and triple hit B-cell lymphomas. Leukemia research.
Cotari, J.W., Voisinne, G., and Altan-Bonnet, G. (2013). Diversity training for signal transduction: leveraging cell-to-cell variability to dissect cellular signaling, differentiation and death. Current opinion in biotechnology *24*, 760-766.
Custodio, A., Mendez, M., and Provencio, M. (2012). Targeted therapies for advanced non-small-cell lung cancer: current status and future implications. Cancer treatment reviews *38*, 36-53.
de Bruin, E.C., McGranahan, N., Mitter, R., Salm, M., Wedge, D.C., Yates, L., Jamal-Hanjani, M., Shafi, S., Murugaesu, N., Rowan, A.J*., et al.* (2014). Spatial and temporal diversity in genomic instability processes defines lung cancer evolution. Science (New York, NY) *346*, 251-256.
Ding, L., Getz, G., Wheeler, D.A., Mardis, E.R., McLellan, M.D., Cibulskis, K., Sougnez, C., Greulich, H., Muzny, D.M., Morgan, M.B*., et al.* (2008). Somatic mutations affect key pathways in lung adenocarcinoma. Nature *455*, 1069-1075.
Fidler, I.J. (1978). Tumor heterogeneity and the biology of cancer invasion and metastasis. Cancer research *38*, 2651-2660.
Fidler, I.J., and Kripke, M.L. (1977). Metastasis results from preexisting variant cells within a malignant tumor. Science (New York, NY) *197*, 893-895.
Gazdar, A.F. (2010). Should we continue to use the term non-small-cell lung cancer? Annals of oncology : official journal of the European Society for Medical Oncology / ESMO *21 Suppl 7*, vii225-229.
Gerlinger, M., Rowan, A.J., Horswell, S., Larkin, J., Endesfelder, D., Gronroos, E., Martinez, P., Matthews, N., Stewart, A., Tarpey, P*., et al.* (2012). Intratumor heterogeneity and branched evolution revealed by multiregion sequencing. The New England journal of medicine *366*, 883-892.
Giesen, C., Wang, H.A., Schapiro, D., Zivanovic, N., Jacobs, A., Hattendorf, B., Schuffler, P.J., Grolimund, D., Buhmann, J.M., Brandt, S*., et al.* (2014). Highly multiplexed imaging of tumor tissues with subcellular resolution by mass cytometry. Nature methods *11*, 417-422.
Gough, A.H., Chen, N., Shun, T.Y., Lezon, T.R., Boltz, R.C., Reese, C.E., Wagner, J., Vernetti, L.A., Grandis, J.R., Lee, A.V*., et al.* (2014). Identifying and quantifying heterogeneity in high content analysis: application of heterogeneity indices to drug discovery. PloS one *9*, e102678.
Govindan, R., Ding, L., Griffith, M., Subramanian, J., Dees, N.D., Kanchi, K.L., Maher, C.A., Fulton, R., Fulton, L., Wallis, J*., et al.* (2012). Genomic landscape of non-small cell lung cancer in smokers and never-smokers. Cell *150*, 1121-1134.
Hanahan, D., and Weinberg, R.A. (2011). Hallmarks of cancer: the next generation. Cell *144*, 646-674.
Harris, M.B., Chang, C.C., Berton, M.T., Danial, N.N., Zhang, J., Kuehner, D., Ye, B.H., Kvatyuk, M., Pandolfi, P.P., Cattoretti, G*., et al.* (1999). Transcriptional repression of Stat6-dependent interleukin-4-induced genes by BCL-6: specific regulation of iepsilon transcription and immunoglobulin E switching. Molecular and cellular biology *19*, 7264-7275.
Hasenauer, J., Heinrich, J., Doszczak, M., Scheurich, P., Weiskopf, D., and Allgower, F. (2012). A visual analytics approach for models of heterogeneous cell populations. EURASIP journal on bioinformatics & systems biology *2012*, 4.
Hatzi, K., and Melnick, A. (2014). Breaking bad in the germinal center: how deregulation of BCL6 contributes to lymphomagenesis. Trends in molecular medicine *20*, 343-352.
Hawkins, R.A., Roberts, M.M., and Forrest, A.P. (1980). Oestrogen receptors and breast cancer: current status. The British journal of surgery *67*, 153-169.

Heppner, G.H., and Miller, B.E. (1983). Tumor heterogeneity: biological implications and therapeutic consequences. Cancer metastasis reviews *2*, 5-23.
Higgs, M.R., Lerat, H., and Pawlotsky, J.M. (2013). Hepatitis C virus-induced activation of beta-catenin promotes c-Myc expression and a cascade of pro-carcinogenetic events. Oncogene *32*, 4683-4693.
Hohenforst-Schmidt, W., Zarogoulidis, P., Darwiche, K., Vogl, T., Goldberg, E.P., Huang, H., Simoff, M., Li, Q., Browning, R., Turner, F.J*., et al.* (2013). Intratumoral chemotherapy for lung cancer: re-challenge current targeted therapies. Drug design, development and therapy *7*, 571-583.
Imielinski, M., Berger, A.H., Hammerman, P.S., Hernandez, B., Pugh, T.J., Hodis, E., Cho, J., Suh, J., Capelletti, M., Sivachenko, A*., et al.* (2012). Mapping the hallmarks of lung adenocarcinoma with massively parallel sequencing. Cell *150*, 1107-1120.
Ischenko, I., Liu, J., Petrenko, O., and Hayman, M.J. (2014). Transforming growth factor-beta signaling network regulates plasticity and lineage commitment of lung cancer cells. Cell death and differentiation *21*, 1218-1228.
Iwakawa, R., Kohno, T., Kato, M., Shiraishi, K., Tsuta, K., Noguchi, M., Ogawa, S., and Yokota, J. (2011). MYC amplification as a prognostic marker of early-stage lung adenocarcinoma identified by whole genome copy number analysis. Clinical cancer research : an official journal of the American Association for Cancer Research *17*, 1481-1489.
Jeannot, V., Busser, B., Brambilla, E., Wislez, M., Robin, B., Cadranel, J., Coll, J.L., and Hurbin, A. (2014). The PI3K/AKT pathway promotes gefitinib resistance in mutant KRAS lung adenocarcinoma by a deacetylase-dependent mechanism. International journal of cancer Journal international du cancer *134*, 2560-2571.
Ju, Y.S., Lee, W.C., Shin, J.Y., Lee, S., Bleazard, T., Won, J.K., Kim, Y.T., Kim, J.I., Kang, J.H., and Seo, J.S. (2012). A transforming KIF5B and RET gene fusion in lung adenocarcinoma revealed from whole-genome and transcriptome sequencing. Genome research *22*, 436-445.
Juan, J., Muraguchi, T., Iezza, G., Sears, R.C., and McMahon, M. (2014). Diminished WNT -> beta-catenin -> c-MYC signaling is a barrier for malignant progression of BRAFV600E-induced lung tumors. Genes & development *28*, 561-575.
Jung, M.J., Rho, J.K., Kim, Y.M., Jung, J.E., Jin, Y.B., Ko, Y.G., Lee, J.S., Lee, S.J., Lee, J.C., and Park, M.J. (2013). Upregulation of CXCR4 is functionally crucial for maintenance of stemness in drug-resistant non-small cell lung cancer cells. Oncogene *32*, 209-221.
Kahn, M. (2014). Can we safely target the WNT pathway? Nature reviews Drug discovery *13*, 513-532.
Kim, H.S., Mendiratta, S., Kim, J., Pecot, C.V., Larsen, J.E., Zubovych, I., Seo, B.Y., Kim, J., Eskiocak, B., Chung, H*., et al.* (2013). Systematic identification of molecular subtype-selective vulnerabilities in non-small-cell lung cancer. Cell *155*, 552-566.
Kwak, E.L., Bang, Y.J., Camidge, D.R., Shaw, A.T., Solomon, B., Maki, R.G., Ou, S.H., Dezube, B.J., Janne, P.A., Costa, D.B*., et al.* (2010). Anaplastic lymphoma kinase inhibition in non-small-cell lung cancer. The New England journal of medicine *363*, 1693-1703.
Larsen, J.E., Cascone, T., Gerber, D.E., Heymach, J.V., and Minna, J.D. (2011). Targeted therapies for lung cancer: clinical experience and novel agents. Cancer journal (Sudbury, Mass) *17*, 512-527.
Larsen, J.E., and Minna, J.D. (2011). Molecular biology of lung cancer: clinical implications. Clinics in chest medicine *32*, 703-740.
Lee, K.B., Ye, S., Park, M.H., Park, B.H., Lee, J.S., and Kim, S.M. (2014). p63-Mediated activation of the beta-catenin/c-Myc signaling pathway stimulates esophageal squamous carcinoma cell invasion and metastasis. Cancer letters *353*, 124-132.
Leinonen, T., Pirinen, R., Bohm, J., Johansson, R., Ropponen, K., and Kosma, V.M. (2006). Expression of matrix metalloproteinases 7 and 9 in non-small cell lung cancer. Relation to clinicopathological factors, beta-catenin and prognosis. Lung cancer (Amsterdam, Netherlands) *51*, 313-321.

Li, Y., Gao, Q., Yin, G., Ding, X., and Hao, J. (2012). WNT/beta-catenin-signaling pathway stimulates the proliferation of cultured adult human Sertoli cells via upregulation of C-myc expression. Reproductive sciences (Thousand Oaks, Calif) *19*, 1232-1240.
Li, Z., Wang, X., Yu, R.Y., Ding, B.B., Yu, J.J., Dai, X.M., Naganuma, A., Stanley, E.R., and Ye, B.H. (2005). BCL-6 negatively regulates expression of the NF-kappaB1 p105/p50 subunit. Journal of immunology *174*, 205-214.
Lin, P., and Medeiros, L.J. (2013). The impact of MYC rearrangements and "double hit" abnormalities in diffuse large B-cell lymphoma. Current hematologic malignancy reports *8*, 243-252.
Lindsley, R.C., and LaCasce, A.S. (2012). Biology of double-hit B-cell lymphomas. Current opinion in hematology *19*, 299-304.
Loo, L.H., Lin, H.J., Steininger, R.J., 3rd, Wang, Y., Wu, L.F., and Altschuler, S.J. (2009). An approach for extensibly profiling the molecular states of cellular subpopulations. Nature methods *6*, 759-765.
Loo, L.H., Wu, L.F., and Altschuler, S.J. (2007). Image-based multivariate profiling of drug responses from single cells. Nat Methods *4*, 445-453.
Lubin, R., Zalcman, G., Bouchet, L., Tredanel, J., Legros, Y., Cazals, D., Hirsch, A., and Soussi, T. (1995). Serum p53 antibodies as early markers of lung cancer. Nature medicine *1*, 701-702.
Makino, S. (1956). Further evidence favoring the concept of the stem cell in ascites tumors of rats. Annals of the New York Academy of Sciences *63*, 818-830.
Massague, J. (2008). TGFbeta in Cancer. Cell *134*, 215-230.
Massague, J. (2012). TGFbeta signalling in context. Nature reviews Molecular cell biology *13*, 616-630.
Massague, J., and Gomis, R.R. (2006). The logic of TGFbeta signaling. FEBS letters *580*, 2811-2820.
Massague, J., Seoane, J., and Wotton, D. (2005). Smad transcription factors. Genes & development *19*, 2783-2810.
McCutcheon, J.N., and Giaccone, G. (2015). Next-Generation Sequencing: Targeting Targeted Therapies. Clinical cancer research : an official journal of the American Association for Cancer Research.
Nunez, R. (2001). DNA measurement and cell cycle analysis by flow cytometry. Current issues in molecular biology *3*, 67-70.
Oki, Y., Noorani, M., Lin, P., Davis, R.E., Neelapu, S.S., Ma, L., Ahmed, M., Rodriguez, M.A., Hagemeister, F.B., Fowler, N.*, et al.* (2014). Double hit lymphoma: the MD Anderson Cancer Center clinical experience. British journal of haematology *166*, 891-901.
Oliveras-Ferraros, C., Vazquez-Martin, A., Queralt, B., Adrados, M., Ortiz, R., Cufi, S., Hernandez-Yague, X., Guardeno, R., Baez, L., Martin-Castillo, B.*, et al.* (2011). Interferon/STAT1 and neuregulin signaling pathways are exploratory biomarkers of cetuximab (Erbitux(R)) efficacy in KRAS wild-type squamous carcinomas: a pathway-based analysis of whole human-genome microarray data from cetuximab-adapted tumor cell-line models. International journal of oncology *39*, 1455-1479.
Padua, D., and Massague, J. (2009). Roles of TGFbeta in metastasis. Cell research *19*, 89-102.
Palomba, M.L., Piersanti, K., Ziegler, C.G., Decker, H., Cotari, J.W., Bantilan, K., Rijo, I., Gardner, J.R., Heaney, M., Bemis, D.*, et al.* (2014). Multidimensional single-cell analysis of BCR signaling reveals proximal activation defect as a hallmark of chronic lymphocytic leukemia B cells. PloS one *9*, e79987.
Pao, W., and Hutchinson, K.E. (2012). Chipping away at the lung cancer genome. Nature medicine *18*, 349-351.
Paramanathan, A., Solomon, B., Collins, M., Franco, M., Kofoed, S., Francis, H., Ball, D., and Mileshkin, L. (2013). Patients treated with platinum-doublet chemotherapy for advanced non--small-cell lung cancer have inferior outcomes if previously treated with platinum-based chemoradiation. Clinical lung cancer *14*, 508-512.
Pennell, N.A. (2012). Selection of chemotherapy for patients with advanced non-small cell lung cancer. Cleveland Clinic journal of medicine *79 Electronic Suppl 1*, eS46-50.

Phan, R.T., and Dalla-Favera, R. (2004). The BCL6 proto-oncogene suppresses p53 expression in germinal-centre B cells. Nature *432*, 635-639.
Phan, R.T., Saito, M., Basso, K., Niu, H., and Dalla-Favera, R. (2005). BCL6 interacts with the transcription factor Miz-1 to suppress the cyclin-dependent kinase inhibitor p21 and cell cycle arrest in germinal center B cells. Nature immunology *6*, 1054-1060.
Phougat, N., Khatri, S., Singh, A., Dangi, M., Kumar, M., Dabur, R., and Chhillar, A.K. (2014). Combination therapy: the propitious rationale for drug development. Combinatorial chemistry & high throughput screening *17*, 53-67.
Planchon, S.M., Waite, K.A., and Eng, C. (2008). The nuclear affairs of PTEN. Journal of cell science *121*, 249-253.
Ramskold, D., Luo, S., Wang, Y.C., Li, R., Deng, Q., Faridani, O.R., Daniels, G.A., Khrebtukova, I., Loring, J.F., Laurent, L.C*., et al.* (2012). Full-length mRNA-Seq from single-cell levels of RNA and individual circulating tumor cells. Nature biotechnology *30*, 777-782.
Ranuncolo, S.M., Polo, J.M., Dierov, J., Singer, M., Kuo, T., Greally, J., Green, R., Carroll, M., and Melnick, A. (2007). Bcl-6 mediates the germinal center B cell phenotype and lymphomagenesis through transcriptional repression of the DNA-damage sensor ATR. Nature immunology *8*, 705-714.
Ranuncolo, S.M., Polo, J.M., and Melnick, A. (2008). BCL6 represses CHEK1 and suppresses DNA damage pathways in normal and malignant B-cells. Blood cells, molecules & diseases *41*, 95-99.
Rasband, W.S., ImageJ, and National Institutes of Health, B., Maryland, USA, http://rsb.info.nih.gov/ij/ (1997-2009).
Ritz, O., Rommel, K., Dorsch, K., Kelsch, E., Melzner, J., Buck, M., Leroy, K., Papadopoulou, V., Wagner, S., Marienfeld, R*., et al.* (2013). STAT6-mediated BCL6 repression in primary mediastinal B-cell lymphoma (PMBL). Oncotarget *4*, 1093-1102.
Safranek, J., Holubec, L., Jr., Topolcan, O., Pesta, M., Klecka, J., Vodicka, J., Finek, J., Kormunda, S., and Pesek, M. (2007). Expression of mRNA MMP-7 and mRNA TIMP-1 in non-small cell lung cancer. Anticancer research *27*, 2953-2956.
Sasaki, H., Yukiue, H., Moiriyama, S., Kobayashi, Y., Nakashima, Y., Kaji, M., Kiriyama, M., Fukai, I., Yamakawa, Y., and Fujii, Y. (2001). Clinical significance of matrix metalloproteinase-7 and Ets-1 gene expression in patients with lung cancer. The Journal of surgical research *101*, 242-247.
Sato, M., Larsen, J.E., Lee, W., Sun, H., Shames, D.S., Dalvi, M.P., Ramirez, R.D., Tang, H., DiMaio, J.M., Gao, B*., et al.* (2013). Human lung epithelial cells progressed to malignancy through specific oncogenic manipulations. Molecular cancer research : MCR *11*, 638-650.
Scharl, M., Huber, N., Lang, S., Furst, A., Jehle, E., and Rogler, G. (2015). Hallmarks of epithelial to mesenchymal transition are detectable in Crohn's disease associated intestinal fibrosis. Clinical and translational medicine *4*, 1.
Shaffer, A.L., Yu, X., He, Y., Boldrick, J., Chan, E.P., and Staudt, L.M. (2000). BCL-6 represses genes that function in lymphocyte differentiation, inflammation, and cell cycle control. Immunity *13*, 199-212.
Shalek, A.K., Satija, R., Shuga, J., Trombetta, J.J., Gennert, D., Lu, D., Chen, P., Gertner, R.S., Gaublomme, J.T., Yosef, N*., et al.* (2014). Single-cell RNA-seq reveals dynamic paracrine control of cellular variation. Nature *510*, 363-369.
Siegel, R., Naishadham, D., and Jemal, A. (2013). Cancer statistics, 2013. CA: a cancer journal for clinicians *63*, 11-30.
Singh, D.K., Ku, C.J., Wichaidit, C., Steininger, R.J., 3rd, Wu, L.F., and Altschuler, S.J. (2010). Patterns of basal signaling heterogeneity can distinguish cellular populations with different drug sensitivities. Molecular systems biology *6*, 369.
Slack, M.D., Martinez, E.D., Wu, L.F., and Altschuler, S.J. (2008). Characterizing heterogeneous cellular responses to perturbations. Proceedings of the National Academy of Sciences of the United States of America *105*, 19306-19311.

Sottoriva, A., Spiteri, I., Piccirillo, S.G., Touloumis, A., Collins, V.P., Marioni, J.C., Curtis, C., Watts, C., and Tavare, S. (2013). Intratumor heterogeneity in human glioblastoma reflects cancer evolutionary dynamics. Proceedings of the National Academy of Sciences of the United States of America *110*, 4009-4014.
Stahel, R., Peters, S., Baas, P., Brambilla, E., Cappuzzo, F., De Ruysscher, D., Eberhardt, W.E., Felip, E., Fennell, D., Marchetti, A.*, et al.* (2013). Strategies for improving outcomes in NSCLC: a look to the future. Lung cancer (Amsterdam, Netherlands) *82*, 375-382.
Supernat, A., Lapinska-Szumczyk, S., Majewska, H., Gulczynski, J., Biernat, W., Wydra, D., and Zaczek, A.J. (2014). Tumor Heterogeneity at Protein Level as an Independent Prognostic Factor in Endometrial Cancer. Translational oncology.
Tamiya, A., Naito, T., Takahashi, T., Endo, M., and Yamamoto, N. (2010). [Comparison between single-agent and platinum-doublet chemotherapy in elderly patients with non-small cell lung cancer]. Gan to kagaku ryoho Cancer & chemotherapy *37*, 1897-1901.
Tan, X., Carretero, J., Chen, Z., Zhang, J., Wang, Y., Chen, J., Li, X., Ye, H., Tang, C., Cheng, X.*, et al.* (2013). Loss of p53 attenuates the contribution of IL-6 deletion on suppressed tumor progression and extended survival in Kras-driven murine lung cancer. PloS one *8*, e80885.
Tran, P.T., Fan, A.C., Bendapudi, P.K., Koh, S., Komatsubara, K., Chen, J., Horng, G., Bellovin, D.I., Giuriato, S., Wang, C.S.*, et al.* (2008). Combined Inactivation of MYC and K-Ras oncogenes reverses tumorigenesis in lung adenocarcinomas and lymphomas. PloS one *3*, e2125.
Tunyaplin, C., Shaffer, A.L., Angelin-Duclos, C.D., Yu, X., Staudt, L.M., and Calame, K.L. (2004). Direct repression of prdm1 by Bcl-6 inhibits plasmacytic differentiation. Journal of immunology *173*, 1158-1165.
Walker, S.R., Liu, S., Xiang, M., Nicolais, M., Hatzi, K., Giannopoulou, E., Elemento, O., Cerchietti, L., Melnick, A., and Frank, D.A. (2015). The transcriptional modulator BCL6 as a molecular target for breast cancer therapy. Oncogene *34*, 1073-1082.
Wang, D., Long, J., Dai, F., Liang, M., Feng, X.H., and Lin, X. (2008). BCL6 represses Smad signaling in transforming growth factor-beta resistance. Cancer research *68*, 783-789.
Wang, Z.L., Fan, Z.Q., Jiang, H.D., and Qu, J.M. (2013). Selective Cox-2 inhibitor celecoxib induces epithelial-mesenchymal transition in human lung cancer cells via activating MEK-ERK signaling. Carcinogenesis *34*, 638-646.
Weir, B.A., Woo, M.S., Getz, G., Perner, S., Ding, L., Beroukhim, R., Lin, W.M., Province, M.A., Kraja, A., Johnson, L.A.*, et al.* (2007). Characterizing the cancer genome in lung adenocarcinoma. Nature *450*, 893-898.
Wendt, M.K., Balanis, N., Carlin, C.R., and Schiemann, W.P. (2014). STAT3 and epithelial-mesenchymal transitions in carcinomas. Jak-Stat *3*, e28975.
Xie, C., Pan, Y., Hao, F., Gao, Y., Liu, Z., Zhang, X., Xie, L., Jiang, G., Li, Q., and Wang, E. (2014). C-Myc participates in beta-catenin-mediated drug resistance in A549/DDP lung adenocarcinoma cells. APMIS : acta pathologica, microbiologica, et immunologica Scandinavica *122*, 1251-1258.
Xiong, A., Yu, W., Liu, Y., Sanders, B.G., and Kline, K. (2015). Elimination of ALDH+ breast tumor initiating cells by docosahexanoic acid and/or gamma tocotrienol through SHP-1 inhibition of Stat3 signaling. Molecular carcinogenesis.
Xu, J., Chen, Y., Huo, D., Khramtsov, A., Khramtsova, G., Zhang, C., Goss, K.H., and Olopade, O.I. (2015). beta-catenin regulates c-Myc and CDKN1A expression in breast cancer cells. Molecular carcinogenesis.
Yamamoto, T., Oshima, T., Yoshihara, K., Nishi, T., Arai, H., Inui, K., Kaneko, T., Nozawa, A., Adachi, H., Rino, Y.*, et al.* (2012). Clinical significance of immunohistochemical expression of insulin-like growth factor-1 receptor and matrix metalloproteinase-7 in resected non-small cell lung cancer. Experimental and therapeutic medicine *3*, 797-802.

Yan, L.X., Liu, Y.H., Luo, D.L., Zhang, F., Cheng, Y., Luo, X.L., Xu, J., Cheng, J., and Zhuang, H.G. (2014). MYC expression in concert with BCL2 and BCL6 expression predicts outcome in Chinese patients with diffuse large B-cell lymphoma, not otherwise specified. PloS one *9*, e104068.
Yang, X., Li, L., Huang, Q., Xu, W., Cai, X., Zhang, J., Yan, W., Song, D., Liu, T., Zhou, W.*, et al.* (2015). Wnt signaling through Snail1 and Zeb1 regulates bone metastasis in lung cancer. American journal of cancer research *5*, 748-755.
Zhang, J., Fujimoto, J., Zhang, J., Wedge, D.C., Song, X., Zhang, J., Seth, S., Chow, C.W., Cao, Y., Gumbs, C.*, et al.* (2014). Intratumor heterogeneity in localized lung adenocarcinomas delineated by multiregion sequencing. Science (New York, NY) *346*, 256-259.
Zhang, J.H., Chung, T.D., and Oldenburg, K.R. (1999). A Simple Statistical Parameter for Use in Evaluation and Validation of High Throughput Screening Assays. Journal of biomolecular screening *4*, 67-73.
Zhang, S., Li, Y., Wu, Y., Shi, K., Bing, L., and Hao, J. (2012a). Wnt/beta-catenin signaling pathway upregulates c-Myc expression to promote cell proliferation of P19 teratocarcinoma cells. Anatomical record (Hoboken, NJ : 2007) *295*, 2104-2113.
Zhang, X., Yue, P., Page, B.D., Li, T., Zhao, W., Namanja, A.T., Paladino, D., Zhao, J., Chen, Y., Gunning, P.T.*, et al.* (2012b). Orally bioavailable small-molecule inhibitor of transcription factor Stat3 regresses human breast and lung cancer xenografts. Proceedings of the National Academy of Sciences of the United States of America *109*, 9623-9628.
Zhang, X.D. (2007). A pair of new statistical parameters for quality control in RNA interference high-throughput screening assays. Genomics *89*, 552-561.